RMZ – MATERIALS AND GEOENVIRONMENT

PERIODICAL FOR MINING, METALLURGY AND GEOLOGY

RMZ – MATERIALI IN GEOOKOLJE

REVIJA ZA RUDARSTVO, METALURGIJO IN GEOLOGIJO

Historical Rewiev

More than 80 years have passed since in 1919 the University Ljubljana in Slovenia was founded. Technical fields were joint in the School of Engineering that included the Geologic and Mining Division while the Metallurgy Division was established in 1939 only. Today the Departments of Geology, Mining and Geotechnology, Materials and Metallurgy are part of the Faculty of Natural Sciences and Engineering, University of Ljubljana.

Before War II the members of the Mining Section together with the Association of Yugoslav Mining and Metallurgy Engineers began to publish the summaries of their research and studies in their technical periodical Rudarski zbornik (Mining Proceedings). Three volumes of Rudarski zbornik (1937, 1938 and 1939) were published. The War interrupted the publication and not untill 1952 the first number of the new journal Rudarsko-metalurški zbornik - RMZ (Mining and Metallurgy Quarterly) has been published by the Division of Mining and Metallurgy, University of Ljubljana. Later the journal has been regularly published quarterly by the Departments of Geology, Mining and Geotechnology, Materials and Metallurgy, and the Institute for Mining, Geotechnology and Environment.

On the meeting of the Advisory and the Editorial Board on May 22nd 1998 Rudarsko-metalurški zbornik has been renamed into "RMZ - Materials and Geoenvironment (RMZ -Materiali in Geookolje)" or shortly RMZ - M&G.

RMZ - M&G is managed by an international advisory and editorial board and is exchanged with other world-known periodicals. All the papers are reviewed by the corresponding professionals and experts.

RMZ - M&G is the only scientific and professional periodical in Slovenia, which is published in the same form nearly 50 years. It incorporates the scientific and professional topics in geology, mining, and geotechnology, in materials and in metallurgy.

The wide range of topics inside the geosciences are wellcome to be published in the RMZ -Materials and Geoenvironment. Research results in geology, hydrogeology, mining, geotechnology, materials, metallurgy, natural and antropogenic pollution of environment, biogeochemistry are proposed fields of work which the journal will handle. RMZ - M&G is co-issued and co-financed by the Faculty of Natural Sciences and Engineering Ljubljana, and the Institute for Mining, Geotechnology and Environment Ljubljana. In addition it is financially supported also by the Ministry of Higher Education, Science and Technology of Republic of Slovenia.

<div align="right">Editor in chief</div>

Table of Contents – Kazalo

Original Scientific Papers – Izvirni znanstveni članki

Short Papers – Strokovni članki

In Memoriam

Microstructural stability of gray iron thin section castings for enameling

Mikrostrukturna stabilnost sive litine z lamelnim grafitom v tankih stenah za emajliranje

Snježana Zeljko[1], Zoran Glavaš[2, *], Katarina Terzić[2], Faruk Unkić[2]

[1]Plamen International, d. o. o., Njemačka ulica 36, p. p. 209, 34000, Pozega, Croatia
[2]University of Zagreb, Faculty of Metallurgy, Aleja narodnih heroja 3, 44103 Sisak, Croatia

*Corresponding author. E-mail: glavaszo@simet.hr

Abstract: The influences of chromium on the stabilization of pearlite in the microstructure of gray iron thin section castings and distortion of castings during enameling were analyzed in this paper. Chromium content varied from the mass fractions 0.08 % to 0.37 %. It is found that the distortion of castings with or without the addition of chromium in the as-cast condition was in the acceptable range. The microstructure of castings in as-cast condition was consisted of pearlitic metal matrix and graphite flakes dispersed throughout. The results showed that the distortion of castings containing the mass fractions 0.08 % and 0.17 % of chromium was outside the acceptable range after enameling, due to decomposition of pearlite and transformation to austenite during enameling. After enameling, distortion of castings containing 0.37 % chromium was acceptable. Decomposition of pearlite was considerably lower than in castings containing 0.08 % and 0.17 % chromium. The obtained results confirmed the beneficial effect of chromium on the stabilization of iron carbide and prevention of decomposition of pearlite at elevated temperatures.

Izvleček: V delu je narejena analiza vpliva kroma na stabilnost perlita v mikrostrukturi sive litine z lamelnim grafitom v tankih stenah ter deformacije ulitkov med procesom emajliranja. Masni delež kroma se spreminja med 0,08 % in 0,37 %. Ugotovljeno je bilo, da je deformacija ulitkov z dodatka kroma ali brez njega v litem stanju v

zadovoljivih mejah. Mikrostruktura ulitkov v litem stanju sestoji iz perlitne matrice in grafitnih lamel v njej. Rezultati analiz kažejo, da je deformacija ulitkov, ki vsebujejo med 0,08 % in 0,17 % kroma, zunaj dovoljenega območja po izvedenem emajliranju. Vzrok za to je razpad perlita in transformacija avstenita med emajliranjem. Po izvedenem emajliranju je za ulitke, ki vsebujejo masni delež Cr 0,37 %, ugotovljeno, da je deformacija v sprejemljivih mejah. Razpad perlita je značilno manjši v tem primeru kot v litinah, ki imajo masni delež Cr 0,08 in 0,17 %. Dobljeni rezultati potrjujejo ugoden učinek kroma na stabilizacijo železovih karbidov in preprečujejo razpad perlita pri delovnih temperaturah.

Key words: gray iron, microstructure, enameling
Ključne besede: siva litina z lamelnim grafitom, mikrostruktura, emajliranje

Introduction

Gray iron refers to a broad class of ferrous casting alloys normally characterized by a microstructure of flake graphite in a ferrous metal matrix which is usually a fully pearlitic.[1, 2] They are relatively inexpensive and easy to produce. They have high thermal conductivity and damping capacity, low modulus of elasticity and an ability to withstand thermal shock.[3] This make them suitable for castings subjected to local or repeated thermal stressing, such as components of ovens and stoves.[3]

The components of ovens and stoves are in many cases enameled in order to improve corrosion resistance, thermal stability, appearance and many other features.[4] Enamels are inorganic vitreous coatings applied to products or parts made of cast iron to improve ap-

pearance and to protect the metal surface. They may be applied to the surface of components by either the wet process or the dry process. After that, they are fused to the casting surface at temperatures 780–800 °C during the firing process.[4]

During enameling, distortion of castings may occur due to high firing temperatures.[4] Distortion of castings results from low metal strength at the firing temperature, thermal stresses due to non-uniform heating and cooling, decomposition of pearlite and transformation to austenite.[4] Changes in design of the components and firing practice alleviate the first two causes, and properly alloying minimizes decomposition of pearlite and transformation to austenite. Moreover, dimensional stability of gray iron castings at elevated temperatures is affected by factors

such as growth, scaling, and creep rate. [5–9] To prevent these processes, alloying elements must be added to stabilize pearlite.[5–10]

The objective of this paper was to determine the influence of various additions of chromium on the stabilization of pearlite and distortion of castings during enameling.

MATERIALS AND METHODS

The gray iron melts were produced in two mains frequency coreless induction furnaces from a charges consisting of pig iron, steel scrap, gray iron returns, ferrophosphorus, silicon carbide and recarburizer. To obtain desired chromium content in the melts, granulated ferrochromium containing the mass fraction 65,0 % of chromium

was added. During charging, heating and melting the induction furnaces followed the same power-time program as a means to keep the thermal history of the melts as controlled as possible in the "furnace" phase.

Gray iron melts from induction furnaces were tapped and then poured at 1400–1420 °C into vertically-parted green sand molds produced in vertically parted molding machine. The dimensions of the molds were: 800 mm × 1000 mm × 250 mm. Pouring was performed by automatic pouring system (pressurized pouring furnace). Late (stream) inoculation was performed with 0.1 % of calcium/aluminum/strontium containing ferrosilicon. Poured castings were used as components of stoves.

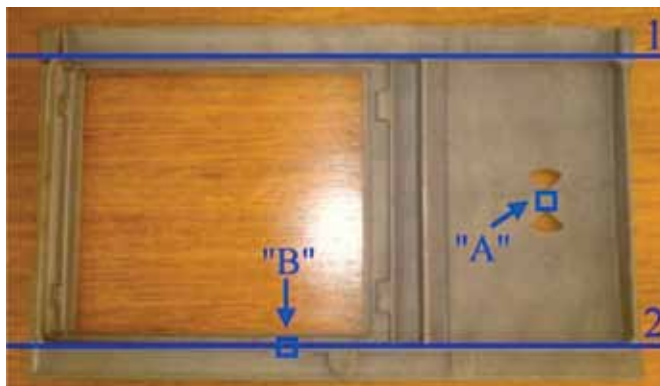After shakeout and blasting, castings were inspected for defects and distor-

Figure 1. Casting after shakeout and blasting. Distortion was measured along the marked lines (1 and 2). Samples for metallographic examinations were cut from areas marked with the letters "A" and "B"

tion. Distortion, i.e. concavity of castings was measured along the ribs 1 and 2 according to figure 1. Maximum acceptable distortion was 1.0 mm.

Enamel was applied to both sides of the castings by wet process (spraying). Fusing of the enamel coating to the castings surface was done in a continuous furnace. Coated castings were fired at 780 °C. Firing time was 10 min. After enameling, distortion of the enameled castings was measured on the previously described manner. The maximum allowable distortion of the castings after enameling was 1.0 mm.

Hardness of the castings before and after enameling was measured by Brinell tester. Metallographic examinations of the castings in as-cast condition and enameled castings were performed by a light metallographic microscope with a digital camera and the image analysis system. Samples were cut from two places as shown in Figure 1: between openings ("A" sample) and from the rib ("B" sample), due to different section thickness (4.0 mm and 6.0 mm). Kinetics of phase transformations in the castings containing 0.08 % and 0.37 % chromium was analyzed by differential scanning calorimetry. The conditions were the same as in the enameling process. Samples were heated at 780 °C and then held at that temperature for 10 min. Heating rate was 40 K/min. The cooling rate after holding at 780 °C was 30 K/min.

Results and discussion

The chemical compositions of examined gray iron heats are given in table 1.

Table 1. Chemical composition of examined gray iron heats in mass fractions, $w/\%$

Gray iron heat	Chemical composition, $w/\%$							
	C	Si	Mn	P	S	Cr	Cu	CE
1	3.55	2.44	0.43	0.370	0.064	0.08	0.09	4.49
2	3.56	2.54	0.44	0.360	0.066	0.17	0.10	4.53
3	3.55	2.47	0.42	0.370	0.071	0.37	0.09	4.50

Table 2. Distortion of castings before and after the enameling

Gray iron heat	The number of castings	Distortion of castings. mm			
		Along the rib 1 (see figure 1)		Along the rib 2 (see figure 1)	
		Before enameling	After enameling	Before enameling	After enameling
1	20	0.15–0.25	1.70–1.90	0–0.20	1.85–1.95
2	50	0.20–0.25	1.20–1.30	0.25	1.20–1.30
3	40	0.10–0.20	0.35–0.50	0.35–0.50	0.30–0.50

With a carbon content in the gray iron melts in the range from 3.55 % to 3.56 %, silicon content in the range from 2.44 % to 2.54 % and a phosphorus content in the range from 0.36 % to 0.37 % carbon equivalents in the range from 4,49 to 4,53 were achieved. This corresponds to slightly hypereutectic compositions. Total carbon and silicon contents were in the target range. If both are low, the iron tends to be brittle and to blister during enameling. If both are high, the iron is soft and warps easily when reheated for enameling. Phosphorus was added intentionally to increase the fluidity of the gray iron melts. Within this range (0.36 % to 0.37 %), phosphorus has a negligible effect on the strength of the gray iron castings at enameling firing temperatures. However, these contents of phosphorus may result in the formation of phosphide eutectic (steadite). The sulfur content was balanced with manganese to promote the formation of manganese sulfides. They were distributed through the structure and acted as nuclei for eutectic graphite. Chromium was added intentionally in gray iron melts number 2 and 3 to stabilize pearlite in the microstructure of castings. Copper promotes pearlite formation, but its content was low in all melts.

The results of measuring distortion (concavity) of castings before and after enameling are given in table 2.

It can be observed from table 2 that in all cases distortion of castings before enameling was in the acceptable range. After enameling distortion of casting containing 0.08 % and 0.17 % chromium was exceeded the maximum allowed value, while the distortion of castings containing 0.37 % chromium was acceptable.

The results of metallographic examinations show that the chromium has pronounced effects on microstructural stability of gray iron castings at firing temperatures (Figures 2 to 4).

It can be observed from figures 2 to 4 that all castings in as-cast condition were fully pearlitic. Types B, C and D graphite flakes were found in thinner "A" samples. In thicker "B" samples, types B and C graphite flakes were present. A large volume fraction of coarse type C graphite flakes was obtained due to hypereutectic compositions. This type of graphite flakes is desirable in applications requiring a high degree heat transfer and high resistance to thermal shock, such as components of stoves. Types B and D graphite flakes are undercooled forms which form when solidification occurs at a large undercooling. Undercooling was occurred due to inadequate nucleation of graphite for a given high cooling rates. The increase of the undercooling during the solidification results in increasing of volume fraction of type D flake

Figure 2. Optical micrographs of the microstructure of gray iron casting containing 0.08 % chromium: a) "A" sample before enameling (as-cast condition), b) "B" sample before enameling (as-cast condition), c) "A" sample after enameling, d) "B" sample after enameling

graphite. High phosphorus contents were resulted in the formation of another microstructural constituent, steadite. Due to the high cooling rates and chromium addition, a small amount of carbides was also found (especially in the microstructure of castings containing 0.37 % chromium).

The results of examinations show that enameling was altered the metal matrix, but no effect on size and shape of graphite achieved during solidification (figures 2 to 4). The pearlite content in the metal matrix decreases after enameling. However, decomposition of the pearlite to ferrite and graphite and transformation to austenite in microstructure of castings containing 0.37 % chromium was considerably lower than in castings containing 0.08 % and 0.17 % chromium. Due to
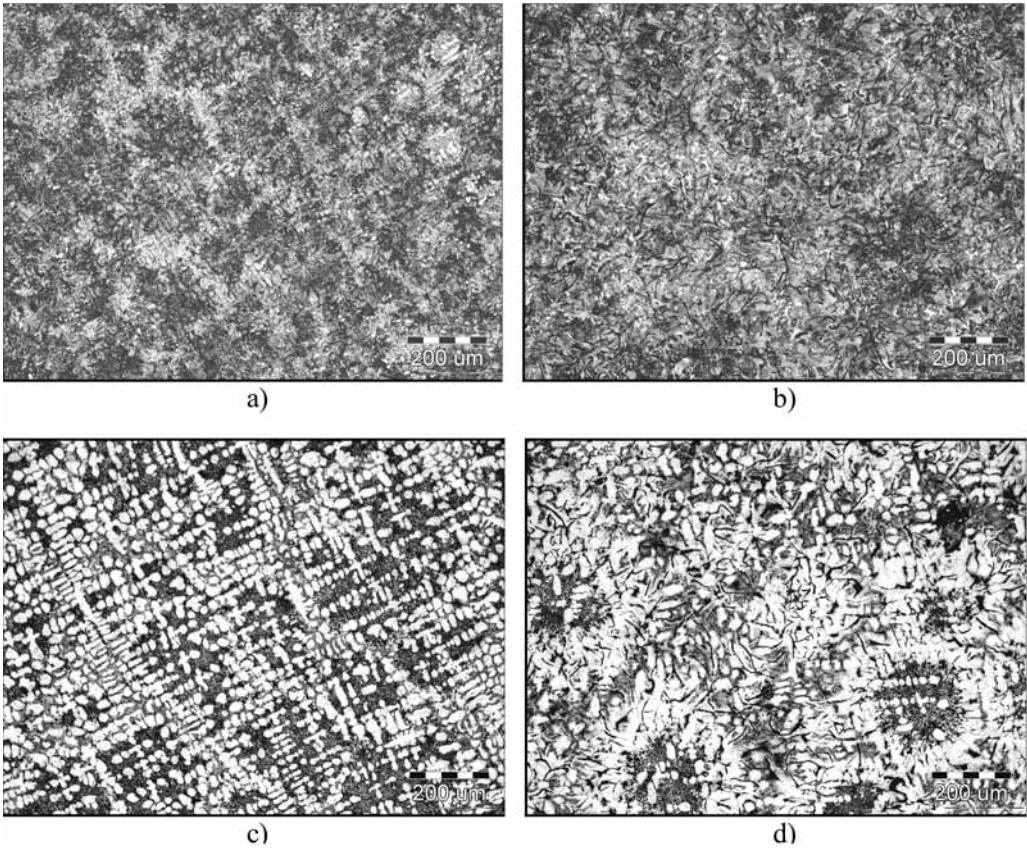
Figure 3. Optical micrographs of the microstructure of gray iron casting containing 0.17 % chromium: a) "A" sample before enameling (as-cast condition), b) "B" sample before enameling (as-cast condition), c) "A" sample after enameling, d) "B" sample after enameling

that, distortion of castings containing 0.37 % after enameling was acceptable. It is obviously that chromium stabilizes iron carbide and therefore prevents the breakdown of pearlite at the firing temperature. This improves the dimensional stability of gray iron castings during enameling.

Although the size and type of the graphite flakes was unaffected by firing process, the size and type had a marked influence on the carbon kinetics during firing process. In castings with a high volume fraction of fine type D graphite flakes, the carbon diffusion paths were shorter, which facilitates the decomposition of pearlite. If pearlite was not stabilized, shorter carbon diffusion paths resulted in higher ferrite volume fraction in the metal matrix after enameling.
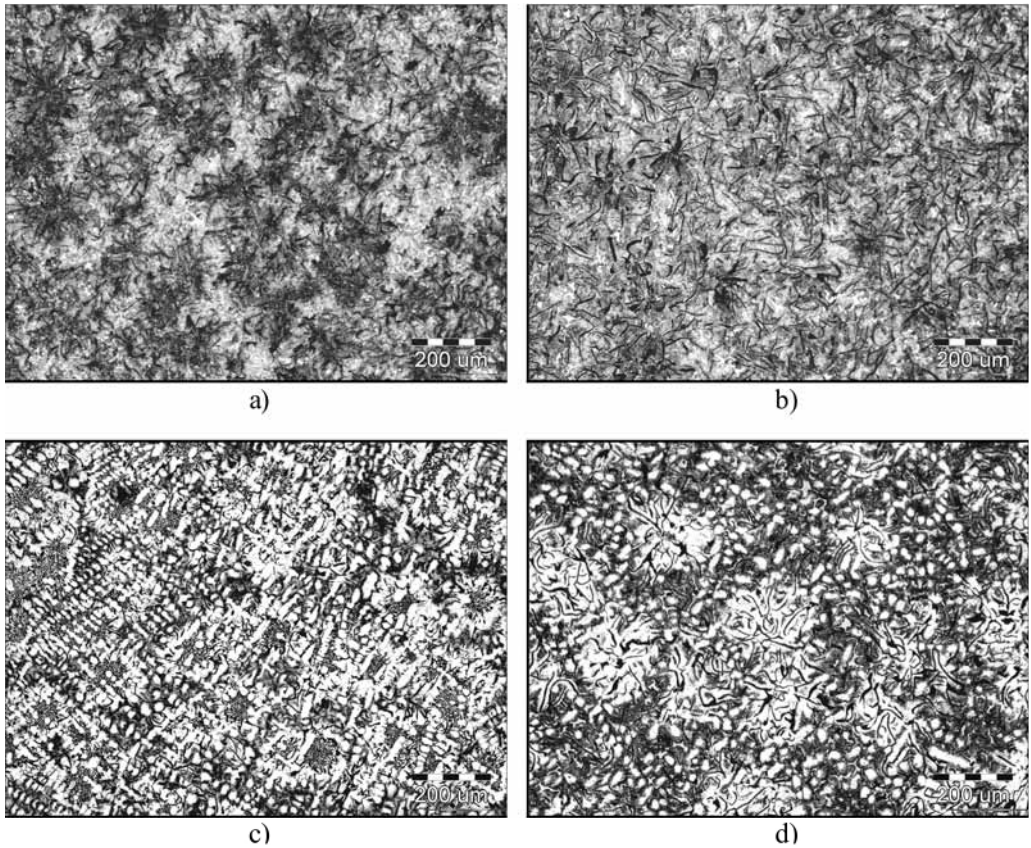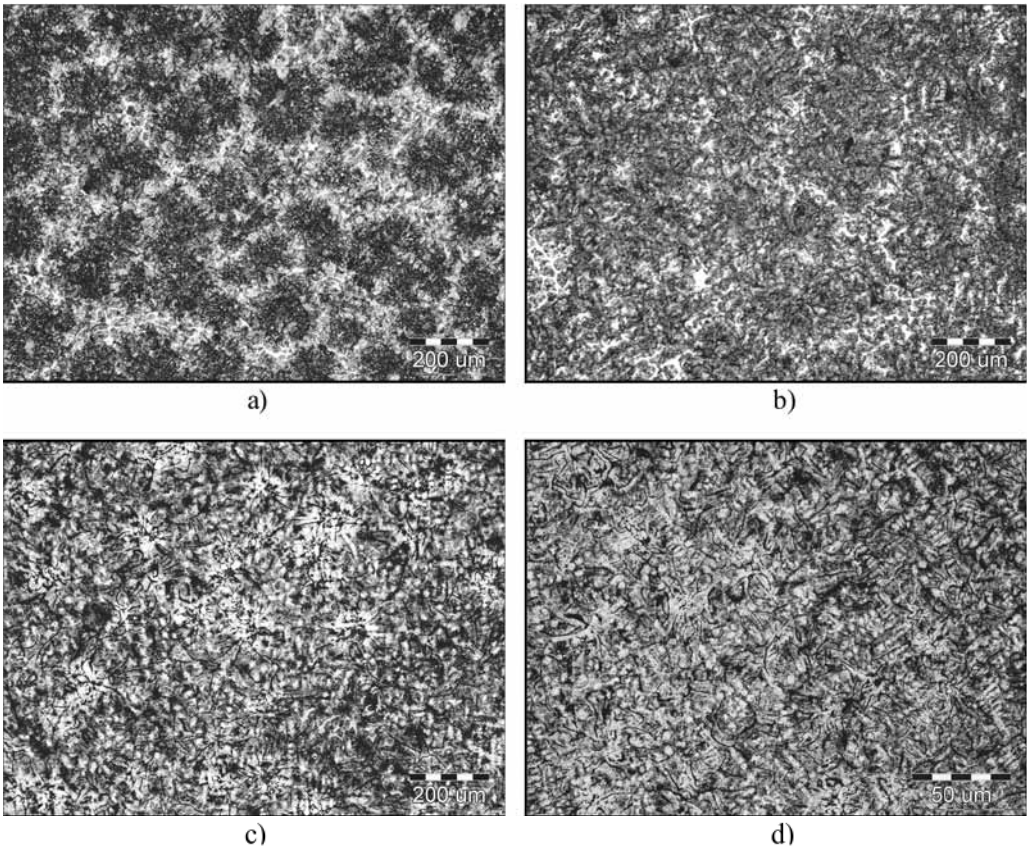
Figure 4. Optical micrographs of the microstructure of gray iron casting containing 0.37 % chromium: a) "A" sample before enameling (as-cast condition), b) "B" sample before enameling (as-cast condition), c) "A" sample after enameling, d) "B" sample after enameling

DSC analysis (figure 5) confirmed the results of metallographic examinations. Heating curve of the sample containing 0.08 % chromium shows that a significant decomposition of pearlite occurred already at ≈350 °C. Decomposition of pearlite progressed very intensively with a further increase in temperature. The maximum was reached at ≈620 °C. Decomposition of the pearlite to ferrite and graphite occurred due to instability at elevated temperatures. Growth, residual stresses and dimensional instability of the casting are the results of the breakdown of the pearlite and transformation to austenite, which occurred at ≈742 °C.

Heating curve of the sample containing 0.37 % chromium shows that the decomposition of pearlite to ferrite and graphite and transformation to austen-

ite was considerably lower than in sample containing 0.08 % chromium. Very small decomposition of pearlite occurred up to 550 °C. Small increase in pearlite decomposition occurred in the range 550–650 °C. This confirms beneficial effect of chromium on the stabilization of iron carbide and the prevention of breakdown of pearlite during enameling. Because of that growth and residual stresses are reduced and the dimensional stability is increased.

The obtained results show that the hardness of all castings decreases after enameling, due to the decomposition of pearlite (table 3). However, castings containing 0.37 % chromium had lower decrease in hardness after enameling than castings containing 0.08 % and 0.17 % chromium, due to much more stable pearlite. The hardness of all castings in as-cast condition and after enameling did not exceed the maximum allowable 230 HB.
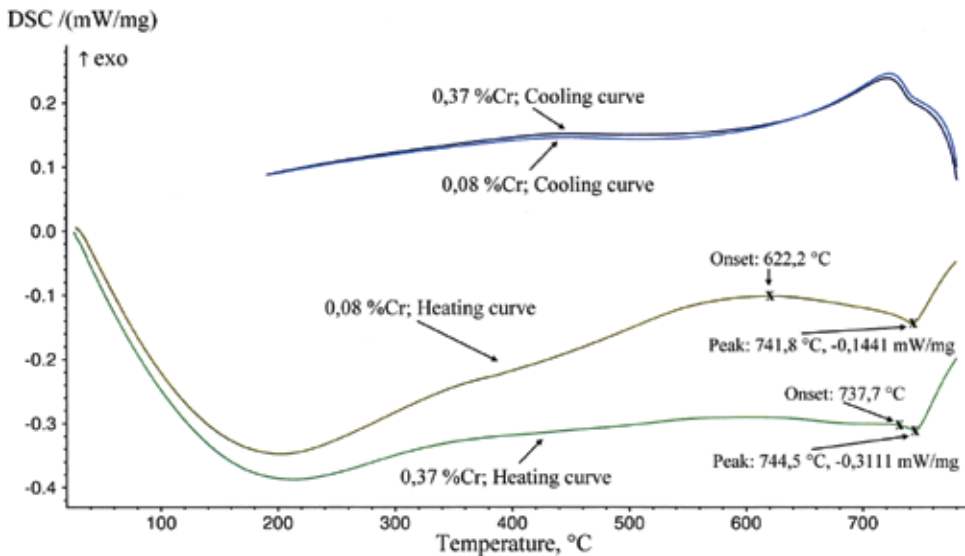
Figure 5. Simultaneous thermal analysis of gray iron samples containing 0.08 % and 0.37 % chromium by DSC method

Table 3. Hardness of castings before and after enameling

Gray iron heat	Hardness of castings, HB			
	Between openings ("A" sample, see figure 1)		On the rib ("B" sample, see figure 1)	
	Before enameling	After enameling	Before enameling	After enameling
1	206	144	214	149
2	216	163	217	166
3	217	183	229	186

Conclusions

The obtained results indicated that the chemical composition has a significant effect on the microstructure of gray iron castings after enameling. During enameling, due to high firing temperatures, decomposition of pearlite and transformation to austenite occurs if pearlite is not stabilized. Phase transformations may result in distortion and dimensional changes of castings. To prevent these processes, alloying elements must be added to stabilize pearlite.

The results of this examinations show that the chromium, when added in proper amount, stabilizes the iron carbide and therefore prevents the breakdown of pearlite during enameling process. Chromium is very effective in stabilization of pearlite, but the use of higher chromium content is limited. It is a strong chill and carbide former, and therefore, high chromium additions can be detrimental to machinability. It is obvious that the chromium content in gray iron casting for enamelling is an important process parameter and must be adapted depending on the required metal matrix structure and section thickness of castings.

Highly branched Type D graphite flakes reduce carbon diffusion distances, which facilitates the decomposition of pearlite. High cooling rates (thin sections) and low nucleation state of melt favors the formation of Type D graphite flakes and carbides. Due to that, melts must be prepared with suitable charge materials (such as pig iron) and properly inoculated.

References

[1] Craig, D. B., Hornung, M. J., McCluhan, T. K. (1988): Gray Iron, chapter in the book: *Metals Handbook, Vol. 15, Casting*. ASM International, Metals Park, Ohio, 1988, pp. 629.

[2] ASM International (1999): Metallurgy and Properties of Gray Irons, chapter in the book: *Cast Irons, ASM Specialty Handbook*. ASM International, Materials Park, Ohio, pp. 32.

[3] Elliott, R. (1988): Cast Iron Technology, *Butterworths & Co., London,* pp. 11.

[4] Technical Publications Committee Of The Porcelain Enamel Institute (1998): Porcelain Enameling, chapter in the book: *ASM Handbook, Vol. 5, Surface Engineering*. ASM International, Materials Park, Ohio, pp. 1343.

[5] ASM International (1999): Elevated-Temperature Properties, chapter in the book: *Cast Irons, ASM Specialty Handbook*. ASM International, Materials Park, Ohio, pp. 409.

[6] ASM International (1997): Alloy Cast Irons, chapter in the book: *Heat-Resistant Materials, ASM Special-*

ty Handbook. ASM International, Materials Park, Ohio, pp. 179.

[7] ASM INTERNATIONAL (1999): Metallurgy and Properties of High-Alloy Graphitic Irons, chapter in the book: *Cast Irons, ASM Specialty Handbook*. ASM International, Materials Park, Ohio, pp. 123.

[8] NOVOSEL, M. (1988): Procesi žarenja sivog lijeva. I. dio. *Livarstvo*; Vol. 3, No. 2, pp. 35–44.

[9] NOVOSEL, M. (1988): Procesi žarenja sivog lijeva. II. dio. *Livarstvo*; Vol. 3, No. 3, pp. 67–72.

[10] AFS CAST IRON DIV. (2000): Stabilizing Pearlite in Gray Cast Iron. *Modern Casting*; Vol. 90, No. 11, pp. 40–43.

The effect of cooling rates on microstructures and hot workability of BRCMO2 tool steel

Vpliv ohlajevalnih hitrosti na mikrostrukturo in vročo preoblikovalnost orodnega jekla BRCMO2

T. Večko Pirtovšek[1], M. Fazarinc[1], G. Kugler[1], P. Mrvar[1], M. Terčelj[1, *]

[1]Faculty for Natural Sciences and Engineering, University of Ljubljana, Aškerčeva 12, 1000 Ljubljana, Slovenia

*Corresponding author: milan.tercelj@omm.ntf.uni-lj.si

Abstract: The influence of solidification and cooling rate on obtained microstructure is especially emphasized in BRCMO2 tool steel. Various cooling rates during solidification process result in considerably different size of grains as well as in different type, size, shape and distribution of carbides. Cast ingot is solidified with different cooling rates across its section leading to different hot workability. Consequently dimensions of ingot are very important since they determine the lowest acceptable cooling rate of the tool steel. Time course of temperature field during the solidification of ingot made from BRCMO2 tool steel has been simulated and obtained microstructures have been analyzed. Finite element analysis was used for estimation of cooling rates and calculation of fractions of solid/liquid at various locations of selected cross-sections of ingot during its cooling. The hot workability of BRCMO2 tool steel was studied using hot compression tests at different deformation conditions on Gleeble 1500D testing equipment.

Izvleček: Vpliv hitrosti strjevanja in ohlajanja na mikrostrukturo je posebej poudarjen pri hitroreznem orodnem jeklu BRCMO2. Tako različne hitrosti ohlajanja med procesom strjevanja kritično vplivajo na različno velikost in razporeditev zrn, prav tako pa tudi na tip, velikost, obliko ter razporeditev karbidov. To se pogosto zgodi pri vlitju jekla v ingot, kjer so hitrosti strjevanja in ohlajanja različne v različnih delih ingota. To ima za posledico tudi različno preobliko-

---

Original scientific paper

valnost v vročem. Tako so dimenzije ingota zelo pomemben parameter, saj določajo najpočasnejšo ohlajevalno hitrost v njem. V tem delu je bil analiziran potek temperature v različnih delih ingota med strjevanjem in ohlajanjem. Z metodo končnih elementov je bila ocenjena ohlajevalna hitrost ter razmerje med talino in trdnim stanjem. Z uporabo naprave Gleeble 1500D je bila preiskana vroča preoblikovalnost na podlagi tlačnih preizkusov.

Keywords: BRCMO2 tool steels, hot workability, cast microstructure, carbide distribution, effect of cooling rates

Ključne besede: orodno jeklo BRCMO2, vroča preoblikovalnost, lita mikrostruktura, razporeditev karbidov, vpliv ohlajevalnih hitrosti

Introduction

The dissolution of alloying elements and precipitation of carbides in ledeburitic tool steels result in a high strength and hardness, small deformation during the heat treatment, a very good wear resistance, and poor hot plasticity. Thus, tool steels usually exhibit a decreased but sufficient hot deformability only in a relatively narrow hot-working range, and as such belong to the group of low-deformable steels.[1–4]

During hot working of ledeburitic tool steels a large number of mutually dependent process parameters influence the intrinsic material properties that make an investigation in this area very specific. Solidification rate can essentially influence the obtained microstructure. During solidification, heating, soaking and hot deformation, various processes take place in

the tool material: the formation of carbides, their decomposition, dissolution, growth, etc. Consequently the size, distribution, type and fraction of carbides, the thermo-mechanical history, the temperature range, etc., have a major influence on the hot workability of ledeburitic tool steels. As a result, hot workability cannot be considered as a constant, but rather as a variable property.[4–8]

BRCMO2 tool steel has excellent hot hardness and wear resistance and is commonly employed to machine hard materials in high speed cutting applications as well as for cold-working dies. But on other hand the tool steel exhibits very poor hot deformability in industrial practice thus improvement in its production is desired. In this contribution time course of temperature in various cross-sections of ingot during solidification of BRCMO2 ledeburitic tool

steel have been calculated by FEA. Additionally, microstructures at various cooling rates were determined and their influence on hot workability has been investigated.

MATERIALS AND METHODS

Materials

BRCMO2 is a molybdenum type tool steel. The chemical composition is given in Table 1. The samples for metallographic analysis were cut from various spots on three various cross section of ingot, i.e. ingot head, ingot bottom, ingot half height, and on various distances from ingot surface, i.e. ingot surface, 10 mm, 50 mm, 90 mm from the surface, and in ingot center.

Optical microscopy (OM, Carl Zeiss AXIO Imager.A1m) was applied for the observation of the microstructure and measurements of the size of eutectic cells where intercept method was applied. The specimens for the optical microscopy were grinded with a sequence of sand papers from 180 to 1200 meshes of granulation, followed by polishing with diamond paste of 1 μm and 0.25 μm granulation and then etched with Nital.

Simulation of cooling rates in ingot using ProCast software

The measured temperature of the melt in the ladle was 1490 °C. It was considered that this temperature was also temperature of the melt in the filled ingot. The simulation of filling and solidification of ingots was calculated using finite element casting simulation program, ProCast. Fluid flow was calculated according to Navier-Stokes equations and solidification properties were based on heat flow according to Fourier's equation.[9] Whole geometry of molds and other parts needed during ingot solidification were modeled in 3D geometry and meshed in ProCast by tetrahedral elements.

Thermodynamic properties of die material, fireclay, exothermic and insulation materials were taken from the ProCast database. Properties of pouring material were calculated using CompuTherm software on the basis of chemical composition. For better results of solidification and cooling the stress module was activated in the software to account for the effect of gap formation on metal/die interface on cooling of ingot.[9] Initial heat transfer coefficient (HTC) h between solidified ingot and mold was considered to

Table 1. Chemical composition of applied BRCMO2 in mass fractions, w_t/%

C	Si	Mn	Cr	Mo	V	W	Co
1.09	0.26	0.25	3.81	9.32	1.09	1.40	8.20

be around 2000 W/(K m²). In general HTC is decreasing with gap formation during solidification and contraction. When the metal is liquid, HTC between the metal and die is a function of ferrostatic pressure given by the equation:

$$h = h_0 \cdot \left(1 + \frac{P}{A}\right)$$

where h_0 is initial heat transfer coefficient, P is pressure and A is empirical constant to account for contact pressure.[8]

Cooling rates were calculated on the basis of the difference between time and temperature from the start of casting to complete solidification.

Hot compression tests

Hot compression tests were applied for assessment of hot deformability as well as for determination of flow curves. For assessment of hot deformability the procedure described in [1] was used. For determination of flow curves samples were taken so from the surface part as well as form centre of ingot's head. The following testing conditions were selected: temperature range 850–1130 °C, strain rates between 0.001 s⁻¹ and 5 s⁻¹ and a true strain of 0.9. The specimens were heated to 1130 °C with a heating rate of 3 °C/s which was followed by holding them for 10 min at this temperature, and cooling with a rate of 2 °C/s to the deformation temperature, holding for 10 min, followed

by hot compression and water quenching afterwards. Tantalum foil with a thickness of 0.1 mm was inserted between the cylindrical specimen and the compression anvil, and a Ni-based lubricant was used. For the higher strain rates the obtained flow curves were temperature compensated according to the procedure described in [7].

Results and discussion

FEM calculated results on ingot cooling and obtained microstructures

The simulated distribution (Figure 1) of solid fraction (left) and of temperature (right) during solidification of ingot at various times after begin of filling; i.e. 570 s (a), 950 s (b), and 1470 s (c) after casting start. It can be noticed that solidification starts on the bottom of ingot already during its filling. The solidification front is then moving from ingot surface towards the center and up to the head of ingot where solidification ends.

On Figure 2 calculated time courses of temperature on spots with various distances from ingot surface are presented. It is clearly seen that due to rapid fall of temperature spots closer to ingot surface undergo considerably higher cooling rates. Furthermore, it is also clear that that fall of temperature is considerably higher on ingot bottom in comparison to ingot head. Calculated

values of cooling rates in ingot head cross-section are given in Table 2. Calculated cooling rates on ingot surface are higher than 10 ºC/s while in the ingot center these values are higher than 0.18 ºC/s.

Ledeburitic steels solidifie through the eutectic transformation is the last transformation of liquid to solid in the solidification process. Therefore, the nucleation and growth of eutectic (eutectic carbides + austenite) occurs in the remaining liquid area between primary dendrites. As-cast microstructure of ledeburitic tool steel consists of dendrites surrounded by an almost continuous inter-dendritic network of eutectic carbides and the size of eutectic cells is directly dependent on solidification rate. Consequently average size of eutectic cells on ingot surface was relative small and amount ca 21 µm while in ingot center these values are around 121 µm. From point of view of deformability obtained values for size of eutectic cells in ingot center indicates on approaching of upper limit of their size. Figure 3a shows microstructure obtained in the center of ingot's head which underwent slowest cooling rates. In the soft annealed condition the solidified microstructure of BRCMO2 steel consist colonies of eutectic carbides and blocky carbides inserted in the basic microstructure from ferrite and spheroidised carbides. In the vicinity of the ingot surface, where the solidification rate was the highest, eutectic cells are smallest and eutectic carbides are impossible to distinguish from the base microstructure detect using OM (see Figure 3b). With the increasing distance from the ingot surface, the eutectic colonies and eutectic carbides became incomparably coarser and also the size and the number of blocky carbides increase. Thus the size of the eutectic cells increase from few micrometers under the ingot surface up to about 86 µm at the 50 mm distance from the ingot surface (see Figure 3c) and in ingot center are around 121 µm where also some micro-porosity was observed. Through the whole cross-section of the ingot the eutectic carbides have lamellar morphology typical for M_2C type of eutectic.

Table 2: Calculated cooling rates and the size of eutectic cells on ingot head cross-section at various distances from ingot surface.

Distance /mm	Assessed cooling rates	The average size of eutectic cells /µm
Up to 1.7	>10 ºC/s	21
10	>0.8 ºC/s	36
50	>0.23 ºC/s	86
center	>0.18 ºC/s	121
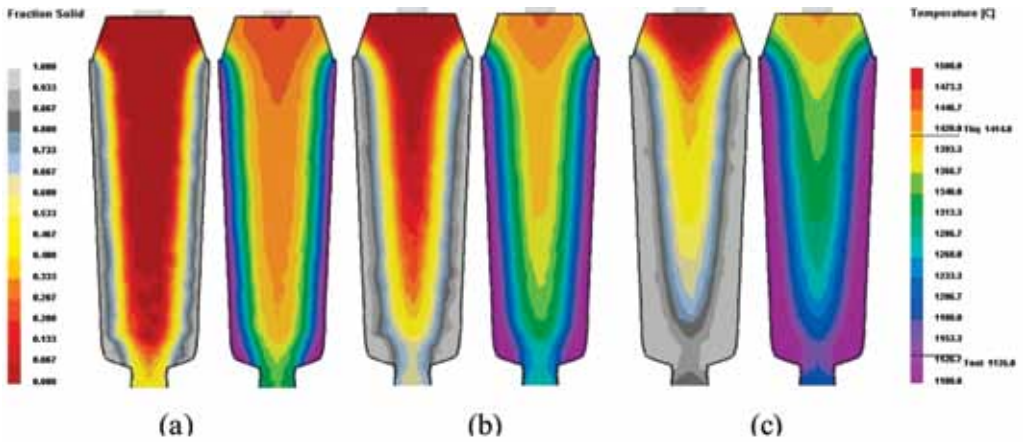
Figure 1. Simulated distribution of solid fraction (left) and of temperature (right) during solidification at: 570 s (a), 950 s (b) and 1470 s (c) after begin of filling.
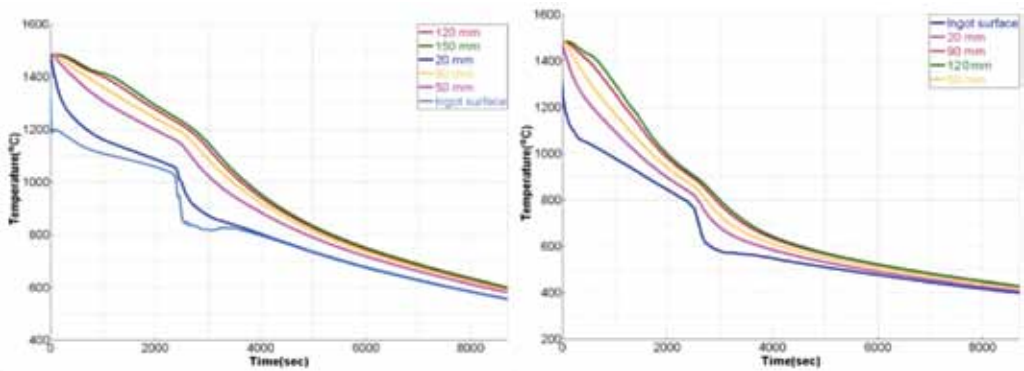

Figure 2. Simulated cooling curves on different depths from ingot surface: top of the ingot (ingot head) (a) and 20 cm from bottom (b).
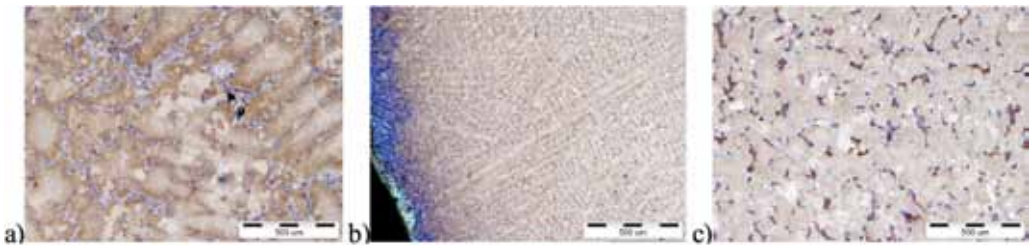

Figure 3. Obtained microstructure on ingot head cross-section: in center (a), on surface (b) and 50 mm from ingot surface.

Hot workability

Different microstructures obtained at different cooling rates result in different hot workability. This was investigated by hot-compression tests at max strain of 0.9, a strain rate of 5 s⁻¹ and various deformation temperatures.[1] The as-cast microstructure (Figure 3b) taken from the region under the ingot surface when cooling at a rate >10 ºC/s does not crack during the upsetting at 1130 °C, whereas the cast microstructure from the ingot core, formed at a cooling rate of 0.18 ºC/s cracks under these deformation conditions. Eutectic cells are believed to be responsible for this behavior. On the other hand at values of strains around 0.6, that are also typical in practice, the cracks were not observed on compressed samples. These results indicate on upper limit of dimensions of ingot since these determine lowest acceptable cooling rate. In laboratory simulation of solidification at cooling rate of 0.167 ºC/s new type of eutectic carbide appeared in microstructure that additionally reduced hot deformability.

As mentioned, flow curves for various temperatures and strain rates were obtained. The comparison of the flow curves is presented in Figure 5. The data gathered from the specimens at the surface of the ingot exhibit higher flow stresses and shape of flow curves indicate on dynamic recrystallization. The samples taken from the center of the ingot reach about 100 MPa lower flow stresses. Samples from ingot center exhibited lower hot deformability since most of them exhibited surface cracking during hot compression at applied strain of 0.9.
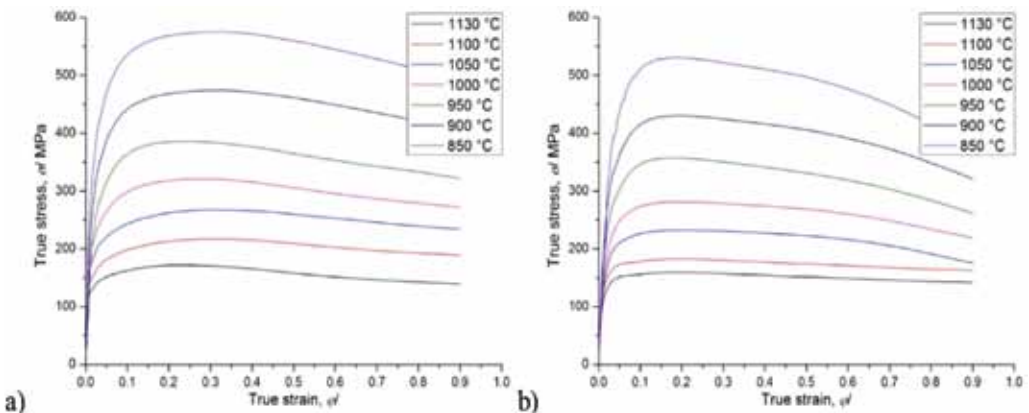

Figure 4. Flow curves measured at different temperatures at strain rate of 5 s⁻¹. Ingot surface (a), center of ingot's head (b).

Conclusions

Calculation of time course of temperatures by FEM on various spots of various cross-sections of ingot during solidification of BRCMO2 tool steel has been carried out. Hot workability of cylindrical samples has been studied by hot compression tests. The following conclusions can be drawn from the presented study:

- Maximal calculated cooling rate on surface area of ingot head amounts >10 ºC/s while the lowest value in centre of ingot head amounts around 0.18 ºC/s.
- BRCMO2 tool steel is very sensitive on cooling rate since this influence on solidified microstructure. Higher cooling rate (>10 ºC/s) results in considerable lower size of dendrites as well as eutectic cells in comparison to lowest calculated cooling rate in solidified ingot.
- From point of view of hot deformability microstructure obtained at cooling rate of about 0.18 ºC/s presents transition from acceptable to non-acceptable microstructure.
- Hot deformability of samples taken from ingot surface does not considerable differ from samples taken from ingot center.
- Applied dimensions of ingot for this tool steel present the upper limit since lower cooling rate would be obtained in ingot with larger dimensions.
- Obtained values for flow curves

of compressed samples from ingot surface are higher in comparison to values of samples taken from ingot center.

References

[1]   Večko Pirtovšek, T., Kugler, G., Godec, M., Terčelj, M. (2011): Materials Characterization; Vol. 62, No. 2, pp. 189–197.

[2]   Ghomashchi, M. R., Sellars, C. M. (1993): Metallurgical transactions A, Vol. 24A, pp. 2171–2180.

[3]   Fajfar, P., Bombač, D., Markoli, B. (2010): RMZ – Materials and Geoenvironment, Vol. 57, No. 2, pp. 159–164.

[4]   Rodenburg, C., Kryzanowski, M., Beynon, J. H., Rainforth, W. M. (2004): Materials Science and Engineering A 386, pp. 420–427.

[5]   Imbert, C., Ryan, N. D., McQueen, H. J. (1984): Metallurgical Transactions A 15A, pp. 1855–1864.

[6]   Milovic, R., Manojlovic, D., Andjelic, M., Drobnjak, D. (1992): Steel Research 63/2, pp. 78–84.

[7]   Imbert, C. A. C. & McQueen, H. J. (2000): Materials Science and Technology, Vol. 16, pp. 532–538.

[8]   Liu, J., Chang, H., Wu, R., Hsu, T. Y., Ruan, X. (2000): Materials Charact. 45, pp. 175–186.

[9]   Kermanpur, A., Eskandari, M., Purmohamad, H., Soltani, M. A., Shateri, R. (2010): Materials and Design 31, pp. 1096–1104.

Effect of heat treatment and test temperature on fracture type of steel Nitronic 60

Vpliv toplotne obdelave in temperature preizkušanja na vrsto preloma jekla Nitronic 60

Almaida Gigović - Gekić[1]*, Mirsada Oruč[2], Aleš Nagode[3], Hasan Avdušinović[1]

[1]University of Zenica, Faculty of Metallurgy and Materials Science, Zenica, Bosnia and Herzegovina
[2]Metallurgical Institute "Kemal Kapetanović", Zenica, Bosnia and Herzegovina
[3]University of Ljubljana, Faculty of Natural Sciences and Engineering, Ljubljana, Slovenia

*Corresponding author. E-mail: almaida.gigovic@famm.unze.ba

Abstract: Nitronic 60 is a commercial name for austenitic stainless steel. Requirements in terms of chemical composition and mechanical properties of steel Nitronic 60 meet the requirements for steel UNS S21800. This steel has an increased content of manganese and silicon, which contributes to its excellent resistance to abrasion and adhesive wear. In this paper the fracture surface of the specimen after tensile test were examined in order to detect changes in ductile properties and the type of fracture depending on the condition of material and test temperature. Analysis of the fracture surface was performed on the stereo, optical and scanning electron microscope.

Izvleček: Nitronic 60 je komercialno ime za avstenitno nerjavno jeklo. Glede na kemijsko sestavo in mehanske lastnosti jeklo Nitronic 60 izpolnjuje zahteve za jeklo UNS S21800. To jeklo ima povečano vsebnost mangana in silicija, ki prispevata k odlični odpornosti proti abraziji in adheziji. V tem delu smo preiskali prelomne površine vzorcev po nateznem preizkusu in spremljali spremembe duktilnih lastnosti ter ugotavljali vrsto preloma v odvisnosti od stanja materiala in temperature preizkušanja. Za analizo prelomnih površin smo uporabili stereo-, optični in elektronski mikroskop.

Original scientific paper

Introduction

Because of the unstable and high nickel price on the world market there is a need for replacing expensive nickel with some other cheaper austenite stabilizing elements.[1, 2] The solution of this problem is substitution a portion of nickel with manganese and nitrogen. In this way a new steel group was created, which according to the UNS (Unified Numbering System) system, referred to as the series 200. In this group of steel nitrogen content ranges from 0.08–0.6 %, manganese 4–19 % and nickel 0.5–18 %.[3, 4] Nitronic 60 is a commercial name for austenitic stainless steel, which according to their chemical composition belonging to series 200. Steel Nitronic 60 has excellent resistance to abrasion and adhesive wear due to an increased content of manganese and silicon. Compared to steel alloyed with nickel and cobalt, Nitronic 60 has the same or better properties and lower price. Also, it has good impact resistance at low temperatures. Steel Nitronic 60 is applied to work at elevated temperatures because of good creep resistance and high temperature corrosion resistance.[5] The ASTM standard for this group of steels prescribes mechanical properties in the annealed condition, hot or cold deformed. This paper presents and discuss the results of the analysis of fracture surface of the specimens after tensile test at room and elevated temperature for three corresponding chemical composition of test material in a rolled and annealed condition.

Materials and methods

Tests were conducted using three melts produced in a vacuum induction furnace (type- Heraeus) at the Metallurgy Institute „Kemal Kapetanović" in Zenica. The results of chemical analysis of the experimental melts and comparative values prescribed by ASTM standards are given in Table 1.

As seen from the Table 1 the chemical composition of test melts is in good agreement with chemical composition as prescribed in ASTM A276. This standard applies to steel S21800, which is taken as a reference for Nitronic 60.

Mechanical and metallographic examinations were conducted on samples in a rolled and solution annealed state. To obtain the austenitic microstructures free of precipitates extracted samples were

Table 1. The chemical composition of melts –Nitronic 60[5] in mass fractions, *w*/%

Melt	Chemical composition, *w*/%							
	C	Si	Mn	Cr	Ni	P	S	N
ASTM A276	≤0.10	3.5–4.5	7–9	16–18	8–9	≤0.006	≤0.03	0.08–0.18
V1694	0.04	3.74	8.6	18.0	8.0	0.007	0.005	0.160
V1696	0.05	3.5	7.9	16.9	8.6	0.005	0.005	0.120
V1697	0.05	3.5	7.2	16.9	8.6	0.005	0.010	0.168

Table 2. Test results of mechanical properties of steel Nitronic 60[5]

Melt	Test condition	Test temperature	Mechanical properties			
			$R_{p0.2}$/(N/mm²)	R_m/(N/mm²)	Z/%	A/%
V1694	rolled	Room temperature	860	1026	50	18.1
V1696			681	874	68	35.6
V1697			779	937	61	27.9
V1694	annealed	Rom temperature	400	750	75	51.8
V1696			331	681	76	57.2
V1697			366	716	68	55.7
V1694	annealed	750 ⁰C	211	292	49	38.7
V1696			158	245	48	45.5
V1697			182	299	42	29.9

Figure 1. Microstructure of austenitic stainless steel Nitronic 60. (aqua regia, × 100)[5]

annealed at a temperature of 1020 °C for 1 h and quenched in water. Microstructure of austenitic stainless steel Nitronic 60 is shown in Figure 1 with polygonal austenite grains with the characteristic twins. The basic parameters of the mechanical properties of tested samples are presented in table 2. Mechanical tests were conducted on a universal hydraulic machine for static testing (200 kN) at the Metallurgical Institute »Kemal Kapetanović« in Zenica. The process of testing and preparing of test specimens for testing performed in accordance with the standards BAS EN 10002-1/02 and BAS EN 10002-5/01. Tensile testing of mechanical properties at room and elevated temperature (750 °C) was carried out on specimens obtained from the Ø 15 mm rod.

Test results from Table 2 for annealed samples tested at room temperature are in agreement with the standard ASTM A276. while the test results for annealed samples tested at elevated temperature are in accordance with the manufacturer demand.

Examination of the fracture surface appearance was performed in three steps.

- Analysis of fracture surfaces on specimens at the stereo microscope Leica with a maximum magnification of 60-times
- 3D simulation of the fracture surface of specimen using Olympus optical microscope with appropriate software. Development of the simulation was based on a series of photographs taken on the optical microscope with magnification of 50-times
- Analysis of the fracture surface using SEM Jeol JSM 5610 at different magnifications.

Results and discussion

Analysis of the tensile test results
Analysis of the results of mechanical tests showed that the material in the rolled condition has the maximum value of tensile properties, while the increase in temperature leads to decreasing of the strength. Specimens tested in annealed condition at room temperature have the best ductile properties. These results are a consequence of the microstructure obtained for different tasted states.

Annealing at temperatures above 1000 °C leads to dissolution of precipitates, mainly $M_{23}C_6$ type of carbides, which have a negative effect on the ductility properties.[6] However, heating austenite steel in the temperature range from 400–900 °C leads to their re-precipitation. Otherwise, the final rolling temperature was an average of 850 °C, which affected the amount of extracted precipitates, and thus the ductility and tensile properties of tested material.

Fracture surfaces analysis

Stereo microscope analysis
Figures 2, 3 and 4 give the appearance of the fracture surfaces of tested specimens made from melts V1696, V1694 and V1697. From Figure 2 and 3 can be seen that the fracture surface of specimens tested at room temperature made of melts V1696 and V1694 have typical Cup-Cone ductile fracture with pronounced plastic deformation while this type of fracture is not present at the specimen made from melt V1697 tested at of 750 ° C
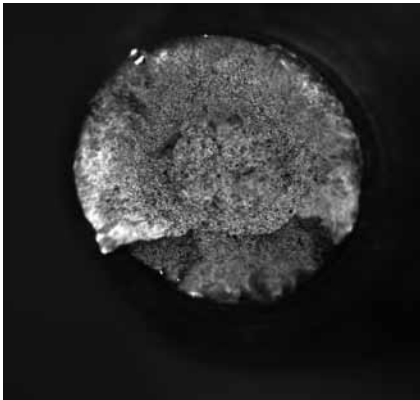
| a) magnification 20-times | b) magnification 12.5-times |
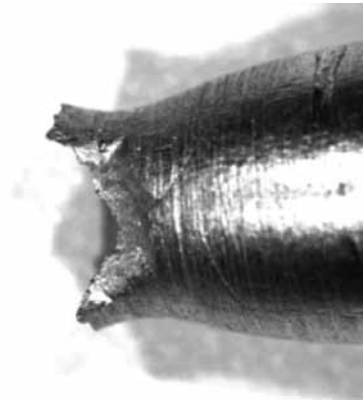
Figure 2. Fracture surface (melt V1696, rolled condition, room temperature)

| a) magnification 16-times | b) magnification 16-times |

Figure 3. Fracture surface (melt V1694, annealed condition, room temperature)

| a) magnification 16-times | b) magnification 12-times |

Figure 4. Fracture surface (melt V1697, annealed condition, tested at 750 °C)

Optical microscope analysis

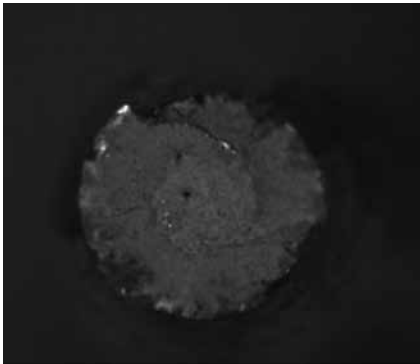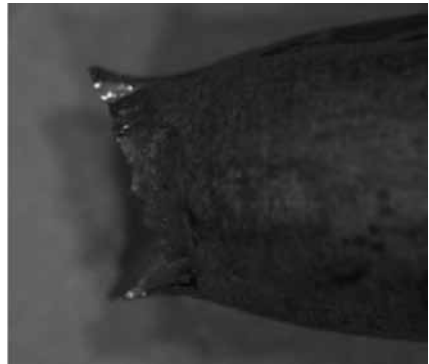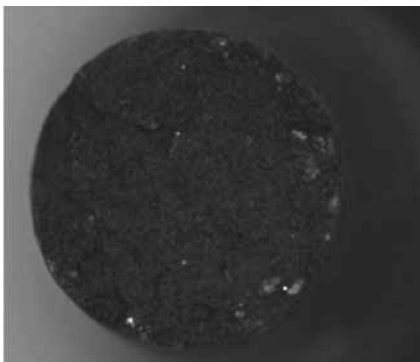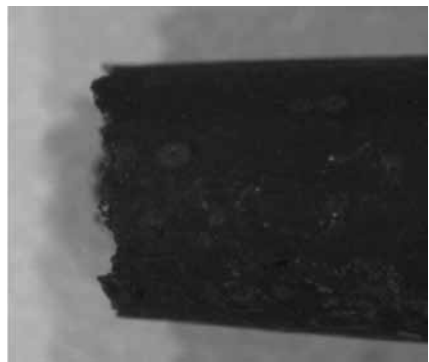Samples presented in the previous chapter were used for 3D analysis of fracture surface. The appearance of the obtained fracture surface is shown in Figures 5, 6 and 7. Analysis of 3D images of the fracture surface confirmed the assumption after observing the samples at a stereo microscope. At the figures 5 and 6 can be observed ductile type of fracture, while in Figure 7 the brittle fracture characteristics can be seen.

Figure 7. 3D view of fractured surface (melt V1697, annealed condition, test temperature 750 °C)

SEM analysis of the fracture surfaces

SEM (scanning electron microscope) analysis was carried out for a detailed analysis of the type of fracture. SEM micrographs were used for confirmation the assumptions made after stereo and optical microscope analysis. The analysis was performed at the University of Ljubljana (Faculty of Natural Sciences and Engineering) at the scanning electron microscope JEOL at different magnifications. Analysis of fracture surfaces showed that the ductile fracture occurs during testing at room temperature in both cases, i.e. in rolled and annealed conditions of samples. Fracture surfaces of samples tested at 750 °C showed the presence of intergranular brittle fracture with small portion of ductile fracture. Appearance of fracture surfaces of specimens is shown in Figures 8, 9,10 and 11 which is consistent with the 3D fracture analysis.
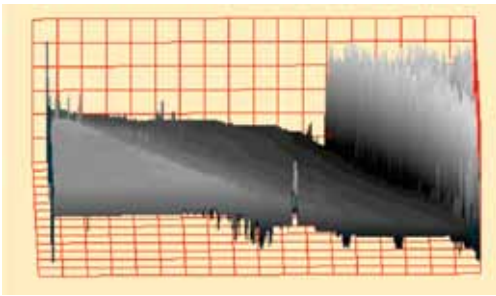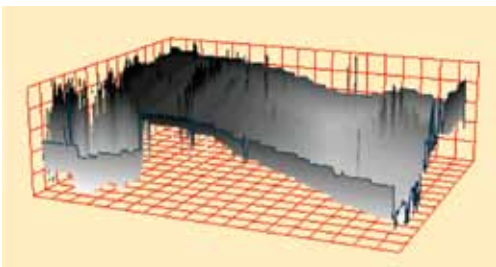

Figure 5. 3D view of fractured surface (melt V1696, rolled condition, room temperature)

Figure 6. 3D view of fractured surface (melt V1694. annealed condition, room temperature)
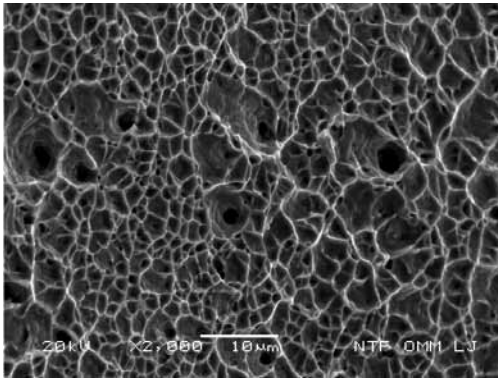
Figure 8. Fracture surface – SEM (melt V1696, rolled condition, room temperature)
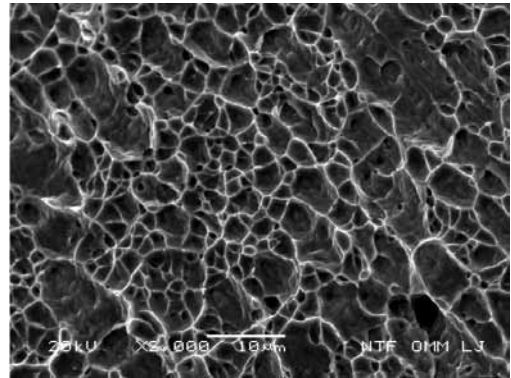
Figure 9. Fracture surface – SEM (melt V1694, annealed condition, room temperature)
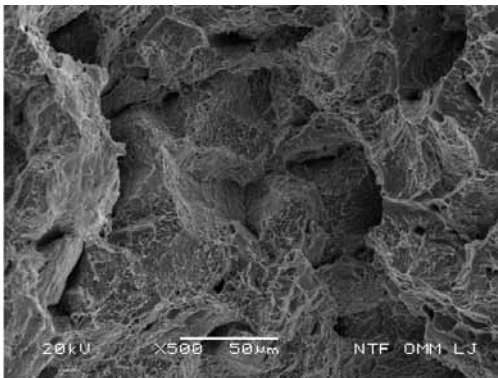
Figure 10. Fracture surface – SEM (melt V1697, annealed condition, tested at 750 °C)
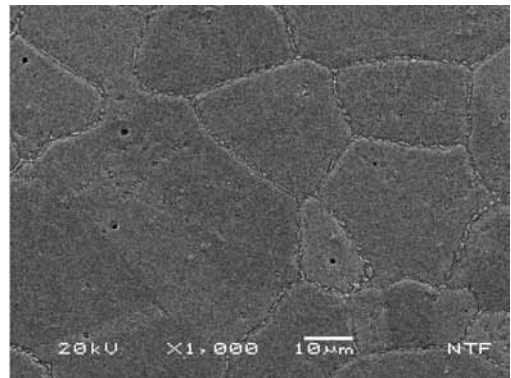
Figure 11. Microstructure of the sample – SEM (melt V1697, annealed condition, tested at 750 °C)

Conclusions

On the basis of the research and analysis of the results it can be concluded that the tensile test specimens tested at room temperature in a rolled and annealed condition have ductile fracture, while during testing at 750 °C appears brittle intergranular fracture.

Samples that were solution annealed have austenitic microstructure without extracted precipitates inside the grains and at grain boundaries what has a significant influence on the ductile properties and the type of fracture.

Temperature rising during testing at 750 °C leads to excretion of the first

precipitates at grain boundaries and then inside the grains, which leads to a decrease in ductile properties and the occurrence of brittle fracture, Figures 10 and 11.[5]

Acknowledgments

References

[1] http://ar.outokumpu.com/2009/this-is-outokumpu/market-review; Market review. (4. 5. 2010)

[2] Oshima, T., Habara, Y., Kuroda, K. (2007): Efforts to save Nickel in Austenitic Stainless Steels. ISIJ International, Vol. 4, No. 3, pp. 359–364.

[3] Beganović, O., Pihura, D., Stergulc, I., Kratina, E.. Fakić, B. (2007): Osvajanje prototipova proizvoda od materijala Nitronic 60 i Nimonic 80A (Osvajanje žice za izradu prototipa pin od čelika Nitronic 60), Metalurški institut „Kemal Kapetanović", Izvještaj br. E-1529, Zenica.

[4] Lula, R. A. (1986): Stainless Steel, American Society for Metals, Ohio.

[5] Gigović-Gekić. A. (2010): Kvantifikacija uticaja alfa-gama obrazujućih elemenata na mehaničke osobine i pojavu delta ferita kod nehrđajućeg austenitnog čelika Nitronic 60. Univerzitet u Zenici. doktorska disertacija, Univerzitet u Zenici, Fakultet za metalurgiju i materijale.

[6] Gigović-Gekić, A., Oruč, M., Vitez, I. (2011): The effect of solution annealing on properties of steel Nitronic 60, Metalurgija, Vol. 50, No. 1, pp. 21–24.

Bacterial indicators of faecal pollution and physiochemical assessment of tributaries of Ganges River in Garhwal Himalayas, India

Bakterijski indikatorji fekalnega onesnaženja in fiziološko-kemijska ocena pritokov reke Ganges v Garhwalski Himalaji v Indiji

Archna Sati[1], Anchal Sood[1], Shivesh Sharma[2, *], Sandeep Bisht[1], Vivek Kumar[3]

[1]Department of Microbiology, SBS Post Graduate Institute of Bio-Medical Sciences and Research Balawala, Dehradun, Uttarakhand, India
[2]Department of Applied Mechanics (Biotechnology), Motilal Nehru National Institute of Technology, Allahabad, Uttar Pradesh, India
[3]Microbiology Section, Department of Soil and Water Research, Public Authority of Agricultural Affairs & Fish Resources, PO Box 21422, Safat-13075, Kuwait

*Corresponding author. E-mail: dr.shiveshsharma@gmail.com

Abstract: A study was undertaken to investigate the water quality of Alaknanda and Bhagirathi rivers (tributaries of River Ganges) in Garhwal Himalayan region during the periods of monsoon, summer and winter seasons. Both the rivers are sacred and are important source of water for drinking and irrigation. Water samples were analyzed for various bacteriological parameters including total viable count (TVC), total coliform (TC), faecal coliform (FC) and faecal streptococci (FS). Also, physicochemical attributes viz. dissolved oxygen (DO), biological oxygen demand (BOD) and chemical oxygen demand (COD) was assessed. Total viable count exceeded the maximum permissible limits in all the samples irrespective to different seasons. The high most probable number (MPN) values and presence of faecal coliforms and streptococci in the water samples suggests the potential presence of pathogenic microorganisms which might cause water borne diseases. A direct effect of season and human activities on the pollution status was

Original scientific paper

observed at all the water sampling sites. The over all objective of this work was to investigate the incidence of these indicator organisms, coliform, faecal coliform, faecal streptococci and physiochemical parameters during different seasons in two main tributaries of Ganges River.

Izvleček: Namen študije je bil raziskati kakovost vode rek Alaknanda in Bhagirathi (pritokov Gangesa) na območju Garhwalske Himalaje v monsunskem, poletnem in zimskem obdobju. Obe reki veljata za sveti in sta hkrati pomemben vir pitne in namakalne vode. V vzorcih vode so določali različne bakteriološke parametre, kot tudi celotno število za življenje sposobnih organizmov (TVC), celotne koliformne organizme (TC), fekalne koliformne organizme (FC) in fekalne streptokoke (FS). Določali so tudi fiziološko-kemijske lastnosti, kot so raztopljeni kisik (DO), biološka potreba po kisiku (BOD) in kemijska potreba po kisiku (COD). Celotno število za življenje sposobnih organizmov presega najvišje dopustne meje v vseh vzorcih, ne glede na čas vzorčenja. Visoke vrednosti najverjetnejšega števila (MPN) in navzočnost fekalnih koliformov ter streptokokov v vzorcih nakazuje možno navzočnost patogenih mikroorganizmov, ki utegnejo povzročati obolenja, ki se širijo z vodo. Na vseh vzorčnih mestih je mogoče opazovati vpliv letnega odobja in človekovih dejavnosti na stanje onesnaženosti. Poglavitni namen dela je bil raziskati pogostnost indikatorskih organizmov, koliformov, fekalnih koliformov, fekalnih streptokokov in fiziološko-kemijskih parametrov v različnih obdobjih leta v dveh glavnih pritokih reke Ganges.

INTRODUCTION

The Ganges or Ganga rises in the Northern Himalayas on the Indian side of the Tibet border. Its five headstreams i.e. the Bhagirathi, Alaknanda, Mandakini, Dhauliganga and Pindar rise in Uttarakhand region. Of these, the two main headstreams are the Alaknanda (Latitude: 30°7'60'' N, Longitude: 78°35'60'' E) about 4 402 meter above sea level (the longer of the two), which rises about 30 miles north of the Himalayan Peak of Nanda Devi and the Bhagirathi (Latitude: 30°7'60'' N, Longitude: 78°34'60'' E) about 3 050 meters

above sea level in an ice cave at the foot of the Himalayan glacier known as Gangotri, merges at Dev Prayag to form river Ganges, flows through the northern Indian planes, providing drainage and water for around 400 million people.

In the recent past, expanding human population, industrialization, intensive agricultural practices and discharges of massive amount of wastewater into the river have resulted in deterioration of water quality. The impact of these anthropogenic activities has been so extensive that the water bodies have lost their self-purification capacity to a large extent. Therefore, there is a grown recognition and need that aquatic water bodies or ecosystem like Ganga must be sustained so that they may support human life. This has resulted in scarcity of potable water supply and loss of biodiversity in aquatic system. The health and well being of the human race is closely tied up with the quality of water used (SHARMA et al., 2005).

Most of the people in the Himalayan region use surface water for drinking which is most vulnerable to pollution due to the surface run off. Almost all major rivers have been tapped at source for drinking water supplies, but there is no monitoring of water quantity or quality on regular bases. During bathing the river water is also used for drinking (Aachman), irrespective of its

water quality. But, it is evident from a course of studies carried out by different (SRIVASTAVA et al., 1996; KULSHRESTHA & SHARMA, 2006) that Ganges water is highly contaminated with coliforms.

Microorganisms are widely distributed in nature, and their abundance and diversity may be used as an indicator for the suitability of water (OKPOKWASILI & AKUJOBI, 1996). The use of bacteria as water quality indicators can be viewed in two ways, first, the presence of such bacteria can be taken as an indication of faecal contamination of the water and thus as a signal to determine why such contamination is present, how serious it is and what steps can be taken to eliminate it; second, their presence can be taken as an indication of the potential danger of health risks that faecal contamination posses. The higher the level of indicator bacteria, the higher the level of faecal contamination and the greater the risk of waterborne diseases (PIPES, 1981). A wide range of pathogenic microorganisms can be transmitted to humans via water contaminated with faecal material. These include enteropathogenic agents such as salmonellas, shigellas, enteroviruses, and multicellular parasites as well as opportunistic pathogens like *Pseudomonas aeroginosa*, *Klebsiella*, *Vibrio parahaemolyticus* and *Aeromonas hydrophila* (HODEGKISS, 1988). It is not practicable to test water for

all these organisms, because the isolation and identification of many of these is seldom quantitative and extremely complicated (CAIRNEROSS et al., 1980; WORLD HEALTH ORGANIZATION (WHO), 1983). An indirect approach is based on assumption that the estimation of groups of normal enteric organisms will indicate the level of faecal contamination of the water supply (WHO, 1983). The most widely used indicators are the coliform bacteria, which may be the total coliform that got narrowed down to the faecal coliforms and the faecal streptococci (HARWOOD et al., 2001; PATHAK & GOPAL, 2001; KISTE-MANN et al., 2002). Concurrently, contamination of water by enteric pathogens has increased worldwide (CRAUN, 1986; ISLAM et al., 2001). However, to the best of our knowledge, no report is available on the bacterial as well as physiochemical parameters analysis of two main tributaries of Ganges River in Garhwal Himalayan region. The overall objective of this work was to investigate the incidence of these indicator organisms, coliforms, faecal coliforms and faecal streptococci in relation with physiochemical parameters of Alaknanda and Bhagirathi rivers in different seasons in Garhwal Himalayas, India.

MATERIALS AND METHODS

Collection of water samples

Intensive survey of the study area was done to select different sites from Gangetic river system of Garhwal region. The Ganges River in Garhwal

Figure 1. Map of the study area of Bhagirathi and Alaknanda river system of Garhwal Himalayas**.**

Table 1. Sample collection sites of Alaknanda and Bhagirathi rivers.

	Alaknada		Bhagirathi
A1	Vasundhara	B1	Bhojwasa
A2	Mana	B2	Chirwasa
A3	Badrinath (Gandhi ghat)	B3	Gangotri
A4	Badrinath (Rishi ghat)	B4	Harsil
A5	Gobind ghat	B5	Jhala
A6	Hanuman Chatti	B6	Bhaironghati
		B7	Gaumukh

Himalayas comprises of two tributaries Bhagirathi and Alaknanda, so sampling was done from both the rivers (Figure 1). The total stretch covered in this study was about 250 km, out of which Alaknanda comprised a stretch of 135 km and Bhagirathi about 115 km. Samples were collected during the monsoon, summer and winter seasons. The samples were carefully collected in triplicate from 13 different places (Table 1) in sterile containers, and were transported in ice boxes at 3° C and brought to the laboratory for analysis (SHARMA et al 2010). The results presented in the table are average of triplicate samples of a particular site.

Bacterial analysis
The bacterial population (total viable count, TVC) in different samples was estimated by inoculating nutrient agar plates with 0.1 mL of suitable dilutions. The results were expressed as colony forming units (cfu) per unit volume, enumerated after 48 h of incubation. The water quality was determined by the standard most probable number (MPN) method. Coliforms were de-tected by inoculation of samples into tubes of MacConkey broth and incubation at 37 ± 1 °C for 48 h. The positive tubes were sub cultured into brilliant green bile broth (BGBB) and were incubated at 44.5 ± 1 °C. Gas production in BGBB at 44.5 ± 1 °C was used for the detection of faecal coliform after 48 h incubation. Faecal streptococci were detected by inoculation of water samples into Azide Dextrose broth and incubation at 37.5 ± 1 °C for 24–48 h (APHA et al, 1999). All the culture media were obtained from Hi-Media Pvt. Ltd., Mumbai, India.

Physiochemical analysis
Physicochemical parameters including total dissolved solids (TDS), conductivity and pH were analyzed on site at the time of sample collection by water analysis kit (Model LT-61, Labtronics, Guelph, Ontario, Canada) as per manufacturer instruction. Other parameters i.e. dissolved oxygen (DO), biological oxygen demand (BOD) and chemical oxygen demand (COD) were performed in laboratory by standard titrimetric method (APHA et al, 1999).

The data were analyzed statistically by using analysis of variance (ANOVA) to find out significance at 5 % levels. In figures, error bars indicate standard error of the mean, where error bars are not visible; they are smaller than the marker.

RESULTS

The TVC value showed a regular trend (Figure 2). The values increased in monsoon season, thus generally highest counts were observed, intermediate in summer season and least in winter season for each sampling site. The highest TVC was noted in Badrinath ghat of Alaknanda river and Gangotri of Bhagirathi river, where the values were as high as 22.2×10^3 and 19.8×10^3, respectively. The lowest value 10.2×10^3 were recorded in Gobind ghat of Alaknanda and 10.2×10^3 in Bhairong-hati of Bhagirathi river, respectively. The total coliform count was high in all water samples (Figure 3), values ranged from 24/100 mL to 310/100 mL. The highest MPN (310/100 mL) was recorded during monsoon at Vasundhara of Alaknanda, the least count MPN (24/100 mL) was obtained in summer and winter season from Bharionghati of Bhagirathi. Even the water samples during less human activities in winter season were not found suitable for drinking as per the BUREAU OF INDIAN STANDARDS (BIS), (1991).

Results for FC and FS counts have also shown a similar trend to TVC and TC, i.e. higher in monsoon season, intermediate in summer season and least during winter season (Figure 4 and 5). Highest FC count was observed in Alaknanda at Badrinath (160.4, 122.3, 101.2)/100 mL and lowest count was at Mana (15.3, 10.2, 9.8)/100 mL during monsoon, summer and winter season, respectively. In Bhagirathi the Chirwasa and Gangotri sites showed almost similar trend of highest count (45.7, 35.4, 29.8) and 45.3, 36.9, 32.1)/100 mL during monsoon, summer and winter seasons, while the least was observed in Bhaironghati (5.9, 4.5, 3.9)/100 mL during monsoon, summer and winter seasons. Similar trend was also observed in FS, the higher count in Alaknanda was at Badrinath (25, 20, 18)/100 mL, lowest at Mana (8, 7, 7)/100 mL, while in Bhagirathi, highest at Harsil (12, 11, 10)/100 mL and least at Chirwasa (6, 3, 3)/100L.

The DO value in Alaknanda ranged from 14.2–18.9 mg/L in monsoon samples and 16.9–23.1 mg/L in winter samples. In Bhagirathi DO values ranged from 10.2–15.4 mg/L in monsoon and 13.2–19.8 mg/L in winter season (Figure 6). Badrinath and Chirwasa showed a remarkable increase in DO in winter season. Though, in general the DO content of all the river water samples show a uniform trend with varying seasons i.e. least during
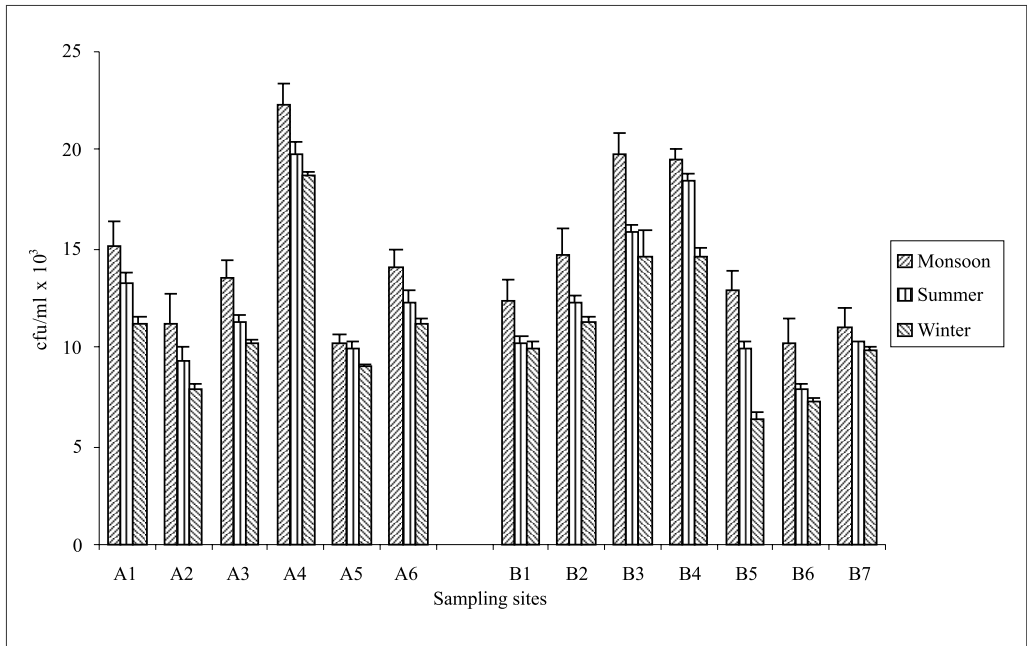
Figure 2. Total viable count (TVC) from Alaknanda and Bhagirathi rivers
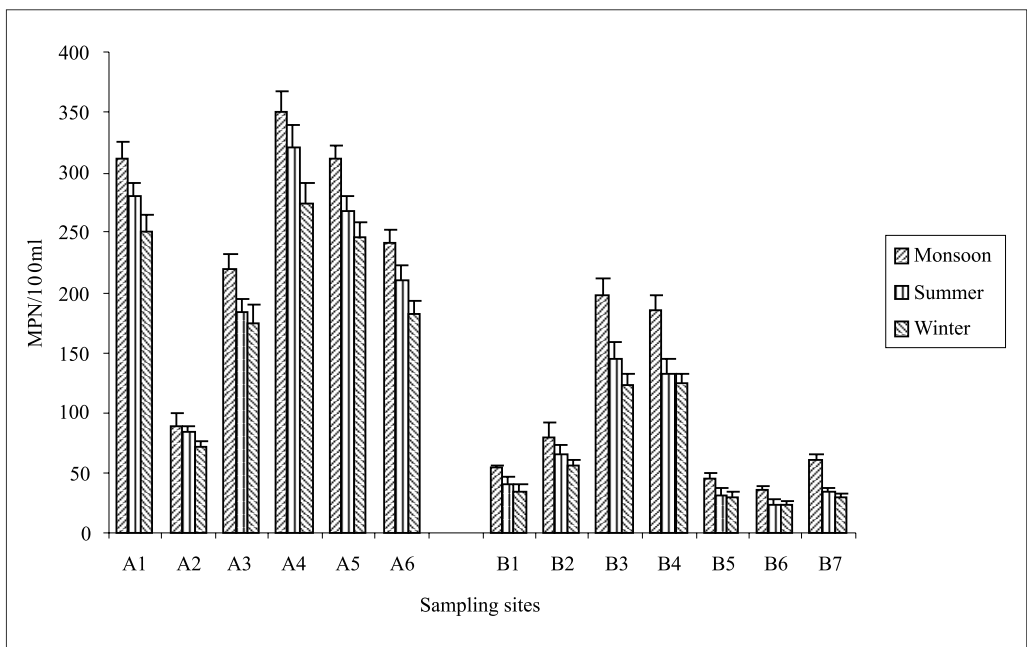
Figure 3. Total coliforms Alaknanda and Bhagirathi rivers
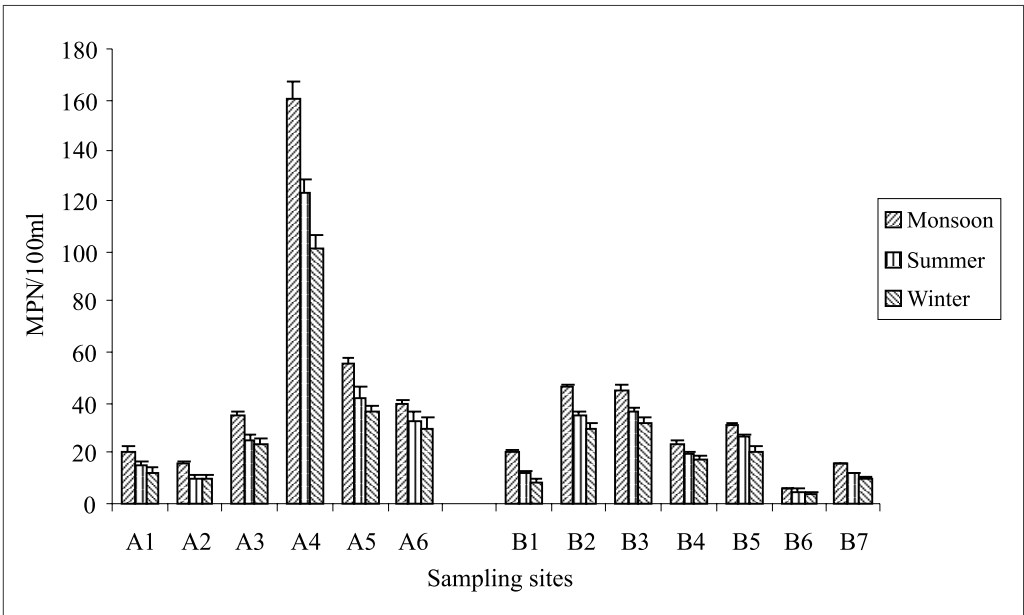
Figure 4. Feacal coliforms count in Alaknanda and Bhagirathi rivers
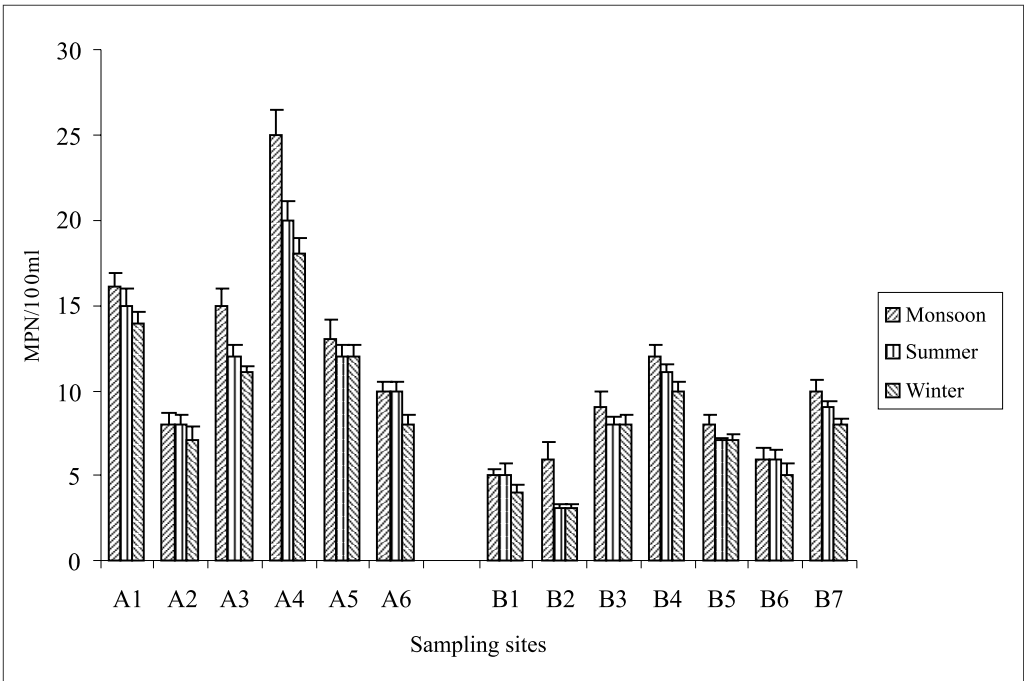
Figure 5. Feacal streptococci from Alaknanda and Bhagirathi rivers

monsoon, highest during winter and intermediate in summer season. However, all the samples were found to be saturated with oxygen and were fit for bathing, wild life and irrigation with respect to the amount of dissolved oxygen. The BOD values for most of the water samples were above the permissible limit (Figure 7), samples in monsoon season have high BOD value, and thus the water was not fit for drinking. Considerably higher COD values were recorded in the monsoon season in all the sites of study area, the COD ranged from 4.5 mg/L to 31 mg/L in all water samples (Figure 8). The effect of season was observed in the pH of water samples throughout this study. The pH was slightly alkaline in winter, but almost neutral in summer and monsoon seasons. Conductivity and TDS in all the sites were found to be well within the minimum prescribed limits (APHA et al, 1999) (data not given).

DISCUSSION

In present study, all sites were found to have high TVC. In fact, the water of Ganga is used for drinking (Aachman) as part of rituals in this region. Although the higher TVC values suggest that this practice should be avoided. Earlier BAGHEL et al, (2005) and SOOD et al., (2008) have also observed high TVC values in the entire stretch of river Ganga in Uttarakhand region. BAGHEL
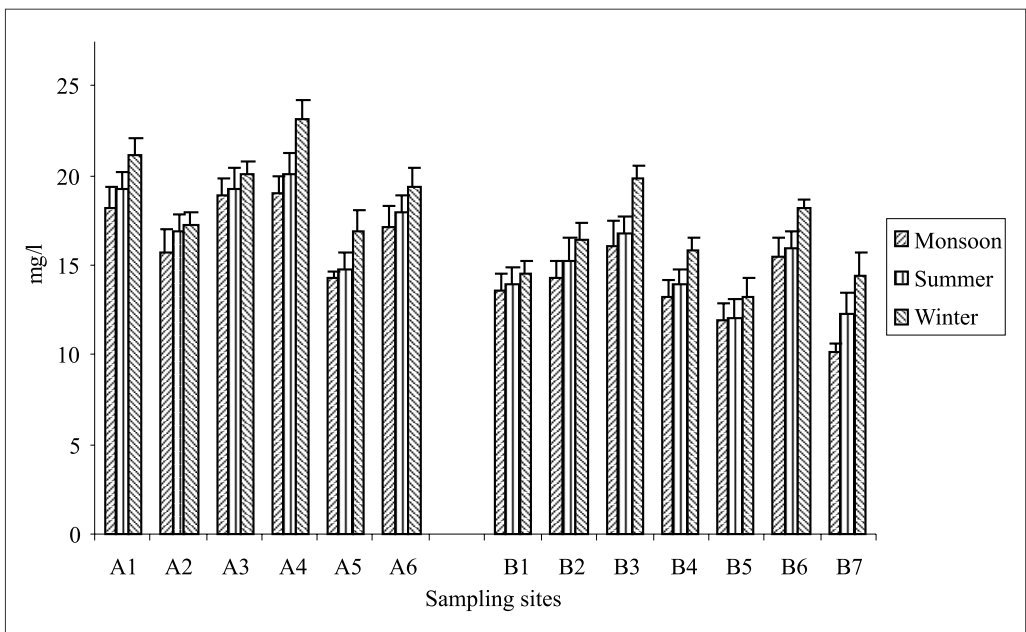
Figure 6. Dissolved oxygen in Alaknanda and Bhagirathi rivers
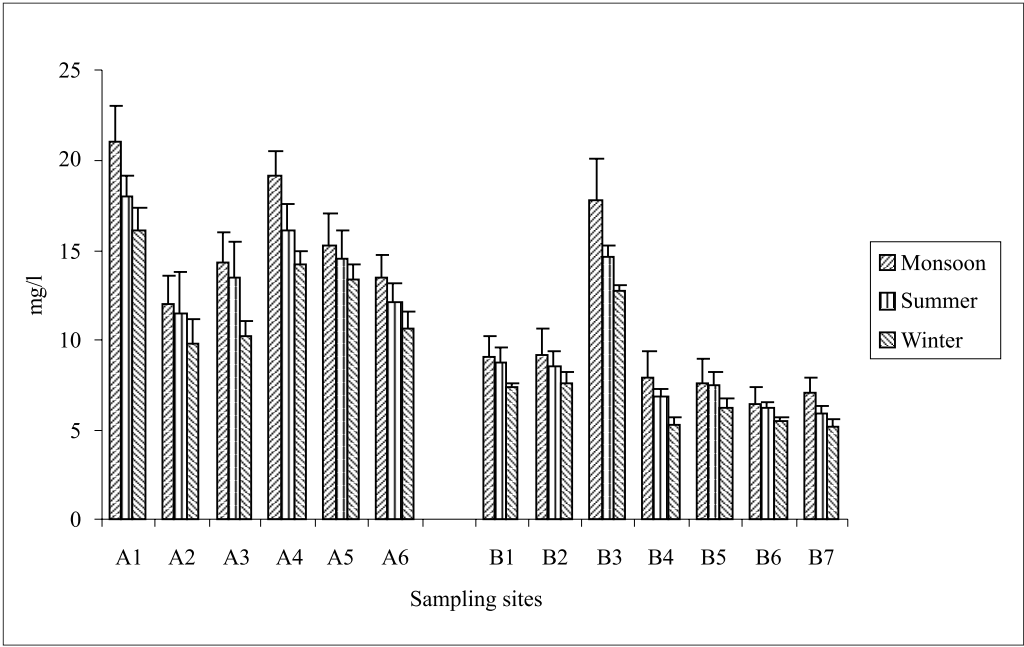
Figure 7. Biological oxygen demand in Alaknanda and Bhagirathi rivers
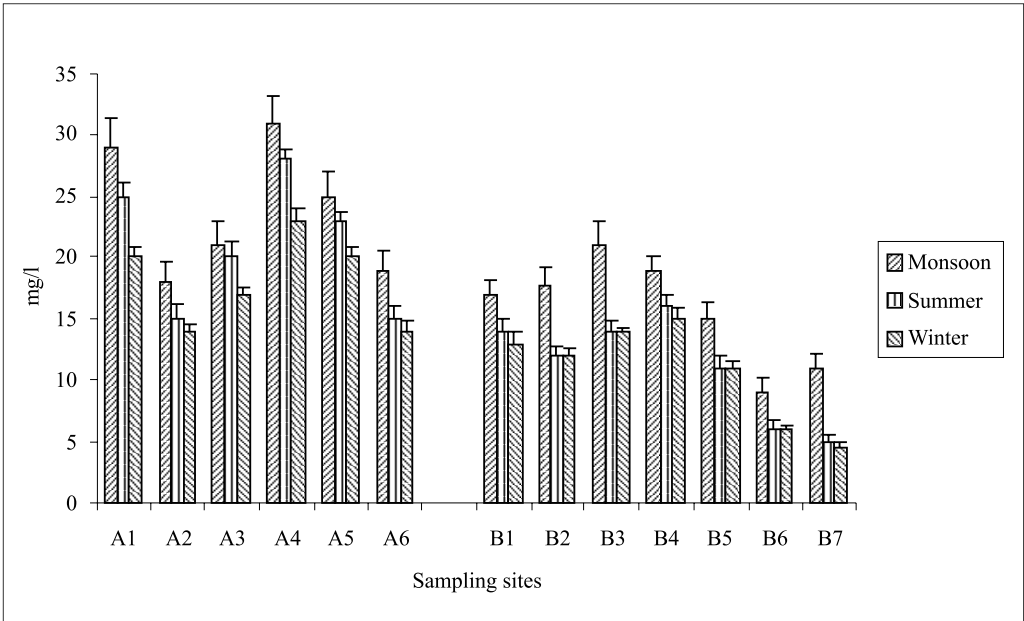
Figure 8. Chemical oxygen demand in Alaknanda and Bhagirathi rivers

et al, (2005) concluded that large number of animals used by natives and pilgrims in upper stretch of Gangetic river system increase FS load.

As a matter of fact, the banks of Alaknanda are more densely populated and face heavy anthropological activity as compared to Bhagirathi. Earlier, FOKMARE & MUSADDIQ (2001) have correlated high content of MPN in surface and ground water of Akola, Maharashtra (India) with the population density. Also the fact that the number of sub-tributaries falling in Alaknanda is more than Bhagirathi may be responsible for the higher coliform count. The less number of FC and FS in most of the sites of study area may be attributed to the fever anthropological activities. All the sites included in this study were found suitable for bathing purpose with respect to the maximum permissible limits of FC and FS counts as per the standards laid by National River Conservation Directorate (NRCD), India.

Earlier, SOOD et al, (2008) have also studied water quality of Ganga in Uttarakhand Himalayas, India and have reported a high level of BOD due to introduction of organic matter into the system as a result of anthropogenic activities. Also these values showed a proportional relation with human activities i.e. the fewer the human activities (in winter), the better the water with respect to physicochemical parameters. Higher BOD values in most of the water samples suggest that either these rivers are rich in organic matter or organic matter is being introduced in the rivers by anthropogenic activities (TIJANI et al, 2005), since, BOD provides a direct measurement of state of pollution. Relationship between BOD, COD and microbial count was found inversely proportional, implying that at high organic loading rates, the ecosystem retards the growth of aerobic microorganisms and favors the growth of anaerobes; our findings draws support from MTUI & NAKAMURS (2006).

The use of coliform bacteria as a measure of the faecal contamination of streams and lakes has been in practice for many years. Our study gives an indication of the extent of relation of microbial pollution and physiochemical parameters; any further addition of wastes may deteriorate the existing hygienic quality in the area. These results suggest that increase of population of coliforms in a river environment are directly proportional to the degree of sewage and human waste pollution, which is reflected by BOD and COD levels. SAH et al. (2000) have stressed on the point that the pollution in rivers and water bodies from industries may adversely affect aquatic life of water bodies' as well human health in the vicinity of rivers/lakes.

In a broad view, the river site with higher catchments area, soil cover and land use are more polluted, owing to more anthropogenic activities. McLellan et al, (2001) stated that faecal pollution indicator organisms can be used to a number of conditions related to the health of aquatic ecosystems and to the potential for health effects among individuals using aquatic environments. The presence of such indicator organisms may provide indication of water-borne problems and is a direct threat to human and animal health. Our studies on microbial ecology and physiochemical analysis in the upper Gangetic tributaries in relation to pollution have clearly revealed that there is significant presence of bacterial indicators of faecal pollution; the situation is serious and alarming. Presence of bacterial indicators of faecal contamination in river water at origin clearly revealed the bacteriological status of the water at that site. For this reason, monitoring of microbial contamination in river should be an essential component of the protection strategy in that area. The base line data generated on bacteriological water quality of rivers may serve as biomonitoring standard and comparisons for other rivers and may be useful for all scientists, decision makers and resource managers working with environmental planning and management of such areas.

Conclusions

The rationale of this study was to evaluate the impact of season and human activities on the pollution status of main upper Gangetic tributaries. This study revealed that tributaries at origin are threatened by high influx of pollutants and enteric pathogenic contamination and it can be concluded that In Alaknanda River, Badrinath is most polluted and Mana is the least, while in Bhagirathi River Gangotri is most polluted and Gaumukh is least. The constant surveillance of these water bodies with respect to the bacterial indicators and physicochemical parameters provides us with the opportunity of true microbiological monitoring of the area as well as proper management actions could be applied in order to improve the quality of these holy rivers and consequently reduce public health risk.

Acknowledgments

REFERENCES

APHA, AWWA, WEF (1998): Standards for Examination of Water and Wastewater, 20th ed. American Public Health Association, Washington DC USA.

BAGHEL, V. S., GOPAL, K., DIWEDI, S. & TRIPATHI, R. D. (2005): Bacterial indicators of faecal contamination of the Gangetic river system right at its source. Ecol. Indicators, Vol. 5, pp 49–56.

BIS (1991): Indian standard specification for drinking water. IS: 10500, Indian Standard Institute.

CAIRNEROSS, S., CARRUTHERS, I., CURTIS, D., FEACHEM, R., BRADLEY, D. & BALDWIN, G. (1980): Evaluation for Village Water Supply Planning. Wiley, Chichester, p. 277.

CRAUN, G. F. (1986): Water Borne Disease in the United States. CRC Press, Boca Raton, FL.

FOKMARE, A. K. & MUSADDIQ, M. (2001): Comparative studies of physico chemical & bacteriological quality of surface & groundwater at Akola (Maharastra). Pollution Res., Vol. 20, No. 4, pp 651–655.

HARWOOD, V. J., BROWNELL, M., PERUSEK, W. & WHITELOCK, J. E (2001): Vancomycin-resistant enterococcus sp. Isolated from waste water and chicken feces in the United States. Appl. & Environ. Microbiol. Vol. 67, pp. 4930–4933.

HODEGKISS, I. J. (1988): Bacteriological monitoring of Hong Kong marine water quality. Environ. Int. Vol. 14, pp. 495–499.

ISLAM, M. S., SIDDIKA, A., KHAN, M. N. H., GOLDAR, M. M., SADIQUE, M. A., KABIR, A. N. M. H., HUQ, A. & COLWELL, R. R. (2001): Microbiological analysis of tube-well water in a rural area of Bangladesh. Appl. & Environ. Microbiol. Vol. 67, pp. 3328–3330.

KISTEMANN, T., CLABEN, T., KOCH, C., DANGENDORF, F., FISCHEDER, R., GEBEL, J., VACATA, V. & EXNER, M. (2002): Microbial load of drinking water reservoir Tributaries during extreme rainfall and runoff. Appl. & Environ. Microbiol. Vol. 68, pp. 2188–2197.

KULSHRESTHA, H. & SHARMA, S. (2006): Impact of mass bathing during Ardhkumbh on water quality status of river Ganga. J. Environ. Biol. Vol. 27, No. 2, 437–440.

McLELLAN, S. L., DANIELS, A. D. & SALMORE, A. K. (2001): Clonal populations of thermotolerant enterobacteriaceaes in recreational water and their potential interference with foecal Escherichia coli counts. Appl. & Environ. Microbiol. Vol. 67, pp. 4934–4938.

MTUI, G. V. S. & NAKAMURS, Y. (2006): Physiochemical and microbiological water quality of lake Sagara in Malagarasi wetlands. J. Eng. & Appl. Sci. Vol. 1, No. 2, pp. 174–180.

OKPOKWASILI, G. C. & AKUJOBI, T. C. (1996): Bacteriological indicators of tropical water quality. Environ. Toxicol. & Water Quality. Vol.11, pp 77–81.

PATHAK, S. P. & GOPAL, K. (2001): Rapid

detection of Escherichia coli as an indicator of faecal pollution in water. Indian J. Microbiol.Vol. 41, pp 139–151.

PIPES,W. O. (1981): Bacterial indicators of pollution. CRC Press Inc., Boca Raton, FL, p. 242.

SAH, J. P., SAH, S. K., ACHARYA P., PANT D. & LANCE V. A. (2000): Assessment of water pollution in the Narayani River, Nepal. Int. J. of Ecol. & Environ. Sci. Vol. 26, pp 235–252.

SHARMA, P., SOOD, A., SHARMA, S., BISHT, S., KUMAR, V., PANDEY, P., GUSAIN, M. P. & GUSAIN, O. P. (2010): Bacterial indicators of faecal pollution and physiochemical assessment of important North Indian lakes. RMZ-Mate. & Geoenviron. Vol. 57, pp 25–40.

SHARMA, S., BAJRACHARYA, R. M., SITAULA, B. K. & MERZ, J. (2005): Water quality in the central Himalaya. Curr. Sci. Vol. 81, pp 774–786.

SOOD, A., SINGH, K. D., PANDEY, P. &

SHARMA, S. (2008): Assessment of bacterial indicators and physicochemical parameters to investigate pollution status of Gangetic river system of Uttarakhand (India). Ecol. Indicators. Vol. 8, 709–717.

SRIVASTAVA, R. K., SINHA, A. K., PANDEY, D. P., SINGH, K. P. & CHANDRA, H. (1996): Water quality of the river Ganga at Phaphamau (Allahabad): Effect of mass bathing during Mahakumbh. Environ. Toxic. Water Quality. Vol. 11, No. 1, pp 1–5.

TIJANI, M. N., BALOGUN, S. A. & ADELEYE, M. A. (2005): Chemical and microbiological assessment of water and bottom-sediments contaminations in Awba lake (U.I), Ibadan, SW-Nigeria. RMZ-Mate. & Geoenviron. Vol. 52, pp. 123–126.

WORLD HEALTH ORGANIZATION (1983): Guidelines for Drinking Water Quality, Vol. 3. World Health Organization, Geneva.

Integrated geophysical and geotechnical investigation of the failed portion of a road in basement complex Terrain, Southwest Nigeria

Povezane geofizikalne in geotehnične preiskave poškodovanega dela ceste na ozemlju metamorfne podlage v Jugozahodni Nigeriji

Osinowo, O. Olawale[1, *], Akanji, A. Olusoji[1], Akinmosin Adewale[2]

[1]University of Ibadan, Department of Geology, Ibadan, Nigeria
[2]University of Lagos, Department of Earth Sciences, Lagos, Nigeria

*Corresponding author. E-mail: wale.osinowo@mail.ui.edu.ng

Abstract: Several efforts by the local authority to fix the bad portions of Ijebu-Ode–Erunwon road, southwest Nigeria have yielded no meaningful result, as the road often get deteriorated shortly after repairs. Geophysical investigation integrated with geotechnical studies were undertaken to determine causes of the consistent failure of the highway. Very Low Frequency Electromagnetic (VLF-EM) and Electrical Resistivity (ER) methods were employed to map sections of the road with anomalous electrical responses and interpreted in-terms of structures, lithology and water saturation.

VLF-EM plots identified positive peaks of filtered real amplitudes greater than 30 % which correspond to major and minor linear fractures within the basement rocks. High current density >30 and low resistivity <10 Ω m delineated rock units underlying the failed pavement to be water saturated. Liquid limit, linear shrinkage and plastic limit index results; 24.0–48.5 %, 2.1–12.9 %, 7.5–27.4 % respectively, indicate excellent to good engineering index properties. However, soaked and unsoaked CBR results; 70.3–83.9 %, and 12.9–31.6 % respectively, indicate percentage reduction in strength with wetness up to 80 %.

Original scientific paper

This study implies that integrated geophysical and geotechnical investigation offers very useful approach for characterizing near surface earth which could be helpful in site preparation prior to construction.

Izvleček: Vrsta poizkusov krajevnih oblasti, da bi popravili slabe odseke ceste Ijebu-Ode–Erunwon v jugozahodni Nigeriji ni bila uspešna, ker se je navadno stanje ceste poslabšalo kmalu nato, ko so jo popravili. Da bi ugotovili vzroke za ponavljajoče se propadanje ceste, so opravili geofizikalne raziskave v povezavi z geotehničnimi študijami. Z zelo nizkofrekvenčno elektromagnetno metodo (VLF-EM) in metodo specifične električne upornosti (ER) so preiskali odseke ceste z anomalnimi električnimi lastnostmi in jih interpretirali z ozirom na zgradbo, litologijo in nasičenost z vodo.

Na diagramih VLF – EM so ugotovili pozitivne vrhove filtriranih realnih amplitud večjih od 30 %, ki ustrezajo večjim in manjšim linearnim razpokam v kamninah podlage. Visoka gostota toka >30 in nizka specifična upornost <10 Ω m sta značilni za zemljine, nasičene z vodo, ki leže pod poškodovanim cestnim površjem. Vrednosti meje tečenja 24.0–48.5 %, meje krčenja 2.1–12.9 % in indeksa meje plastičnosti 7.5–27.4 % nakazujejo od odlične do dobre inženirske indeksne lastnosti. Toda rezultati preskusa CBR v nasičenem in nenasičenem stanju, 70.3–83.9 % in 12.9–31.6 %, kažejo, da se zmanjša nosilnost pri vlagi do 80 %. Raziskava priča o tem, kako uporabno je povezati geofizikalne in geotehnične preiskave za karakterizacijo pripovršinskih tal, kar utegne biti smotrno pri preiskavi terena pred samo gradnjo.

INTRODUCTION

Flexible highway aids easy and smooth vehicular movement, and has been very useful for transportation of people, goods and services from one point to another, especially in developing countries where other means of transportation such as rail, underground tube, air and water transport system have remained largely undeveloped. However, bad portions of road, many of which result from poor construction or being founded on incompetent sub-grade and sub-base materials had been found to do more harm than good. They have been responsible for many fatal accidents, wearing down of vehicles and waste of valuable time during traffic jams. The various types of road failure identified in the study area include failure of the black top surfacing, especially along wheel cracks, pitting or minor dent, shear or massive failure (pot-holes) extending through

the pavement occasionally to the sub-grade. (Plate 1)

The integrity of near surface geophysical investigation methods to complement geotechnical studies in some foundation engineering problems cannot be overemphasized. This research therefore integrates Electromagnetic, Electrical Resistivity and geotechnical techniques to study the causes of consistent failure of Luba–Erunwon axis of Ijebu-Ode–Erunwon road. It involves lateral and vertical probe of the failed, fairly stable, fairly failed and stable portion of the road in order to characterize the near surface geologic materials that constitute the sub-grade, sub-base and the foundation upon which the pavement was founded.

The study area is situated within the southwestern part of Nigeria, it lies between longitudes $6^049'$ N and $6°52'$ N, latitude $3^056'$ E and $3^058'$ E and the studied portion of the pavement is about 2

Plate 1. Failed section of Luba–Erunwon axis of Ijebu-Ode–Erunwon road

km in length. The road was initially constructed in 1983 and have since suffered major failures, especially in the northeastern end, towards Erunwon axis of the road. The road has been repaired severally, the repairs usually include minor repair of the road element and resurfacing. However the northeastern part of the road always starts to deteriorate barely six months after reconstruction.

GEOLOGICAL SETTING

Ijebu-Ode and environ lies within the transitional zone between the Precambrian Basement Complex rocks of the southwestern Nigeria and the Cretaceous sediments of Abeokuta Group in eastern part of Dahomey Basin. The basement rocks occur predominantly in the north, northwest and northeastern parts of the field and it is predominantly a Migmatite Gneiss Complex of biotite granite gneiss, biotite-hornblende gneiss with varying degrees of fracturing (Olayinka and Osinowo, 2009). The southern part of the field is overlain by Ise Member of Abeokuta group that unconformably overlies the basement rocks. Litho-stratigraphically, Abeokuta Group comprise of
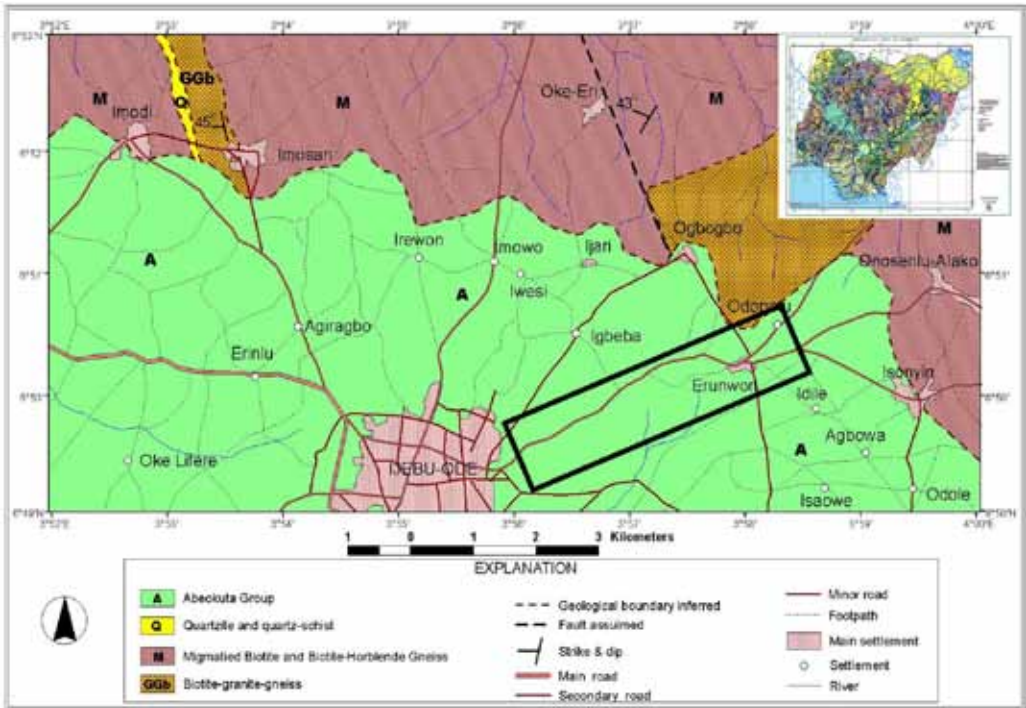
Figure 1. Geological map of Ijebu-Ode and its environ with geological map of Nigeria inserted

grits, arkosic sandstones, siltstones and clay with occasional conglomerate of predominantly arenaceous materials (Omatsola and Adegoke, 1981). Figure 1 shows the geology of Ijebu-Ode and its environ.

MATERIALS AND METHODS

Electromagnetic method is one of the geophysical methods commonly used in foundation investigation and environmental studies (OLORUNFEMI & MESIDA, 1987; SHARMA, 1997). The principle is based on induction of a secondary magnetic field H_s in the subsurface conductor of conductivity σ due to effect of an artificially generated primary field H_p. Electromagnetic measurements are usually presented as the mutual impedance ratio Z/Z_0 or relative charge in the impedance over a conductor which has ability to provide clear information about the subsurface conductivity and structure.

$$Z/Z_0 - 1 = \frac{H_s^z(\omega, \sigma, h, s)}{H_p^z(s)}$$

ABEM WADI was used for VLF-EM measurements, it uses military transmitters as the source of primary electromagnetic waves H_p which is located several kilometers away at the high powered military communication transmission stations. The transmitter's antenna transmits signals continuously at low radio frequency range of 15–30

kHz. The signals generated can travel long distance and able to penetrate the subsurface to induce eddy current in buried conductors. The technique measures the components of Very Low Frequency EM field which are related to the geoelectric structure of the subsurface. (CHOUTEAU et al, 1996). Five VLF-EM profile stations were occupied with the profile length ranging from 250 m to 850 m. Readings were taking at station interval of 3 m and 6 m. Measurements such as raw real, raw imaginary, station's latitude and longitude and the signal strength were recorded against station interval.

Electrical resistivity investigation of the subsurface involved determination of the distribution of ground resistivity based on its response to the flow of electric current injected during surface measurement. True ground resistivity of the subsurface can be estimated and can further be employed to interpret the subsurface qualitatively and quantitatively ((LOKE, 2001). Georesistivity survey involved measurement of potential difference generated by the current electrodes adapted to Wenner and Schlumberger electrode configurations.

$$\rho_a = \Delta V/I \cdot K$$

K is the geometric factor.

Two measurement methods were adopted; 1-D Vertical Electrical Sound-

ing (VES) and 2-D resistivity measurement using Electrical Resistivity Traversing (ERT) technique. The 1D VES measurements aimed at determining the variation in the geoelectric parameters with depth at the probed stations while 2D method mapped resistivity continuity useful to delineate structurally weak zones that could be responsible for continuous failure of the road. Geopulse Tigre resistivity meter was used to measure ground resistance. Current electrodes for 1D measurement were spread from AB/2 of 1 m to 133 m for VES measurement. Two dimensional measurements was made by increasing the electrode spacing along the levels. Ten levels along profiles were covered with electrode spacing range from 3 m to 30 m at incremental step of 3 across 100 m long profile.

Geotechnical studies to determine some engineering index properties of sub-grade and sub-base materials employed to corroborate the geophysical measurements involved collection of twelve disturbed bulk samples from four pits each drilled to depth of 1 m and at sampling depths of 0–0.3 m, 0.3–0.6 m and 0.6–1.0 m from each pit. Sample recovering pits were constructed at the failed, fairly stable, fairly failed and stable parts of the road at 80 m, 247 m, 300 m and 470 m on the road. Mechanical sieving helped determined particle size distribution of gravel and sand proportions of dried coarse fraction. Consistency Limit Tests generally known as the Atterberg limits gave the plasticity characteristics of the cohesive fraction of the sieved samples. The consistency limit test includes; liquid limit, plastic limit and linear shrinkage test. The difference between the liquid and plastic limits gave the plasticity index, which is the range of moisture contents over which the soil remains plastic.

California Bearing Ratio (CBR) test, widely used to characterize and select sub-grade materials for use in road construction was carried out. The test was devised by the California Highway Association and it is simply the ratio of the load that cause a penetration of 2.5 mm or 5.0 mm material to a standard load that causes similar penetration on a standard California sample, notably 13.24 kN and 19.96 kN respectively.

$$C\,B\,R = \frac{\text{Load that caused a penetration of 2.5/5.0 mm} \times 100\,\%}{13.24/19.96\,(kN)}$$

Both soaked and unsoaked CBR tests were carried out and swelling of samples was carefully monitored during the 96 h of soaking period to assess the likely effect of water ingress on the swelling of base material. The samples were compacted at the modified AASHTO level as described under procedure for compaction test in a standard *CBR* mold.

Data processing

The obtained raw real (in-phase) and raw imaginary (quadrature) components contain valuable diagnostic information of the subsurface but in a complex pattern that cannot directly and easily be related to the causative body. They contain noise, the raw real/imaginary data are also often wrongly located on the source along the profile. To correct the above effects and obtain profiles or pseudo-section/images that are easy to interpret, two different data processing techniques were applied. Fraser (1969) and Karous & Hjelt (1977, 1983) filtering operators. Fraser filter is a linear high-frequency band-pass filter that yields semi-quantitative interpretation of data. It transforms the in-phase components into contourable data with noise reduced to the best possible minimum. VLFPROS MATLAB code for processing VLF-EM data developed by Sundararajan et al. (2006) was employed to carry out both the Fraser and the Karous and Hjelt filtering operations.

Electrical resistivity data processing involved cleaning the data to remove spurious readings. Resultant VES data were plotted on bi-log paper and partial curve matched using standard two layer curves and auxiliary curves; Cagniard graph (Koefoed, 1979), to obtain some geoelectrical parameters such as layer depth/thickness and layer resistivity values (Orellana & Mooney, 1966). The obtained geoelectrical parameters from partial curve matching were used as initial model parameters to interpret the geoelectrical sounding curves using inversion model software RESIST (Vander Velpen, 1988) and WinG-Link. The inversion algorithm involves the calculation of curves for observed data by convolving the resistivity transform with appropriate filter coefficient, (Ghosh, 1971 and O'Neill, 1975). The inversion algorithm filters spurious data, enhance signal as well as correct depth matched for obtained geoelectric layers.

Data Quality Check (QC) was carried out on the obtained ERT data for spurious data. The resultant data were inverted using the DIPRO inversion software based on the inversion principle presented by Yi & Kim, (1988). The software is a $2\frac{1}{2}$ dimensional inversion subroutine designed based on the Least Square inversion algorithm and uses two different modeling and smoothening approaches. The FDM Inversion performs smoothness constrained least square inversions based on the finite difference modeling assuming flat topography, while the FEM performs smoothness constrained least square inversion based on finite element modeling. The software automatically determines a two dimensional resistivity model of the subsurface for the obtained data. A forward modeling

subroutine is applied to calculate theoretical apparent resistivity values and a non-linear least squares optimisation techniques was used for the inversion subroutine, (DeGroot-Hedlin & Constable, 1990 and Sasaki, 1989).

Results

Palacky et al. (1981), De Rooy et al. (1986), Hazell et al. (1988) and other authors have shown the relevance of EM method to be in overburden thickness estimation and basement fracture delineation. Figures 2 (a–f) present the VLF-EM plot of raw real and filtered real components against the profile distance in meters. Two basic anomaly types were identified using characteristic feature curves of coincident inflections on real component anomaly curves as well as the amplitude of the filtered real anomaly. The sign 'F' indicates point with positive peak filtered real anomaly with amplitude ranging between 30–60 %. It characterizes regions or points along the profile with major linear displacement at depth <5 m which may represent a fractured or sheared zone. The sign 'f' indicates positive filtered real anomaly of amplitude <30 % and characterizes zones or points with loose materials at depth <5 m.

Five major linear features F_1–F_5 were delineated at 87 m, 178 m, 298 m, 657 m and 810 m of the profile. Features F_1,

F_2 and F_5 were identified at the failed portion while features F_4 and F_3 were found at the fairly failed part of the road respectively. This shows that 60 % of the identified major features underlie the intensely failed portion while 40 % underlies fairly failed portion. Also, features f_1–f_8 were detected around locations 203 m, 330 m, 410 m, 482 m, 553 m, 578 m, 848 m, 1040 m of the profile length.

Figure 3 is the current density plot along profile 1 which traversed the failed, fairly stable and stable portions of the road from NE-SW. The profile indicates relatively high conductive zone as evident by high current density (up to 30) close to the surface in the north-eastern end and central part of the profile. These zones coincide with the failed portion of the road, it also coincides with the highly fractured part. The high conductivity is likely due to high water filled fractures in the basement rock. Similarly, low resistivity section at the north-eastern end of the road (high conductivity) was identified on the 2-D inverted section obtained from the ERT profile (Figure 4) and resistivity section (Figure 5) constructed from VES data around the study area. The stable portion has a relatively thick and dry sandy unit upon which the pavement rests directly. Vertical Electrical Soundings (VES) identified three to four layered earth interpreted as top soil, loose saturated clayey sand unit and highly saturated fractured basement at the failed section of the road. Figure

6 (a and b) present the representative curves and interpreted log of VES data around the stable and failed portion of the road.
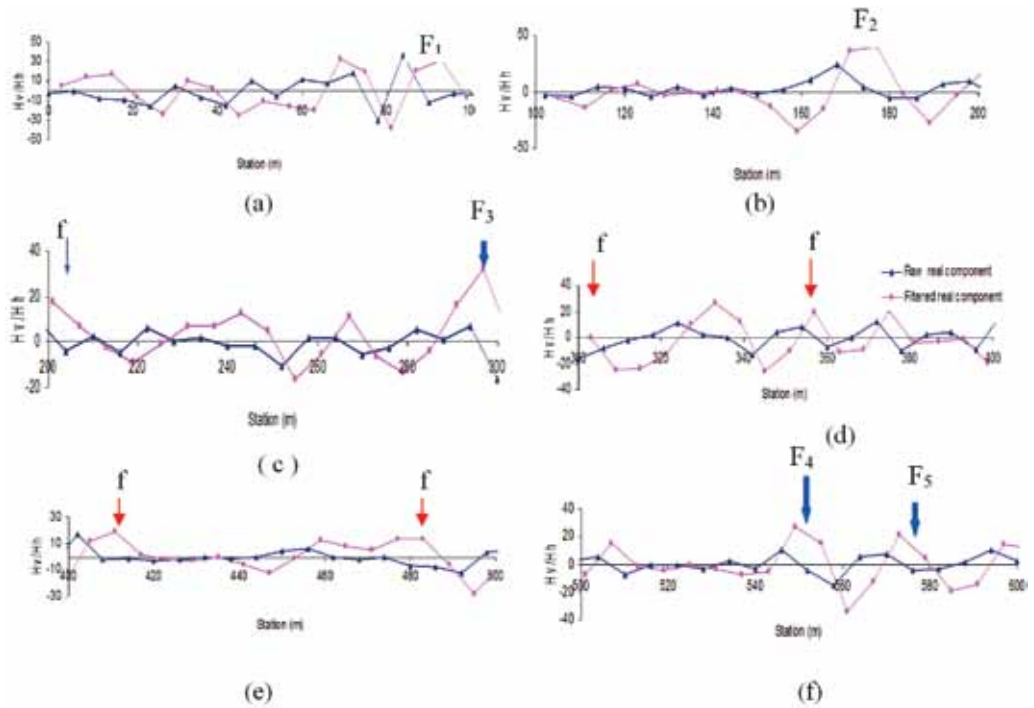
Figure 2. VLF – EM Curve of Raw real and Filtered real Components.
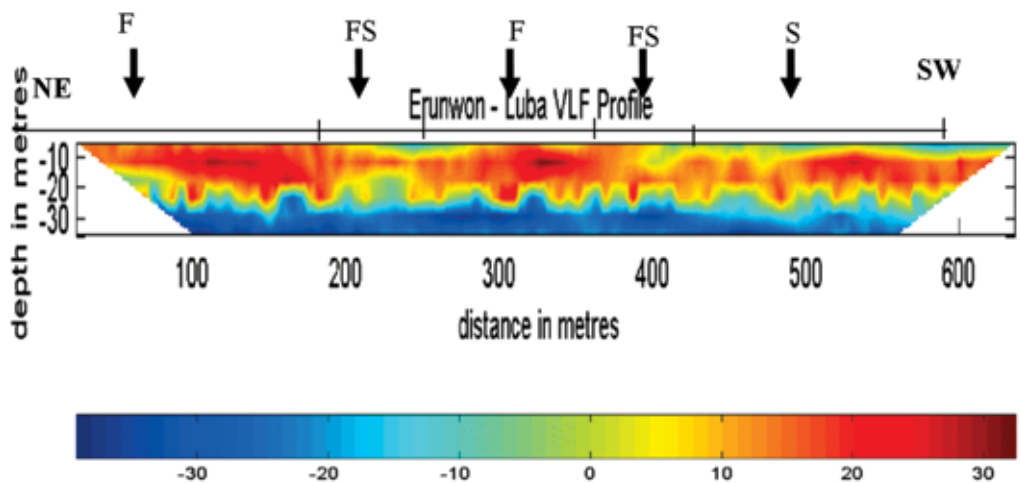
Figure 3. Current density plot along VLF – EM Profile 1 (F = Failed, S = Stable, FS = Fairly Stable)
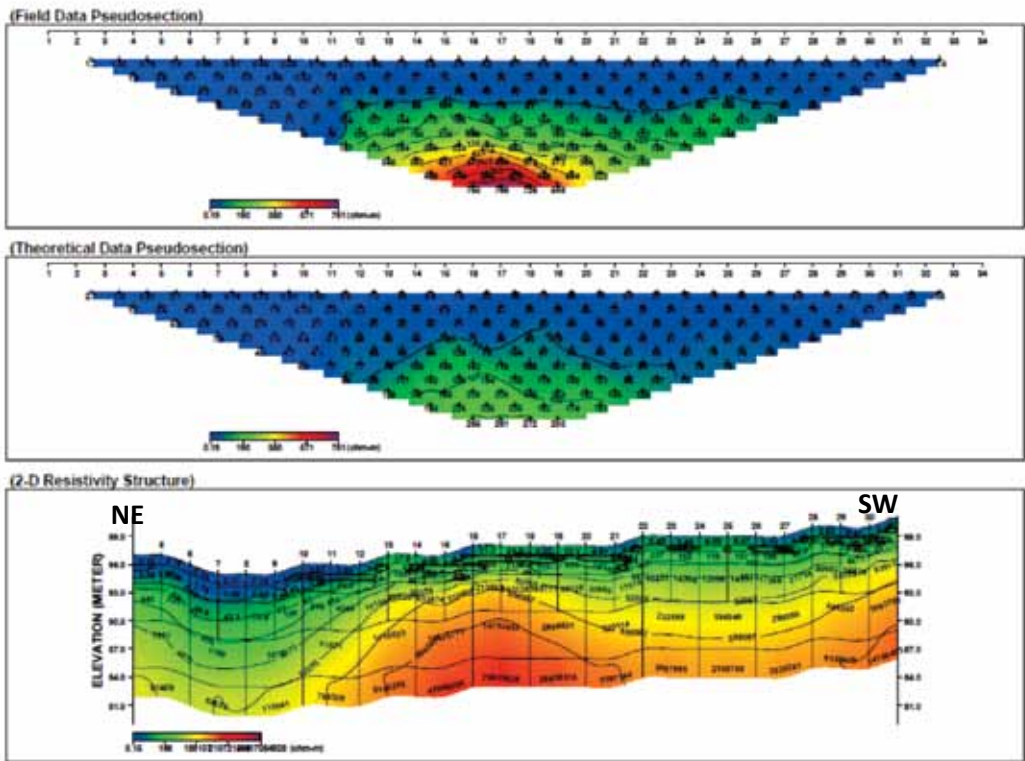
Figure 4. Field data pseudo section, theoretical pseudo section and ERT sections along Ijebu-Ode–Erunwon road.
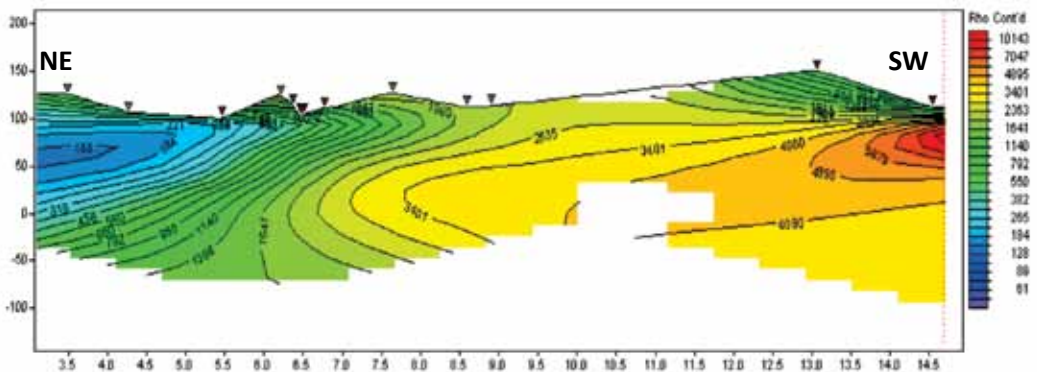
Figure 5. Inverted Electrical Resistivity section from VES data around the study area.

VES 31				
Layers	1	2	3	4
Resistivity (Ω m)	311	77.1	808	2813
Depth (m)	0.45	1.1	18.9	-
Interpretation	Top soil	Sandy clay	Unsaturated sand	Fresh basement rock
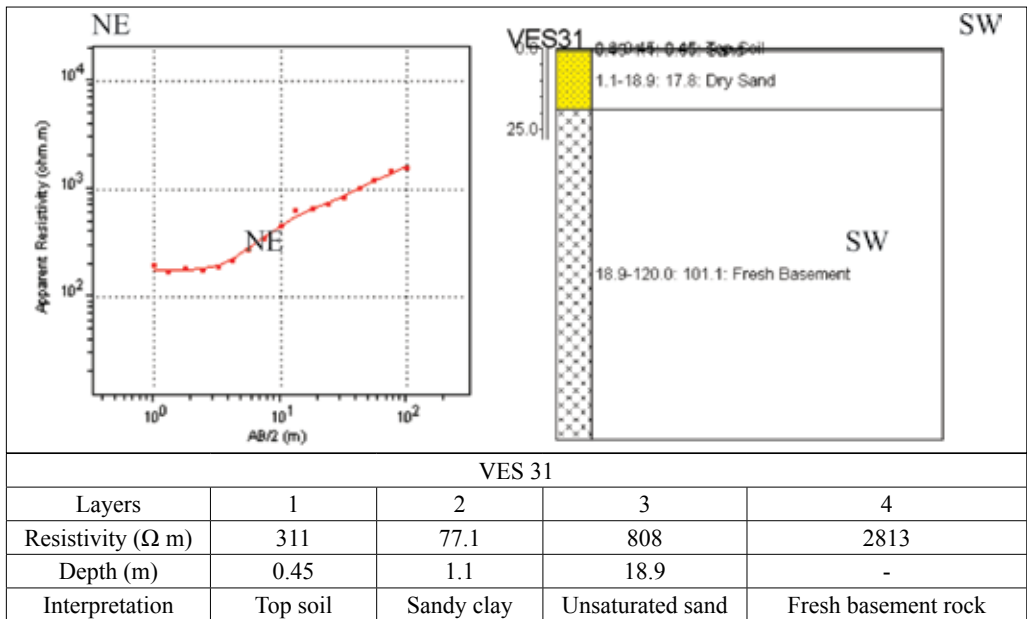
Figure 6a. Representative VES curve and interpreted log around stable part of the Ijebu-Ode–Erunwon road

VES 25					
Layers	1	2	3	4	5
Resistivity (Ω m)	516	283	4144		
Depth (m)	1.57	16.1	-		
Interpretation	Top soil	Fractured basement rock	Fresh basement rock		
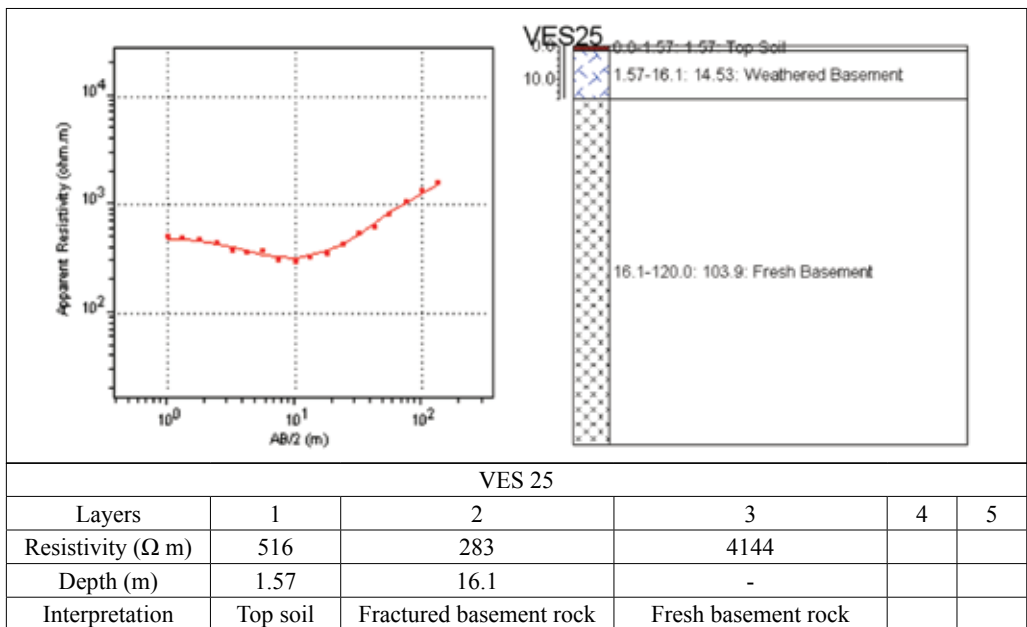
Figure 6b. Representative VES curve and interpreted log around failed part of the Ijebu-Ode–Erunwon road

Results of Geotechnical analysis

Geotechnical investigation of the highway is aimed at ascertaining geotechnical bases for the road failure. Table 1 presents a description of the recovered samples.

Grain size distribution

Table 2 presents the summary of the grain size distribution. Samples 2C, 3B, 3C, 4B and 4C have higher fines constituent than other samples. The percentage of fines ranges from 22–26 %, 23–45 %, 21–37 % and 24–46 % for samples from failed, fairly stable, fairly failed and stable parts of the road respectively. The result indicates that the soil units below the stable parts of the road exhibit better engineering properties than those of the failed, fairly failed and fairly stable portions.

Table 1. Soil profiles in the study area

Depth Range (m)	Road condition	Pit No	Sample code	Colour	Name
0-03		1	1A	Brown	Clayey sand
0.3-0.6	Failed	1	1B	Brown	Clayey sand
0.6-1.0		1	1C	Very brown	Clayey sand
0.0-3		2	2A	Brown	Clayey sand
0.3-0.6	Fairly stable	2	2B	Brown	Sandy clay
0.6-1		2	2C	Reddish brown	Sandy clay
0-0.3		3	3A	Brown	Sandy clay
0.3-0.6	Fairly failed	3	3B	Reddish brown	Silty clay
0.6-1		3	3C	Reddish brown	Silty clay
0-0.3		4	4B	Reddish brown	Silty clay
0.3-0.6	Stable	4	4B	Reddish brown	Silty clay
0.6-1		4	4C	Reddish brown	Silty clay

Table 2. Grain size distribution of the studied soil samples

Sample	Depth (m)	Medium Gravel/%	Fine Gravel %	Coarse Sand/%	Medium Sand/%	Fine Sand %	Fines (Clay and Silt)/%
1A	0–0.3	7.0	7.0	19.0	27.0	14.0	26.0
1B	0.3–0.6	2.0	4.0	20.0	37.0	14.0	23.0
1C	0.6–1.0	1.0	1.5	17.5	38.0	20.0	22.0
2A	0–0.3	0.1	0.1	16.9	42.0	17.0	23.9
2B	0.3–0.6	0.1	0.1	20.8	45.0	13.0	21.0
2C	0.6–1.0	0	0	12.5	40.0	10.5	37.0
3A	0–0.3	3.0	2.0	19.5	39.5	13.0	23.0
3B	0.3–0.6	0.1	1.9	16.0	33.5	10.5	37.0
3C	0.6–1.0	0	0.1	15.9	30.5	8.5	45.0
4A	0–0.3	2.0	1.5	17.5	41.5	13.5	24.0
4B	0.3–0.6	0	0	21.0	27.0	14.5	37.5
4C	0.6–1.0	0	0	15.0	29.5	9.5	46.0

Table 3. Atterberg Limit result of the clay fraction of the recovered samples

Sample	Depth (m)	Road Condition	Liquid Limit (%)	Plastic limit (%)	Plasticity Index	Linear Shrinkage
1A	0–0.3		27.0	15.6	11.4	6.4
1B	0.3–0.6	Failed	26.8	15.0	11.3	7.8
1C	0.6–1.0		24.0	14.7	9.3	6.4
2A	0–0.3		24.0	16.1	7.9	2.1
2B	0.3–0.6	F a i r l y Stable	26.0	18.5	7.5	5.7
2C	0.6–1.0		50.0	29.4	20.6	12.9
3A	0–0.3		24.0	13.7	10.3	2.1
3B	0.3–0.6	F a i r l y Failed	48.5	21.1	27.4	9.3
3C	0.6–1.0		56.0	26.2	29.8	12.1
4A	0–0.3		26.0	13.1	12.9	2.1
4B	0.3–0.6	Stable	36.0	17.7	18.3	8.6
4C	0.6–1.0		51.0	25.3	25.7	10.4

According to the American Association of State Highway and Transportation Official (AASHTO) classification system, samples from failed portions, samples 1A,1B and 1C fell into A-2-6, A-2-6 and A-2-4 groups which are excellent to good materials for sub-grade soil in rating, while samples 3A, 3B and 3C of the fairly failed portions fell into A-2-4, A-7-6, and A-7-6 groups which corresponds to excellent to good and fair to poor soils respectively for sub-grade material. Also, samples 4A, 4B and 4C of the stable portion of the road fell into A-2-6, A-6 and A-4 groups which corresponds to excellent to good and fair to poor soils respectively. Samples 2A, 2B and 2C fell into A-2-4, A-2-4 and A-7-6 groups and also correspond to excellent to good and fair to good soils respectively for sub-grade materials.

Table 3 presents the plastic limit test results, the range and mean values range from 14.7–15.6 % and 15.1 %; 13.7–26.2 % and 20.3 %; 16.1–29.4 % and 21.3 % and 13.1–25.3 % and 18.7 % at the failed, fairly failed, fairly stable and stable portions respectively. The respective plasticity indexes which is the difference between the liquid limits and plastic limits range and mean of 9.3–11.4 % and 10.7 % respectively for failed portion, 10.3–29.8 % and 22.5 % respectively for fairly failed portion, 7.5–20.6 % and 12.0 % respectively for fairly stable portion and 12.9–25.7 % and 19.0 % respectively for stable portion.

Linear Shrinkage

The linear shrinkage at the failed, fairly failed, fairly stable and stable portions have range and mean of 6.4–7.8 % and 6.9 %; 2.1–12.1 % and

7.8 %; 2.1–12.9 % and 6.9 %, and 2.1–10.7 % and 7.1 % respectively. MADEDOR (1983) and ADEYEMI (1992) gave the maximum value of 8 % as linear Shrinkage for highway sub-base materials and maximum of 10 % was specified for sub-grade materials. It can therefore be concluded that at the failed portions the liquid limits, plasticity index and linear shrinkage for samples 1A, 1B and 1C satisfied all the required standards for highway sub-base and while at the fairly failed portion sample 3A satisfied all the require standards for sub-base materials, but samples 3B and BC failed the requirements for sub-grade material. At the stable portions, samples 4A and 4B satisfied the required standard by FMWH (2000) for sub-base and sub-grade soils respectively while samples 4C has slightly higher liquid and plasticity index. At the fairly stable portion, samples 2A and 2B also satisfied the requirements for sub-base and sub-grade materials for highways but samples 2C has slightly higher liquid and linear shrinkage values.

From the Casagrande chart (Figure 7), the classification of the soil samples 1A, 1B, 1C, 3A, 2A, 2B and 4A plotted within the region of low plasticity while samples 2C, 3B, and 4B, 4C plotted within
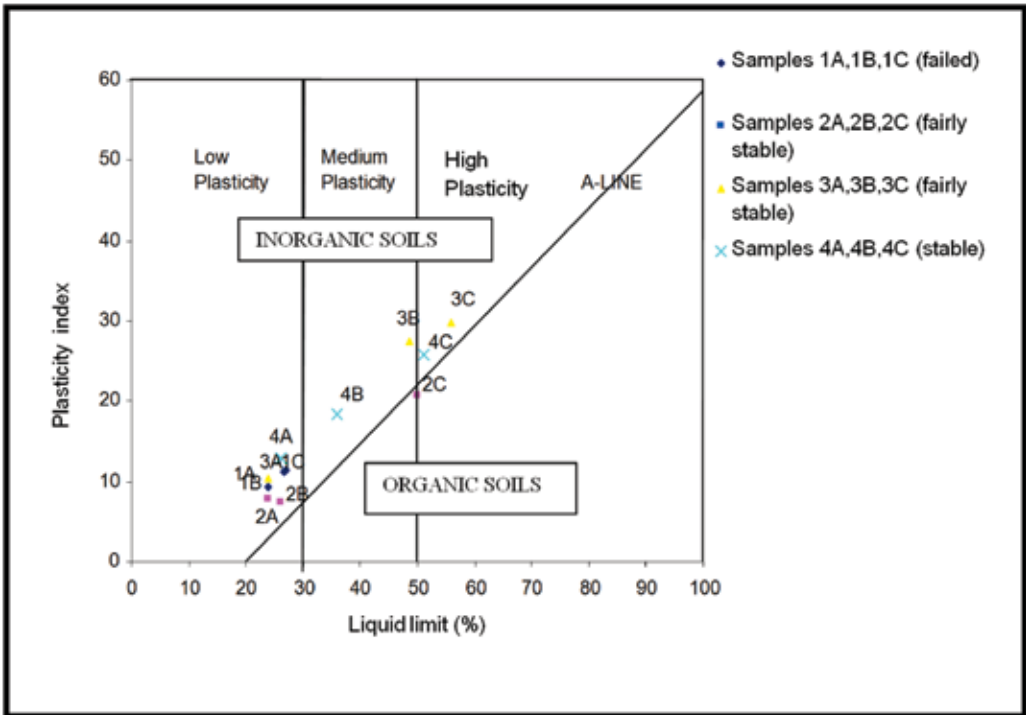
Figure 7. Casagrande Chart Classification of studied samples

region of medium plasticity. Sample 3C plotted completely within region of high plasticity. The result indicates that samples 1A, 1B and1C (of failed portion) 2A, 2B (of fairly stable portion), 3A (of fairly failed portion) 4A, 4B and 4C (of the stable portion) are good sub-base and sub-grade materials while samples 3C of fairly failed portion is unsuitable for sub-grade material.

California Bearing Ratio Strength
The dry density of the soils and optimum moisture content of the soils compacted at the modified AASHTO is shown in the Table 4. It shows percentage reduction in strength as a result of soaking of the compacted samples and it ranges between 55–83 %. Figures 8 (a–e) present the unsoaked and soaked *CBR* curves of the studied samples. Most of the analyzed samples have the required 80 % unsoaked *CBR* value recommended for highway sub-base and sub-grade soils by the FMWH (2000) but only sample 1B satisfied the required unsoaked *CBR* value of 30 %.

Table 4. Maximum dry density and optimum moisture content of the samples compacted at the modified AASHTO level.

Sample	Depth (m)	Road condition	Maximum dry density (kg/m)	Optimum moisture content (%)
1B	0.3–0.6	Failed	1970	10.95
1C	0.6–1.0		1910	10.6
3B	0.3–0.6	Fairly failed	1730	12.4
4B	0.3–0.6	Stable	1830	12.0
4C	0.6–1.0		1780	14.0

Table 5. CBR result

Sample	unsoaked *CBR* (%)	Soaked *CBR* (%)	Percentage Reduction in strength (%)
1B	71.3	31.6	55.68022
1C	83.9	15.3	81.764
3B	76.7	12.9	83.18123
4B	70.3	19	72.97297
4C	77.6	17	78.09278
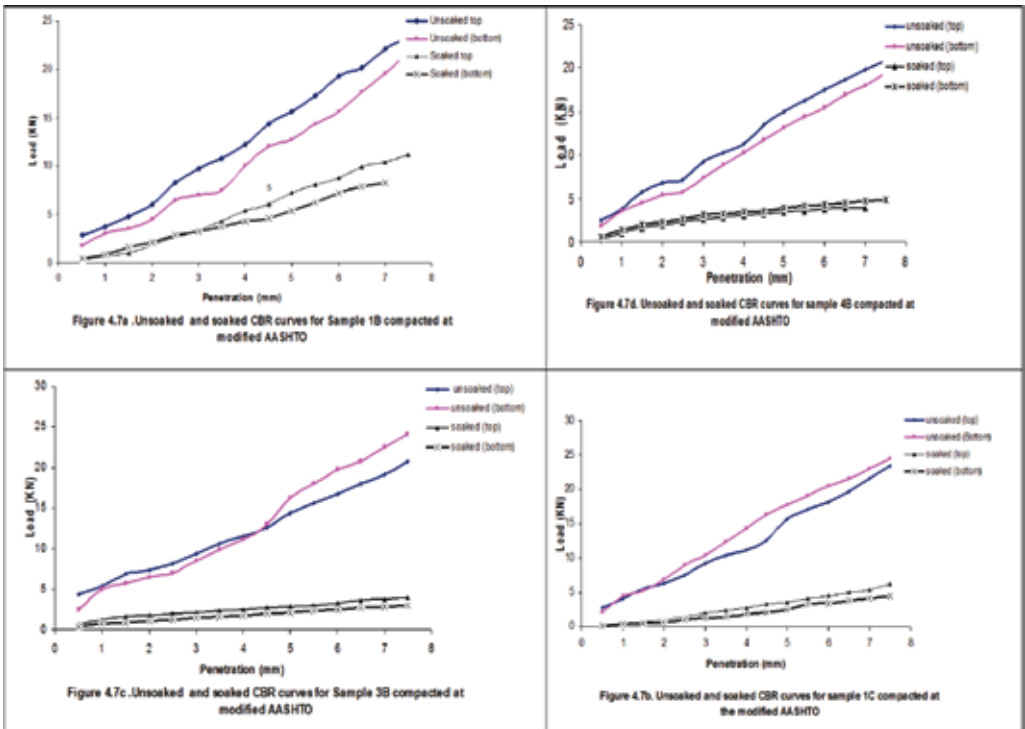
Figure 8. California bearing ratio of the studied soils compacted at the optimum moisture content of the modified AASHTO

Discussion

The geophysical investigation results gave horizontal variation in conductivity of the subsurface materials underlying the flexible highway pavement at different portions in view of ascertaining geophysical bases if any for the causes of the highway failure. The interpretation of the plots of real and filtered real curves of the geophysical survey showed that majority of the identified major and minor linear features which represent zones of anoma-

lously high conductivity were detected at the intensely failed portions of the road. These features are suspected to be numerous fractures in the underlying basement rocks and hence, conductive discontinuity in the shallow overburden.

The geotechnical analysis of the twelve bulk soil samples collected at different portions of the highway helped determined the variation in engineering index properties of the sub-base and sub-grade soils. Geotechnical results revealed that the sub-base

and sub-grade soils in the depth range of 0-1.0m of the failed portions satisfied all the requirements of liquid limits, plasticity index, linear shrinkage, grain size distribution characteristics specified by the Federal Ministry of Works and Housing. These soils also plot within the region of low plasticity on Casagrande chart classification and under AASHTO classification into groups A-2-6, A-2-6 and A-2-4 which indicate that the soils are excellent to good materials for subgrade soils.

In terms of shear strength most of the analyzed samples have adequate values of unsoaked *CBR*. However, they suffered very high reduction in shear strength of up to 80 % in soaked condition. The numerous major and minor linear fractures mapped in the shallow basement as delineated by VLF – EM methods have tendency to increased the permeability of the portion and thus cause the it to be highly saturated. This is evident in high current density and low resistivity values associated with the failed region. This has particularly made the excellent to good sub-base and sub-grade materials to perpetually remain in soaked condition. The geotechnical implication of this is that the highway pavement is resting on sub-grade, sub-base and foundation materials that lost as high as 80 % of shear strength as a result of ingress of water.

Conclusion

Both geophysical and geotechnical investigation methods have been used to characterize different portions of the flexible highway in the study area. The highway was reported to always fail barely six months after reconstruction. Geophysical investigation delineated numerous anomalously high current density and low resistivity zones as well as identified some major and minor linear fractures in the shallow underlying basement rocks. Also, the geotechnical investigations although showed that the samples collected generally displayed excellent to good engineering index properties as sub-base and sub-grade materials, but suffers up to 80 % reduction in strength with wetness. The interaction of the sub-grade and sub-base soils with water from numerous fractures in the basement rocks has greatly reduced shear strengths and therefore incessant failure of the overlying pavement.

Removal and replacement of the sub-grade and sub-base materials upon which the flexible pavement rests (up to 1 m) or soil stabilization / treatment that would improve materials shear strength under wet condition is suggested as well as construction of proper drainage system to drain the whole length of the road. This will address consistent highway pavement failure associated with Erunwon – Ijebu-Ode road.

References

Adeyemi, G. O. (1992): Highway geotechnical properties of lateritized residual soils in the Ajebo-Ishara geological transition zone of southwestern Nigeria. Ph. D thesis. Obafemi Awolowo University, Ile-Ife, Nigeria. 357 pp.

American Association of State Highways and Transport Officials, Mi145. Classification of Soil and aggregate mixtures of highway for construction purpose, highway materials, Vol. 1.1.

Chouteau, M., Zhang, P., Chapellier, D. (1996): Computation of apparent resistivity profiles from VLF-EM data using linear filter. *Geophysical Prospecting,* Vol. 44, pp. 215–212.

DeGroot-Hedlin, C. & Constable, S. C. (1990): Occam's inversion to generate smooth, two-dimensional models from magnetotelluric data. *Geophysics,* Vol. 55, pp. 1613–1624.

De Rooy, C., Kamful, M., Kolawole, L. L. & Olokun, A. (1986): Use of the Eletromagnetic method for Groundwater Prospecting in Nigeria. Paper presented at ate First Annual Symposium of Training Workshop on Groundwater Resources in Nigeria. 23rd–25th July 1986, Lagos, Nigeria.

DIPROTM Version 4.01 (2001): Processing and interpretation software for electrical resistivity data. Korea Institute of Geoscience and Mineral Resources (KIGAM), Dae-jeon, South Korea.

Federal Ministry of Works and Housing (2000): Specification for roads and bridges, Vol. 2, pp. 137–275.

Fraser, D. C. (1969): Contouring of VLF-EM data. *Geophysics,* Vol. 34, pp. 958–967.

Ghosh, D. P. (1971): Inverse filter coefficients for the computation of the apparent resistivity standard curves for horizontally stratified earth. *Geophysical Prospecting,* Vol. 19, pp. 769–775.

Hazell, J. R. T., Gratchley, C. R. & Presion, A. M. (1988): The location of aquifers in crystalline rocks and Alluvium in Northern Nigeria using combined Electromagnetic and Resistivity Techniques. *Quarterly Journal of Engineering Geology*, Vol. 21, pp. 159–175.

Karous, M. R., & Hjelt, S. E. (1983): Linear filtering of VLF dip-angle measurements. *Geophysical Prospecting*, Vol. 31, pp. 782–794.

Karous, M. R. & Hjelt, S. E. (1977): Determination of apparent current density from VLF measurements: Report. Department of Geophysics, University of Oulu, Finland, Contribution, Vol. 89, 19 pp.

Koefoed, O. (1979): *Geosounding Principles 1* Resistivity Sounding Measurements, Elsevier, Amsterdam.

Loke, M. H. (2001): Topographic modelling in resistivity imaging inversion. 62nd EAGE, Conference & Technical Exhibition Extended Abstracts, D-2.

Madedor, A. A. (1983): Pavement design guidelines and practise for differ-

ent geological areas in Nigeria. In Ola, S. A. (Eds): Tropical soils of Nigeria in engineering practise, A. A. Balkema (publishers) Rotterdam, Netherland, pp. 291–298.

OLORUNFEMI, M. O. & MESIDA, E. A. (1987): Engineering geophysics and its application in engineering site investigation – case study from Ile-Ife area. The Nigerian Engineer, Vol. 22, pp. 57–66.

OMATSOLA, M. E. & ADEGOKE, O. S. (1981): Tectonic evolution and stratigraphy of Dahomey basin. Jour. Min. Geol., Vol. 18, pp. 130–137.

O'NEILL, D. J. & MERRICK, N. P. (1984): A digital linear filter for resistivity sounding with generalized electrode array. *Geophys. Prospect.*, Vol. 32, pp. 105–123.

ORELLANA, E. & MOONEY, H. M. (1966): Master Tables and Curves for Vertical Electrical Sounding over Layered Structures. Interientia, Madrid, Spain.

OLAYINKA, A. I. & OSINOWO, O. O. (2009): Integrated geophysical and satellite imagery mapping for groundwater assessment in a geological transition zone in south-western Nigeria. *SAGEEP*, Vol. 22, pp. 977–987.

PALACKY, G. J., RITSEMA, I. L. & DE JONG. S. J. (1981): Electromagnetic prospecting for Groundwater in Precambrian terrains in the Republic of Upper Volta. *Geophysical Prospecting*, Vol. 29, 932–955.

SASAKI, Y. (1989): Two-dimensional joint inversion of magnetotelluric and dipole-dipole resistivity data. *Geophysics*, Vol. 54, pp. 254–262.

SHARMA, P. V. (1997): Environmental and Engineering Geophysics, Cambridge University press, 173 pp.

SUNDARARAJAN, N., RAMESHBABU, V., PRASAD, N. S. & SRINIVAS, Y. (2006): VLFPROS- A MATLAB code for processing of VLF-EM data. *Computers & Geosciences,* Vol. 32, pp. 1806–1813.

YI, M. J. & KIM, J. H. (1998): Enhancing the resolving power of the least squres inversion with Active Constraint Balancing, SEG Expanded Abstracts, 68 Annual Meeting, New Orleans, pp. 485–488.

Sequence stratigraphic framework of K-field in part of Western Niger delta, Nigeria

Sekvenčna stratigrafija naftnega polja K v zahodnem delu delte reke Niger, Nigerija

M. E. Nton[1,*] & Tope Shade Ogungbemi[1]

[1]University of Ibadan, Department of Geology, Ibadan, Nigeria

*Corresponding author. E-mail: ntonme@yahoo.com

Abstract: A sequence stratigraphic approach was applied to K-Field, within the western Niger Delta by integrating wireline logs of four wells; 001,003, 004 and 005; and high resolution biostratigraphic data of wells 001, 004 and well 005. The study is aimed at deducing key bounding surfaces, depositional sequences and their corresponding systems tracts as well as the palaeodepositional environment of the hydrocarbon bearing Agbada Formation in the study area.

Two sequence boundaries at 8900 ft (2697 m) and 9050 ft (2742 m), and one maximum flooding surface at a depth of 7650 ft (2318 m) were recognized in well 5 and used to subdivide the stratigraphic succession into depositional sequences and their corresponding systems tracts. Highstand and Transgressive systems tracts were recognized in each of the three depositional sequences. Marker shale, characterized by *Chloguebelina* 3 (16.0 Ma) was used to date the key bounding surfaces with the aid of the Niger Delta chronostratigraphic chart as Early to Late Miocene. The Highstand systems tracts are characterized by shale-rich upward coarsening sands, having poor reservoir quality while the lowstand systems tracts are characterized by thick sandstone units, indicating good quality seals to reservoirs. From the SP logs motifs, the depositional environments inferred include tidal channel, shoreface and shelf environments which typify a marine depositional setting.

Izvleček: Na podlagi karotažnih vrtin in detajlnih biostratigrafskih podatkov iz štirih vrtin (001, 003, 004 in 005) smo izdelali sekvenčno strati-

grafijo naftnega polja K v zahodnem delu delte reke Niger. Namen študije je bil določiti glavne mejne površine, depozicijske sekvence, sistemske trakte in okolje sedimentacije. Podatke smo analizirali s programsko opremo Petrel.

V preučenih zaporedjih smo določili tri depozicijske sekvence, ki so ločene s sekvenčnimi mejami na globini 2697 m ter 2742 m. Za vsako izmed sekvenc smo določili transgresivne sistemske trakte (TST) in sistemske trakte visoke gladine morja (HST). Zgodnje- do poznomiocenska starost preučevanega zaporedja je bila določena na podlagi plasti kronostratigrafske lestvice delte Nigra in glinavcev s *Chloguebelino* 3 (16.0 Ma). Sistemski trakti visoke gladine morja vsebujejo z glino bogate peske, ki so rezervoar slabše kvalitete. Transgresivni sistemski trakti pa so sestavljeni iz debelih enot, ki so dobre zaporne plasti rezervoarja. Na podlagi SP-motivov iz vrtin smo določili naslednja sedimentacijska okolja: plimske kanale ter obalna in šelfna okolja.

INTRODUCTION

The Niger Delta is situated in the Gulf of Guinea and extends throughout the Niger Delta province (KLETT et al, 1997). The Niger Delta is a large arcuate type, situated on the west coast of central Africa between latitudes 3° and 6° N and longitudes 5° and 8° E (REIJERS et al, 1997). It ranks among the world's most prolific petroleum producing Tertiary deltas. This province contains one identified petroleum system known as the Tertiary Niger Delta (Akata-Agbada) petroleum system (EKWEOZOR & DAUKORU, 1984: KULKE, 1995).

Over 80 % of Nigeria's revenue comes from oil and gas, with the Niger Delta basin as the main target. In order to satisfy the need for increasing production of the vast hydrocarbon resources, it was necessary to improve the existing geological knowledge of the region by application of a modern concept of sequence stratigraphy.

Sequence stratigraphy, which is the underlying concept for this work, is the study of the subdivision of sedimentary basin fills into genetic packages bounded by unconformities and their correlative conformities. The knowledge of sequence stratigraphy can provide a chronostratigraphic framework for the correlation and mapping of sedimentary facies and for stratigraphic predictions.

Present study therefore focuses on developing sequence stratigraphic framework for K-Field within the Niger Delta basin, based on the integration of data from well logs and biostratigraphic data sets.

Study area and regional geologic setting

The study area is the K-Field, located in the onshore portion of the western part of the Tertiary Niger Delta (Figure 1). The K-Field, which contains four wells used in this study, is within the Shell Petroleum Development Company of Nigeria concession (Figure 1).

On the basis of sand-shale ratios, the subsurface Tertiary section of the Niger Delta is divided into three formations (Figure 2), representing prograding depositional facies. These formations are from oldest to youngest; Akata, Agbada and Benin Formations. The
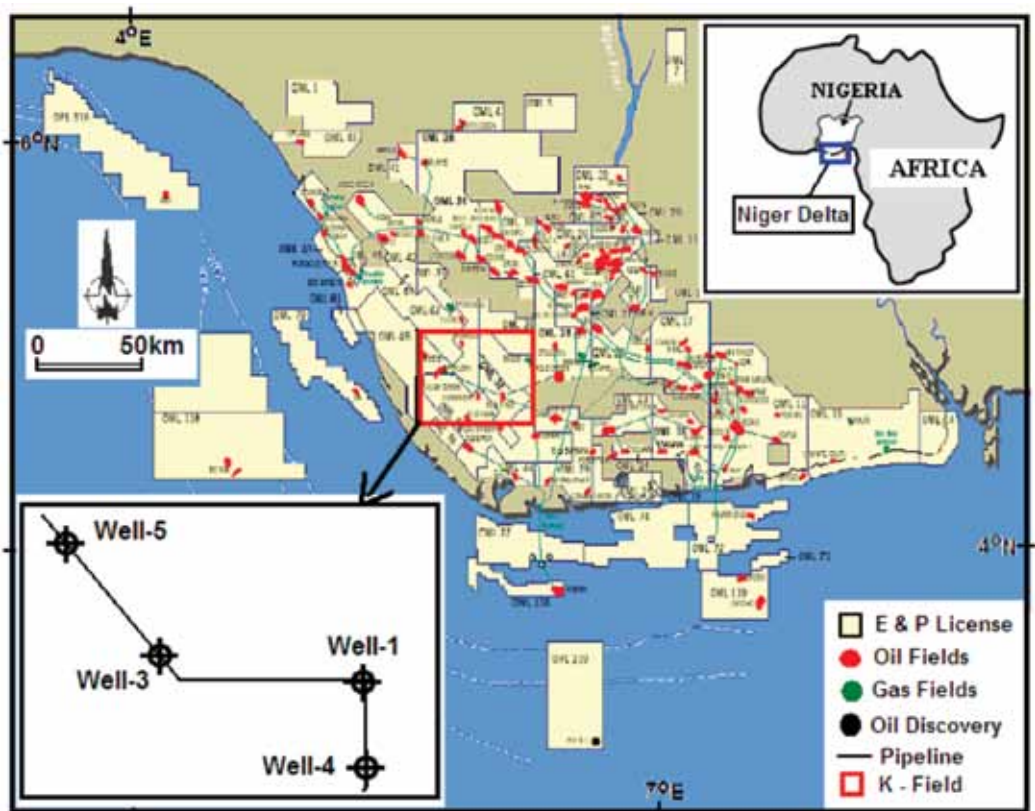

Figure 1. Concession map of Niger Delta showing location of K-Field with base map of four wells shown. Map of Africa inset (Modified from ENI/NAOC, 2002 Brochure on Nigeria
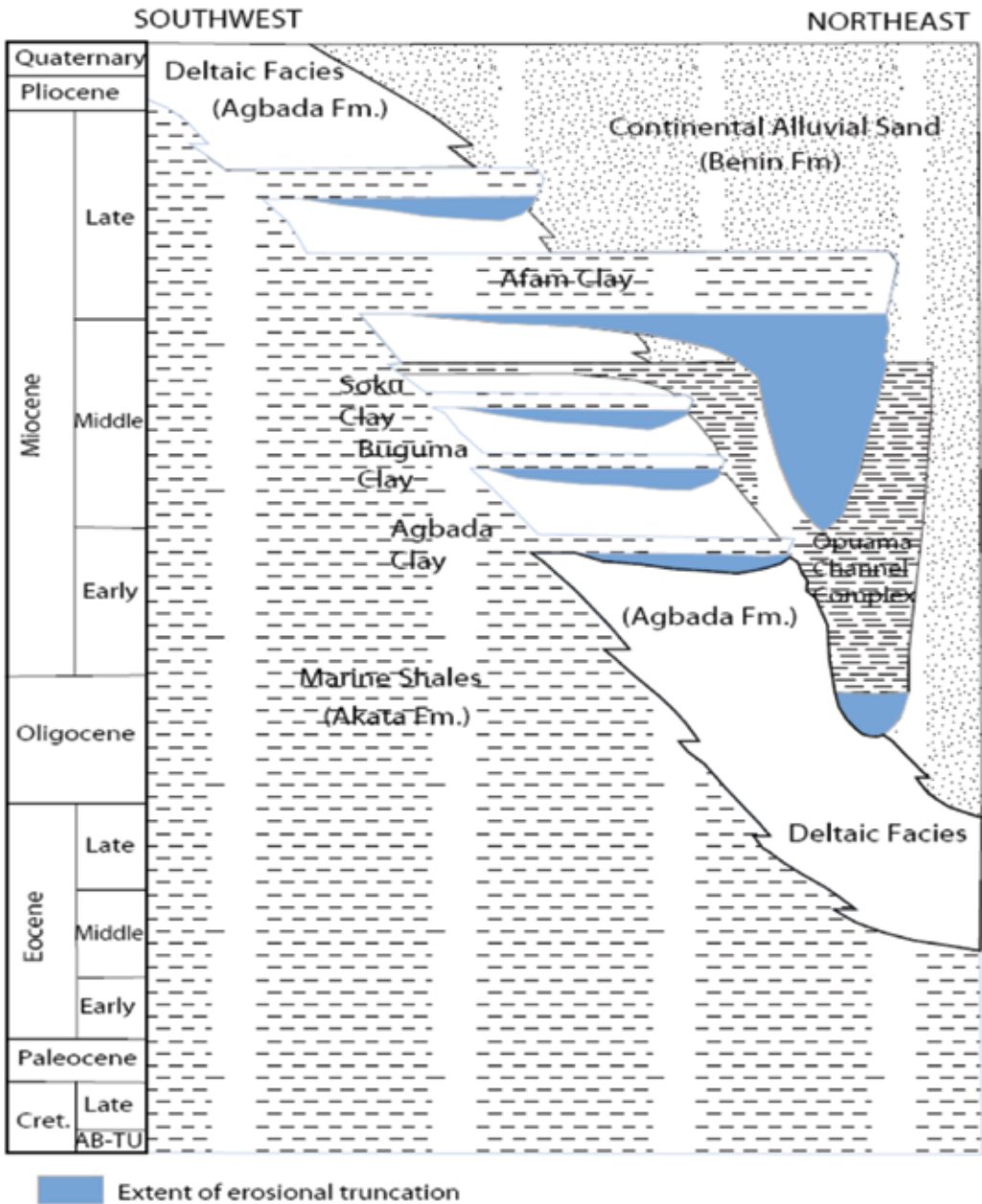
Figure 2. Stratigraphic column showing the three Formations of the Niger Delta (DOUST & OMATSOLA, 1990)

type sections of these formations are described in SHORT & STÄUBLE (1967) and summarized in a variety of papers (e. g. AVBOBVO, 1978; DOUST & OMATOLA, 1990; KULKE, 1995).

The Akata Formation at the base of the delta, is of marine origin and is composed of thick shale sequences (potential source rock), turbidite sand (potential reservoirs in deep water), and minor amounts of clay and silt. Beginning in the Cretaceous in the proximal part of the delta and Recent in the distal offshore, the Akata Formation formed within a deep water environment, when terrestrial organic matter and clays were transported to deep water areas characterized by low energy conditions and oxygen deficiency (STACHER, 1995). It is estimated that the formation is up to 7 000 m thick (DOUST & OMATSOLA, 1990). The Akata Formation underlies the entire delta, and is typically overpressured. Turbidity currents likely deposited deep sea fan sands within the upper Akata Formation during the development of the delta (BURKE, 1972).

The Agbada Formation, which is the major petroleum-bearing unit, overlies the Akata Formation. The formation began in the Eocene in the proximal part of the delta and presently deposited in the nearshore shelf domain. It consists of paralic siliciclastics, over 3 700 m thick and represents the actual deltaic portion of the sequence. These clastics accumulated in delta-front, delta-topset, and fluvio-deltaic environments. In the lower part of the Agbada Formation, shale and sandstone beds were deposited in equal proportions, however, the upper portion is mostly sand with only minor shale interbeds. The Benin Formation is the youngest lithostratigraphic succession in the Niger Delta and comprised sandstone, grits, claystone and streaks of lignite. It is about 2 000 m thick and ranges in age from Oligocene in the proximal part of the delta to Recent. The Benin Formation consists of thick sections of continental sediments with coastal plain and shallow marine sandstones. The formation water is fresh with high resistivity.

The structural development within the Niger delta is controlled by differential loading of the underlying prodelta shales of the Akata Formation, which consists of three basic elements; the northern (proximal) megastructure boundary fault, a southern counter-regional terminating fault and/or toe-thrust belt and the intervening central rigid block between the two fault systems (EVAMY et al, 1978). Most known traps in the Niger Delta are structural, although stratigraphic traps are not uncommon (Figure 3). The growth faults which formed the structural traps developed during synsedimentary deformation of the Agbada paralic sequence (EVAMY et al., 1978; STACHER, 1995). DOUST & OMATSOLA (1990) described a

variety of structural trapping elements, including those associated with simple rollover structures; structures with multiple growth faults, structures with antithetic faults, and collapsed crest structures. Nton & Adesina (2009) identified two major growth faults, three antithetic and two synthetic faults, offshore Niger Delta. They also noted structural closures as rollover anticlines displayed on the time/depth structure maps which suggest probable hydrocarbon accumulation at the downthrown side of the major growth fault. Schematic sketches showing the development of growth-fault-bounded depobelts during progradation of unstable Niger Delta clastics have been presented in Knox & Omatsola (1989). The formation of interest is the Agbada Formation which contains the hydrocarbon producing reservoirs in the study area.
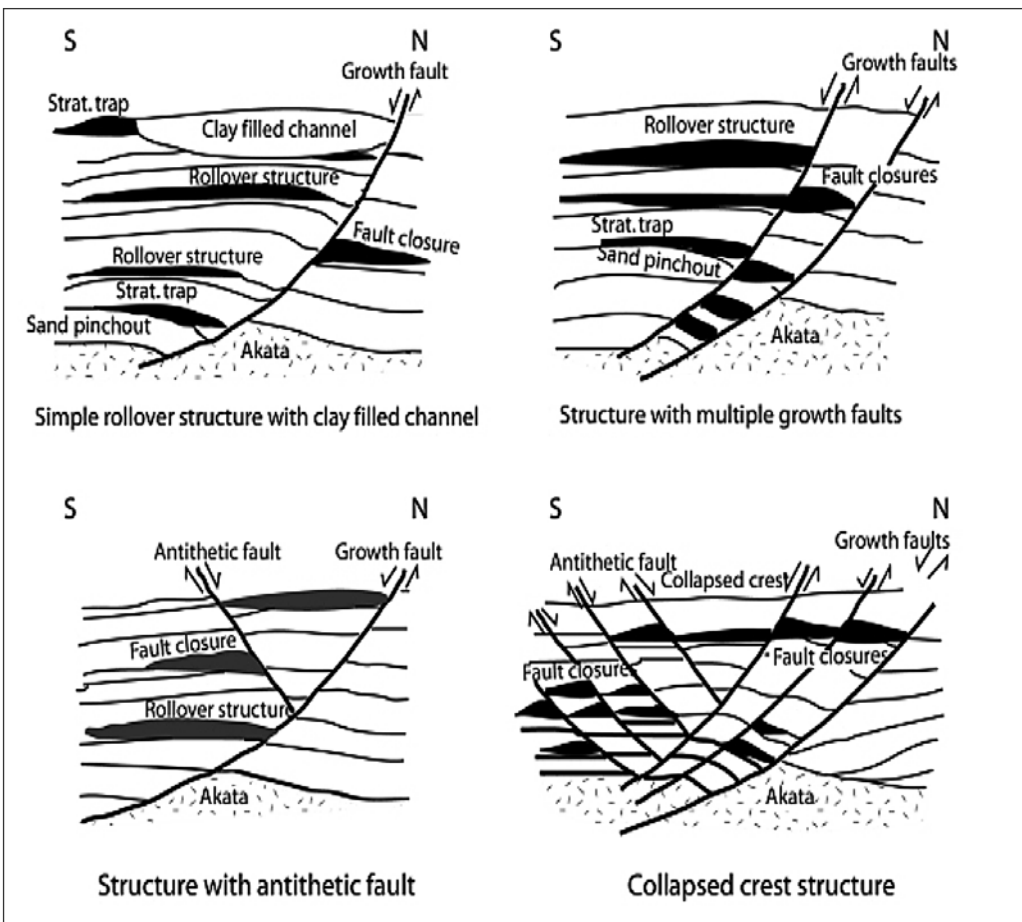

Figure 3. Examples of Niger Delta Oil Field Structure and associated trap types. (STACHER, 1995)

Materials and methods

A suite of well logs, in ASCII format , were obtained from four wells namely; 001, 003, 004, and 005, drilled within the K- Field in the western Niger Delta. Biostratigraphy data, summarized with Pollen(P) and Foram(F) zones from three wells notably; 001, 004, and 005 plus deviation data were utilised in this study. The above dataset were obtained from the Shell Petroleum Development Company of Nigeria Limited. The well logs, made of the gamma ray, self potential and resistivity logs were analysed using the PETREL software (version 2003) at the workstation of the Department of Geophysics, Federal University of Technology, Akure, Nigeria.

A detailed analysis and interpretation of the suite of well logs was carried out, followed by biostratigraphic interpretation of the data. The various analyses were integrated and interpreted to deduce a sequence stratigraphic framework of the Field of study. Detailed analytical procedures are documented in Ogungbemi (2009).

Recognition of Sequence Boundaries
The recognition of sequence boundaries (SB) in this study was based on the concept of Van Wagoner et al. (1990). The sequence boundaries were identified by a sand-rich facies, within a coarsening upward sequence. These are usually located between two maximum flooding surfaces and are recognized by an erosional surface between a lowstand and a highstand system tract.

Recognition of Maximum Flooding Surfaces
The Maximum Flooding Surface caps the Transgressive System Tracts (TST). It represents the most landward transgression of the shoreline. The 3rd order MFS identifiable in the Niger delta chronostratigraphic chart where mapped on the wells. It was identified through the biostratigraphic data made available and interpreted. When integrated with the biostratigraphic interpretation, it is also represented on the well log as the point where the resistivity logs which corresponds to the highest value on the SP logs.

Recognition of Systems Tracts
This was recognized by first locating the3rd order and 4th order maximum flooding sufaces within major condensed sections on the logs, followed by the location of the highstand system tracts, transgressive system tract and the lowstand system tract subdividing. The Lowstand System Tract comprises the basin floor fan, the slope fan and the prograding complex. The basin floor sands contain massive turbidite sands with the upper boundary characterized by hemipelagic shale (Vail et al., 1992). The slope fan consists of crescent-shaped channel bank units while the, prograding complex is a prograding unit

with an aggradational offlap configuration. It rests directly on the underlying slope fan and basin floor complexes and is characteriesed by turbidities sands and shales. A maximum shale point generally marks the boundary between the slope fan complex and the lowstand prograding complex. The Trangressive System Tract is characterized by electrofacies that is made up of high gamma ray values indicating the presence of deep sea marine shale. The portion of the log with the lowest resistivity was selected as the maximum flooding surface when integrated with the biostratigraphic data. This is based on the concept of Sangree et al., (1990).

The Highstand System Tract is bounded below by a downlap surface of maximum flooding and above by a sequence boundary. According to Vail et al., (1990), log correlations in the highstand commonly indicate interbedded sand and shale lithofacies while the reservoir continuity is fair.

Results and discussion

Based on integration of the available data, the lithologic, depositional energy, stratigraphic surfaces and sequence stratigraphy of the field were analyzed and interpreted. These interpretations aided in the subdivision of stratigraphy into system tracts that aided in better correlation of the wells for an improved search for hydrocarbon in the study area as shown below.

Lithology and Depositional Energy

This study revealed that low SP log readings, ranging from 82.4 mv to 173.7 mv, are good reservoir quality sandstones while SP log reading ranging between 44.3 mv and 82.4 mv, indicates shale interval (Figure 4). This was used in the identification of the sand–shale ratio which aided in interpreting sandstone and shaly lithologies. These sandy lithologies were painted yellow, shaly lithologies were painted green and self potential logs were painted red for easy identification (Figure 4). Most of the sandstone units within the field have some shale intercalations as seen mostly on the upper part of the study interval. The thickness for the small reservoirs ranges between 15 m and 20 m while the very thick sandstone units range between 76 m and 305 m (Figure 4).

The depositional energy trend, which is useful for the identification of sedimentary facies (Posamentier & Vail, 1988), follows two sequences in this study. These are; those with finning upward and coarsening upward sequences (Figures 4 and 5). Those with fining upward sequences are seen to have lesser thicknesses. This forms the lithologic classification indicating the building up of sandstone from coarse to fine grains, with the coarse grains pointing to higher energy of deposition while the finer

Stratigraphic Cross Section of wells 005, 003, 001 and 004:Equally Spaced Logs
Datum : SSTVD   Vertical scale = 1 in per 50 ft 08/08/2008
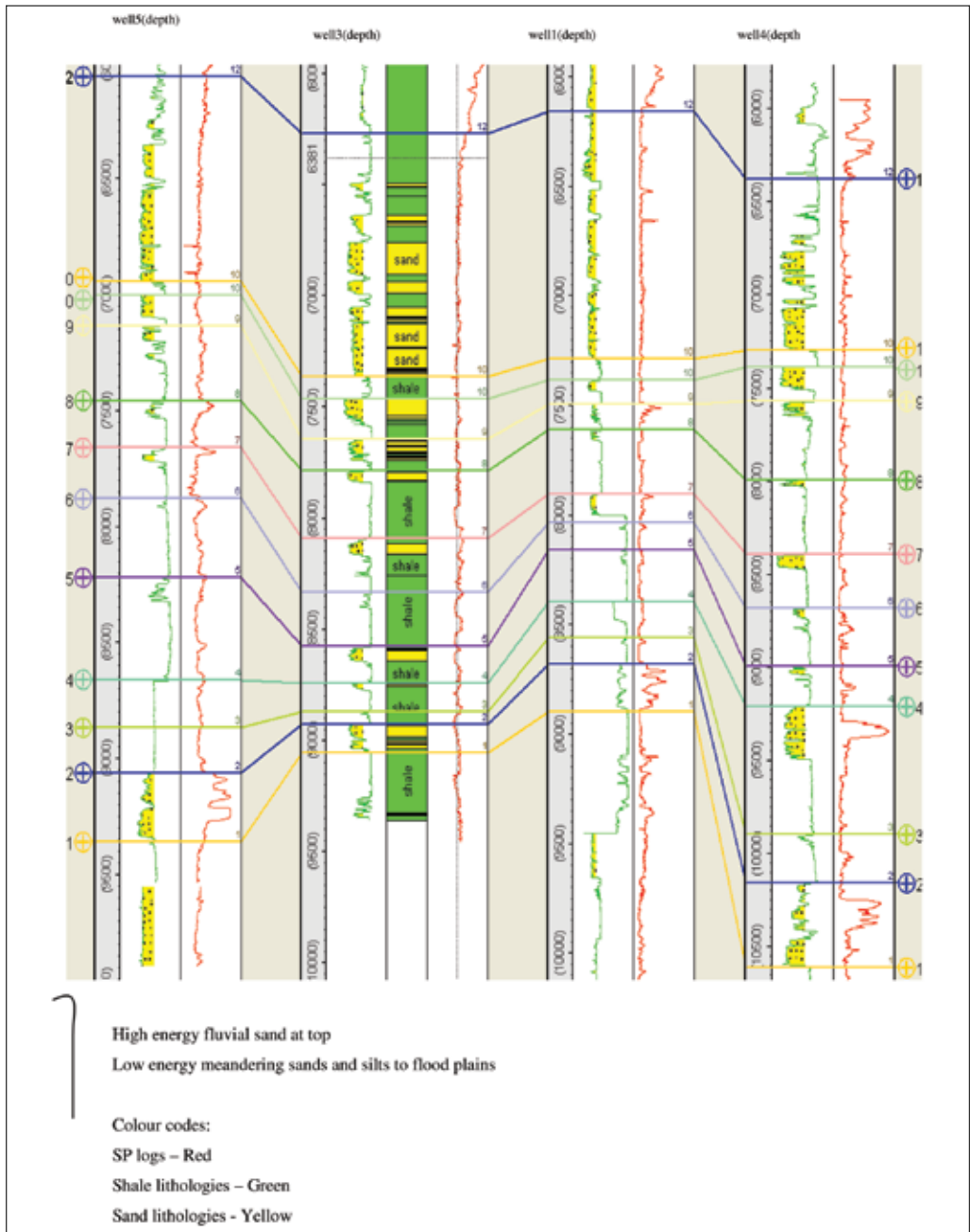

Figure 4. Correlation panels and depositional energy trends based on wells 005, 003, 001 and 004

Stratigraphic Cross Section "Well005.003,001and 004:Equally spaced logs
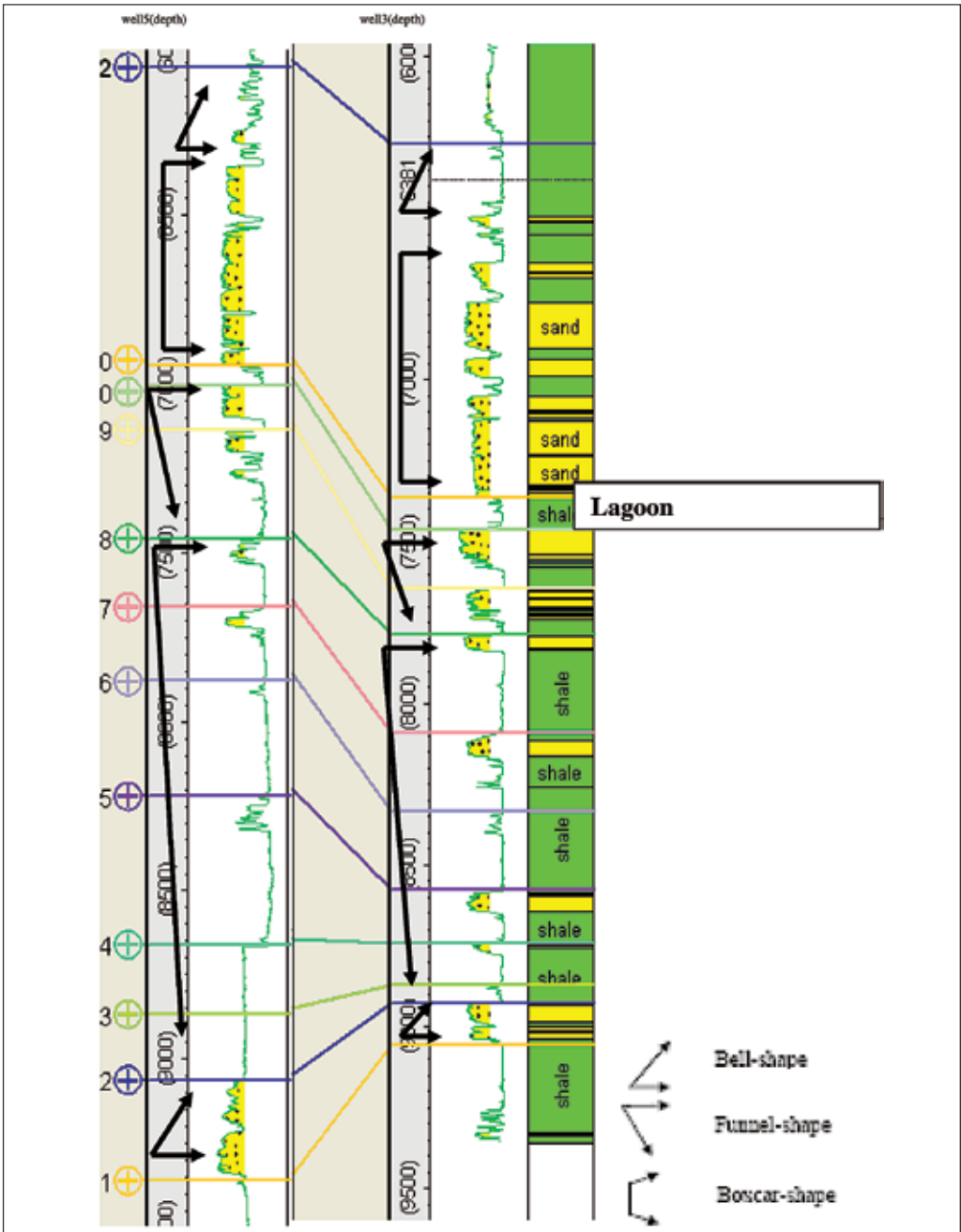Datum : SSTVD Vertical Scale= 1 in per 50ft
08/08/2008

Figure 5. Log trends for depositional environment using Wells 005 and 003

grains indicate a lower energy of deposition. The coarsening upward sequences show a larger thickness of deposits, decreasing from sandstone at the top to shale at the base (Figure 5).

SP logs analysis in the studied interval show three types of log motifs, which are; funnel-shaped, bell-shaped and box car-shaped (Figure 5). The funnel–shaped motif is that which has been identified as upward-coarsening sedimentary sequences (Figure 5). These sedimentary sequences would be inferred to be a prograding complex deposited within a lowstand system tract. They are interpreted as fluvial channel deposited within a continental to coastal environment (Figure 5). These sequences have lesser thickness than others, ranging between 39 ft to 41 ft (11.8 m to 12.4 m).

In the bell-shaped motif, the SP logs of the study interval have a bell motif overlain and underlain by thick shales. They are seen to have upwards fining sedimentary sequences (Figure 5) with thicknesses ranging from 500 ft to 970 ft (152 m to 294 m).This occurs when marine sediments such as shales transgress over continental facies or fluvial sediments. They could also be interpreted as tidal channel sands deposited under high tidal influence over fluvial sands.

The box car-shaped SP log is a convex (outward) view with a box description. The motif is formed due to a build up of clastic sediments at a constant sea level leading to an aggrading sediment deposition. The box car-shaped SP log indicates the truncation of a rapid aggradational deposition with terminal boundaries. They can be inferred to as distributary channel sands. According to Selley (1991), three general categories of environments can be inferred from such depositions; these are tidal channel sand, fluvial channel sand delta distributaries channel sands. It can be deduced from this study therefore that the box-car depositional motif is significant of distributary channel sand deposited within a shallow marine environment.

Third order stratigraphic surfaces and sequences

The sequence stratigraphic framework for K Field is composed of three major third(3rd) order Sequence Boundaries (SB) ranging from 15.9 Ma to 10.4 Ma and one major third (3rd) order sequence of Miocene age, corresponding to Pollen zones P680 to P780 and Foram zones of F9300 to F9800 (Table 1). The maximum flooding surface was tied to the Niger Delta Chronostratigraphic chart (Figure 6)

Maximum Flooding Surface (MFS)

A major third order MFS was identified, and subsequent four fourth order Maximum Flooding Surfaces (Figure 7). The MFS identified was based on the positions of highest abundance and diversity peaks, on the biofacies data.
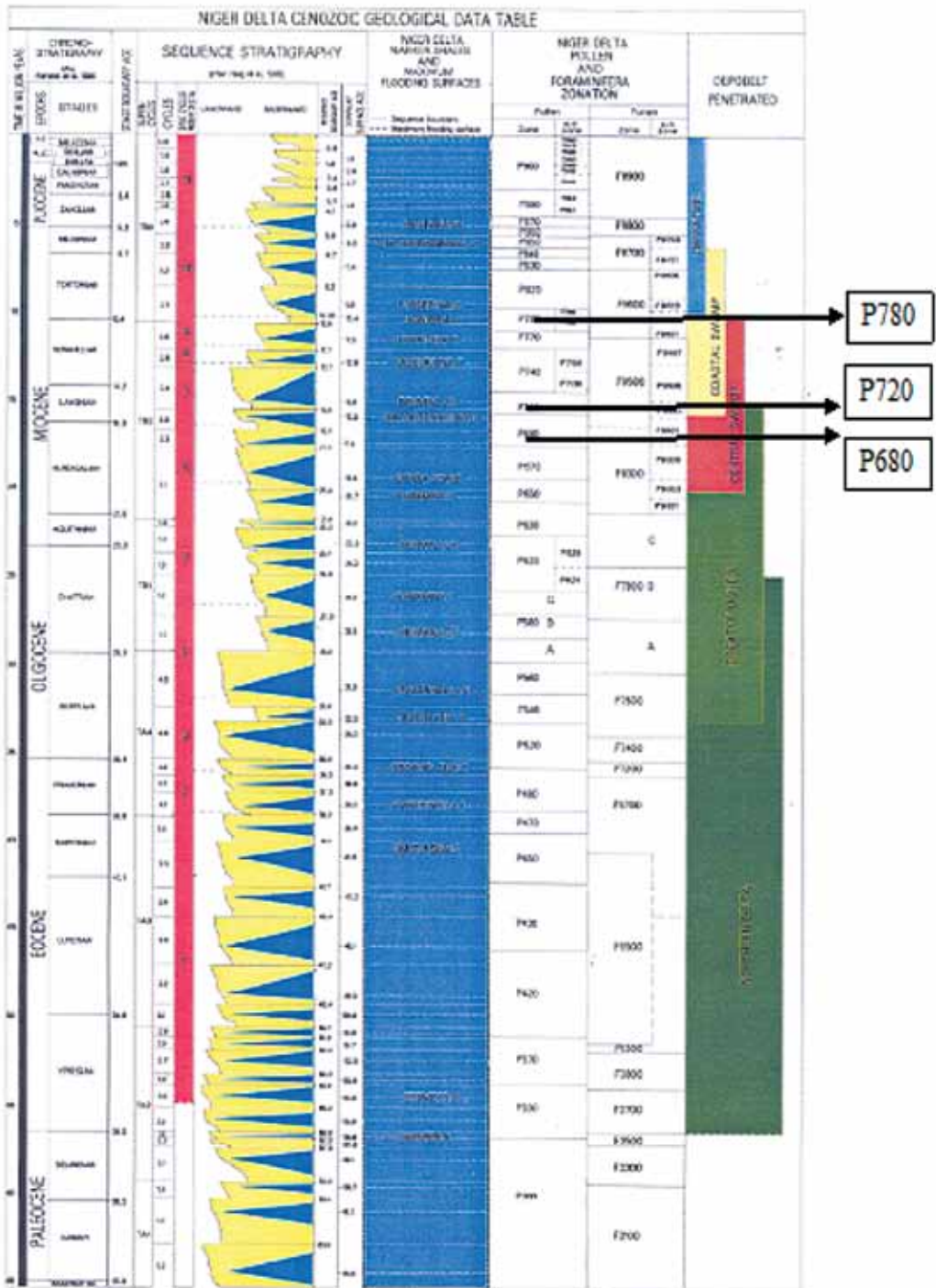
Figure 6. Niger Delta chronostratgraphic chart (HAQ et al, 1988)

On the well logs, they were identified as the flooding surface with the highest resistivity values. This correctly ties with the MFS identified at a depth of 7 650 ft (2 318 m).

Chloguebelina 3 MFS (16.0 Ma).
This MFS penetrated in the studied Field has been tied to the Chloguebelina-3 marker on the Niger Delta Chronostratigraphic chart (Figure 6). They were encountered by Wells 003 and 005 at respective depths of 7 850ft (2 379 m) and 7 650ft (2 318 m) based on well log interpretation. It occurs with the P680 and F9300 biozones. The log patterns show an upward coasening depositional energy succession and downward finning sedimentation with a laterally extensive shaly lithology.

Sequence Boundaries (SB)
The sequence boundaries were identified based on the interpretation of parasequence stacking patterns, log shapes and motifs. The third order sequence boundaries recognized are 15.9 Ma and 10.38 Ma (Figure 6). Resistivity logs

which correspond to the lowest value on the SP log indicates the sequence boundaries mapped (Figure 7)

17.7 Ma SB
This is the oldest sequence boundary identified in the K-Field. It is penetrated by Wells 005 and 003 at depths of 9 050 ft (2 758 m) and 8 950 ft (2 722 m) respectively. This surface was not recognized on well 001 due to the depth in which it was drilled to. This was identified from the well logs with the aid of the biostratigraphic data (Table 1)

Deductions from biofacies interpretations typically show that such horizons are devoid of Pollens, with no indication of Foraminifera. The depositional environment deduced from the log signatures depicts a continental sediment deposited in a shelf environment (Figure 5) based on the concept of BUSCH et al., (1974).

10.38 Ma SB
This is the second sequence boundary penetrated in K-Field and it marks the

Table 1. Biostratigraphic data table

Well	Depth (ft)	Marker shales's (Faunal bed)	Dated Age(ma)	P Zones	F Zones	Epochs
1	6180 76.75	Nonion 6 Chloguembelina 3	10.3 16.0	P780 P680	F9800 F9300	Miocene Miocene
4 3	6400 7550 9000 10010	Nonion 6 Chloguembelina 3 Rich Bolivina 25 Rich Bolivina 25	9.0 16.0 17.7 17.7	P820 P680 P670 P670	F9800 F9300 F9300 9300	Miocene Miocene Miocene Miocene
5	6080 7701	Nonion 6 Chloguembelina 3	10.3 16.0	P780 P680	F9800 F9300	Miocene Miocene

Stratigraphic Cross Section "Well005.003,001and 004:Equally spaced logs
Datum : SSTVD Vertical Scale= 1 in per 50ft
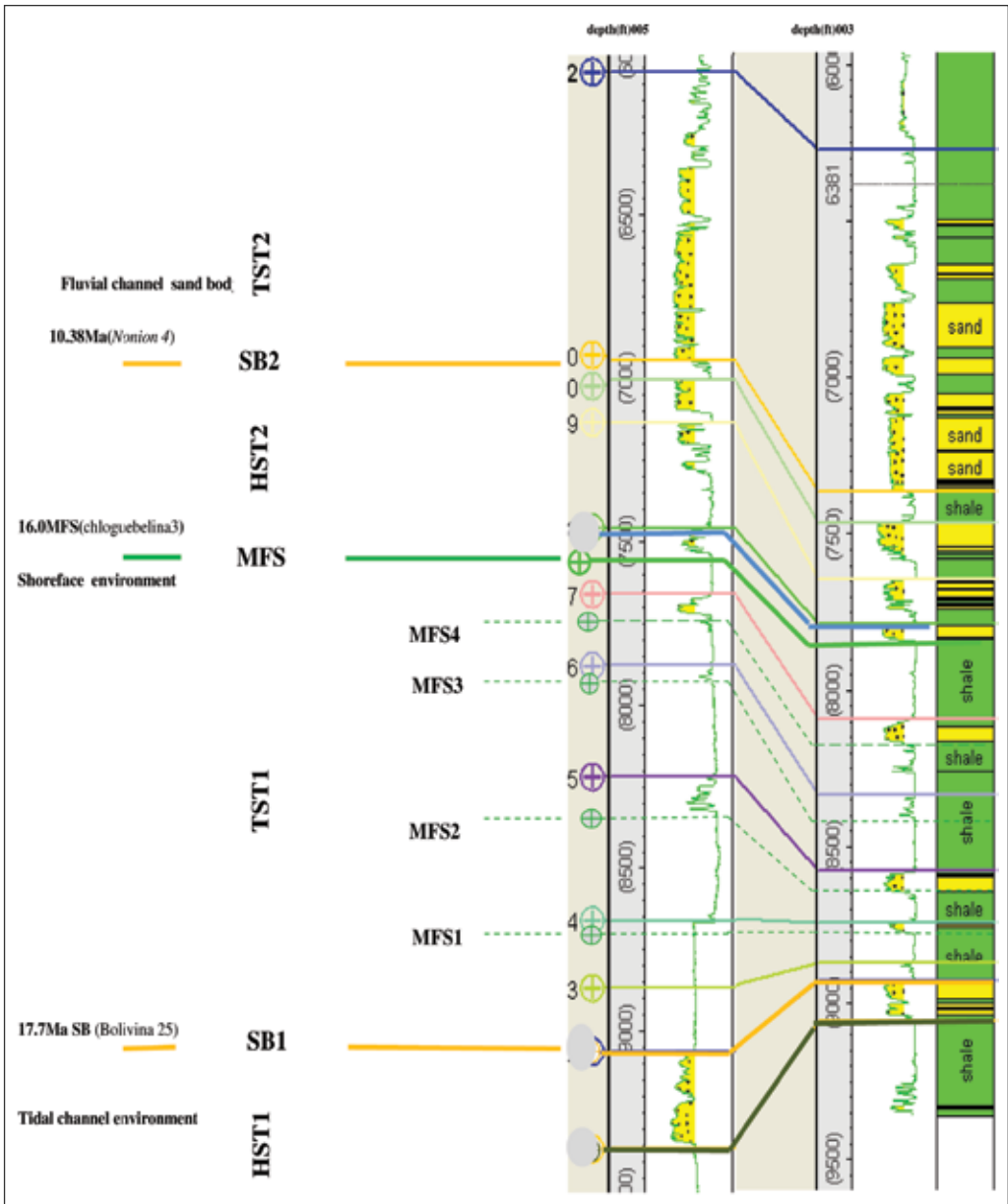18/08/2008

Figure 7. Sequence stratigraphic correlation and depositional environment setting of K-Field showing Wells 005 and 003

base of the Benin Formation. It was penetrated by Wells 005 and 003 at depths 7 000 ft (2 134 m) and 7 300 ft (2 225 m) respectively. This sequence has a blocky log shape which is depicted on the SP log (Figure 5) and indicates a channel sand deposit (Serra, 1985). This is well correlated to the Niger Delta chronostratigraphic chart (Figure 6).

Description of the third order depositonal sequences of wells

Sequence stratigraphic model developed for K-Field was based on the interpretation carried out on Wells 003 and 005 that penetrated different subsurface lithologies. Figures 4, 5 and 7 show the representation of the interpretation of the wells.

Well 003

The sequence 1 of this well ends at 8 575 ft (2 598.5 m) (Figure 7) and is capped by the Highstand Systems Tract. Sequence 2 of this well starts with a cresent shaped log pattern , which grades into a prograding complex. The basal unit starts at a depth of 9 055 ft and ends at 7 000 ft. It is bounded below by the shallow marine deposits (Figure 7) which marks the base of this Sequence Boundary. The Transgressive system tract covers a total depth of about 1 055 ft (320 m) as it exihibits an aggradational parasequence set terminated at the top by the major condensed section embedded in the 16.0 Ma Maximum Flooding Surface.The Highstand sys-

tems tract starts from the top of TST1 at depth 7 450 ft (2 257.6 m) to 6 950 ft (2 106 m). This systems tract terminates at the 10.38 Ma Sequence Boundary.

Well 005

The first sequence in this well started from the base of the well and ends at 8 945 ft (2 710.6 m) (Figure 7). This is capped by high system tract. The second sequence in this well starts at the depth of 8 985 ft (2 723 m) and the depositional episode commenced with the deposition of Trangressive Systems Tracts. These lie unconformably on the lower boundary, culminating in the Transgressive peak at the Maximum Flooding Surface with lowest shale resistivity and high value on the SP log at a depth of 7 550 ft (2 294.8 m). This in turn initiated the blocky sand of the the Highstand Systems Tract, which extends from the top of the Maximum Flooding Surface and terminates at 6 950 ft (2 112.5 m) and (2 226.7 m), at a position which marks the end of the second sequence boundary.

Depositional environment

The depositional environments were delineated based on SP log signatures. Depositional environments delineated in this study include the tidal channel complex and the shelf environment (Figure 7). The blocky shaped pattern is characteristic of the distributary channel sediments deposited in a shallow marine environment (Figure 5). This corroborates the findings of Ser-

ra, (1985) This signature is represented by a kick to the left of the SP baseline. Flooding surfaces, identified with marine shales, can be recognized below as a large right kick on the SP log (Figure 7). This significant signature typifies the shelf environment. The inner shoreface environment is marked generally by an upward decrease in shale content from the proximal to the distal portion of the field. This corroborates the findings of Willis & Bennett, (1994).

A typical model constructed for the Field was done using Well 005 (Figure 7). It shows that the deposited sequence starts with a tidal channel environment, with an interfingering of sandy sediments which is capped by the Transgressive system tract with marine shale marking the maximum flooding surface which also hosts the condensed section. This sequence change into shoreface environment having sand bodies at the base. This typifies the concept described by Emery et al., (1996) Subsequently, the next sequence recognized starts with a fluvial channel sand body, characterized by some extensive marine shale deposits (Figure 7).

Summary and conclusion

The concept of sequence stratigraphy was applied to the K-field, within the western Niger Delta, Nigeria. This was based on biofacies analysis, well log shapes/trends, pollen and foram zones data which were utilized independently and later integrated with well logs to within a chronostratigraphic framework for the field.

Two sequence boundaries at 8 900 ft (2 697 m) and 9 050 ft (2 742.4 m), and one maximum flooding surface at a depth of 7 650 ft (2 318.2 m) were recognized in well 5 and utilized to subdivide the stratigraphic succession into depositional sequences and their corresponding systems tracts. Highstand and Transgressive systems tracts were recognized in each of the three depositional sequences. Marker shale, characterized by *Chloguebelina* 3 (16.0 Ma) was used to date the key bounding surfaces with the aid of the Niger Delta chronostratigraphic chart as Early to Late Miocene.

The Highstand systems tracts are characterized by shale-rich upward coarsening sands, having poor reservoir quality, while the transgressive systems tracts are characterized by thick sandy shale units, indicating good quality seals to reservoirs. Arising from the SP logs motifs, the depositional environments inferred include tidal channel, shoreface and shelf environments, typical of shallow marine depositional setting.

This model will therefore serve as a guide to the development of K-field and assist in further exploration activity.

Acknowledgments

The authors are grateful to the management and staff of the Shell Petroleum Nigeria Limited, for the provision of data. We are grateful for the invaluable assistance of the Department of Applied Geophysics, Federal University of Technology, Akure, Nigeria, for the permission to use their Petrel Work station for the data analysis**.** I appreciate the encouragement of my colleagues, Prof. A. A. Elueze and Dr. M. N.Tijani at all times.

References

AVBOVBO, A. A. (1978): Tertiary lithostratigraphy of Niger Delta: American Association of Petroleum Geologists Bulletin, v. 62, p. 295–300.

BURKE, K. (1972): Longshore drift, submarine canyons, and submarine fans in development of Niger Delta: American Association of Petroleum Geologists, v. 56, p. 1975–1983.

BUSCH, W., SCHNEIDER, G. & MEHNERT, K. R. (1974): Initial melting at grain boundaries. Part II: melting in rocks of granitic, quartz dioritic, and tonalitic composition. *Neues Jahrbuch für Mineralogie, Monatshefte* 345–370.

DOUST, H. & OMATSOLA, M. E. (1990): Niger Delta, In: Edwards, J. D. and Santogrossi, P.A., (eds.) , Divergent/passive Margin Basins, AAPG Memoir 48: Tulsa, American Association of Petroleum Geologists, p. 239–248.

EKWEOZOR, C. M. & DAUKORU, E. M. (1984): Petroleum source bed evaluation of Tertiary Niger Delta--reply: American Association of Petroleum Geologists Bulletin, v. 68, p. 390–394.

EVAMY, B. D., HAREMBOURE, J., KAMERLING, P., KNAAP, W. A., MOLLOY, F. A. & ROWLANDS, P. H. (1978): Hydrocarbon habitat of Tertiary Niger Delta: American Association of Petroleum Geologists Bulletin, v. 62, p. 277–298.

HAQ, B. U., HARDENBOL, J. & VAIL, P. R. (1988): Mesozoic and Cenozoic chronostratigraphy and eustatic cycles. In: Wilgus, C. K., Hasting, B. S., Kendall, C. G. St., Posamentia, H., Ross, C. A., and Van Wagoner, (eds.).Sea-level –an integrated approach, Jour. Soc. Econs. Paleotol. Mineral. Spec. Publi. 42, p. 47–70.

KLETT, T. R., AHLBRANDT, T. S., SCHMOKER, J. W. & DOLTON, J. L. (1997): Ranking of the world's oil and gas provinces by known petroleum volumes: U. S. Geological Survey Open-file Report-97–463, CD-ROM.

KNOX, G. J. & OMATSOLA, M. E. (1989): Development of the Cenozoic Niger Delta in terms of the escalator regression model and impact on hydrocarbon distribution, In: W. J. M van der Linden, S. A. P. L, Cloetingh, J. P. K., Kaasschieter, W. J. E., van der Graff, J., Vandenberghe, and van der Gun, J. A. M., (eds), KNGMG Symposium

on Coastal lowland Geology and Geotechnology, Proceedings: Dordrecht, The Netherlands, Kluwer Academic Publishers, p. 181–202.

Kulke, H. (1995): Nigeria, In: Kulke, H., (ed.), Regional Petroleum Geology of the World. Part II: Africa, America, Australia and Antarctica: Berlin, Gebrüder Borntraeger, p. 143–172.

Nton, M. E. & Adesina, A. D. (2009): Aspects of structures and depositional environment of sand bodies within tomboy field, offshore western Niger Delta, Nigeria. RMZ – Materials and Geoenvironment, Vol. 56, No. 3, pp. 284–303.

Ogungbemi, T. S. (2009): Sequence stratigraphic framework of k-Field in part of Western Niger Delta, Nigeria,. Unpublished M.Sc thesis , Department of Geology, University of Ibadan, 73 p.

Reijers, T. J. A., Petters, S. W. & Nwajide, C. S. (1997): The Niger Delta Basin, in Selley, R.C., ed., African Basins--Sedimentary Basin of the World 3: Elsevier Science, Amsterdam 3, pp. 151–172.

Selley, R. C. (1991): The third age of log analysis--application to reservoir diagenetic studies [abs.]: The Log Analyst, v. 32, no. 4, p. 381–82.

Serra, O. (1985): Sedimentary environments from wireline logs: Schlumberger Technical Services, Paris, Document No. M-081030/ SMP-7008, 211 p. [Extracted from Serra, O., 1986, Fundamentals of well-log interpretation v. 2--the interpretation of logging data, chapters 4-6: Elsevier Science Publishers, Amsterdam, Developments in Petroleum Science No. 15B, 684 p.].

Shannon, P. M. & Naylor N. (1989): Petroleum Basin Studies: London, Graham and Trotman Limited, p 153–169.

Short, K. C. & Stauble, A. J. (1967): Outline of geology of Niger Delta: American Association of Petroleum Geologists Bulletin, v. 51, p. 761–779.

Stacher, P. (1995): Present understanding of the Niger Delta hydrocarbon habitat. In: Oti, M.N., and Postma, G., (eds.), Geology of Deltas: Rotterdam, A.A. Balkema, p. 257–267.

Vail, P. R. (1998): Sequence stratigraphy workbook, fundamentals of sequence stratigraphy: 1999 AAPG Annual convention short course: Sequence stratigraphy interpretation of seismic, well log and outcrop data, presented by P. R. Vail and J. B. Sangree, March 19, 1998, Houston, Texas.

Van Wagoner, J. C., Mitchum, R. M., Campion, K. M. & Rahmanian, V. D. (1990): Siliciclastic sequence stratigraphy in well logs, cores and outcrops: concept for high-resolution correlation of time and facies, AAPG methods in exploration series, No. 7, 55 pp.

Willis K. J. & Bennett K. D. (1994). The Neolithic transition - fact or fiction? Palaeoecological evidence from the Balkans. The Holocene v. 4, p. 326–330.

Environmental impacts of asphalt and cement composites with addition of EAF dust

Okoljski vplivi asfaltnih in cementnih kompozitov z dodatkom EOP-prahu

Tina Oblak[1], Janez Ščančar[1], Mitja Vahčič[1], Tea Zuliani[1], Ana Mladenovič[2] & Radmila Milačič[1, *]

[1]Jožef Stefan Institute, Department of Environmental Sciences, Jamova 39, Ljubljana, Slovenia
[2]Slovenian National Building and Civil Engineering Institute, Dimičeva 12, Ljubljana, Slovenia

*Corresponding author. E-mail: radmila.milacic@ijs.si

Abstract: EAF dust can be used in civil engineering as an appropriate additive in asphalt and cement composites. Before its intended use it is necessary to estimate the environmental impacts. For this purpose leachability tests based on diffusion were performed in water and salt water for six months. Stable compact and ground asphalt composites with addition of 2 % of EAF dust and cement composites with addition of 1.5 % of EAF were studied. Data demonstrated that Cr was leached almost solely as Cr(VI). The results indicated that Cr(VI) was not leached from compact asphalt composites with addition of EAF dust. However, in ground asphalt composites with addition of EAF dust Cr(VI) was leached with water in concentrations up to 220 µg L^{-1} and with salt water up to 150 µg L^{-1}. In compact and ground cement composites with addition of EAF dust leaching of Cr(VI) with water was negligible, while Cr(VI) was leached with salt water in concentrations up to 100 µg L^{-1}. The leaching of Cr(VI) originated primarily from cement. Other metals investigated did not represent an environmental burden. Therefore, from the environmental aspects EAF dust can be safely used as a component in asphalt and cement mixtures.

Original scientific paper

Izvleček: V gradbeništvu lahko EOP-prah uporabimo kot primeren doda-
tek asfaltnim in cementnim kompozitom. Pred tovrstno uporabo pa
je poleg fizikalno-mehanskih, potrebno preučiti tudi okoljske vpli-
ve. V ta namen smo šest mesecev sledili izluževanju kovin z izluži-
tvenimi preizkusi na osnovi difuzije v vodi in slani vodi. Pripravili
smo kompaktne in zdrobljene asfaltne kompozite z dodatkom 2 %
filtrskega prahu in kompaktne ter zdrobljene cementne kompozite
z dodatkom 1,5 % filtrskega prahu. Ugotovili smo, da se je krom
izluževal pretežno kot Cr(VI). Ta se ni izluževal iz kompaktnih
asfaltnih kompozitov z dodatkom EOP-prahu, medtem ko so do-
segle izlužene koncentracije iz zdrobljenih kompozitov vrednosti
do 220 µg L^{-1} Cr(VI). Iz cementnih kompozitov z dodatkom EOP-
-prahu se je Cr(VI) izluževal le s slano vodo v koncentracijah do
100 µg L^{-1}. Izluževanje nekaterih drugih kovin je bilo zanemarlji-
vo. S fizikalno-mehanskega in okoljskega vidika EOP-prah lahko
uporabljamo kot dodatek asfaltnim in cementnim kompozitom za
uporabo v gradbeništvu.

Key words: EAF dust, asphalt and cement composites with addition of
EAF dust, leachability, Cr(VI)
Ključne besede: EOP-prah, asfaltni in cementni kompoziti z dodatkom
EOP-prahu, izluževanje, Cr(VI)

Introduction

In the developed countries industrial
by-products from steel making indus-
try e.g. steel slag [1–6] and electric arc
filter (EAF) dust [7, 8] are widely used in
civil engineering. Waste products are
increasingly used as alternative mate-
rials that successfully substitute natu-
ral raw materials. Re-use of industrial
by-products leads to preservation of
natural resources,[3] substantial reduc-
tion of landfills load and consequently
to the protection of the terrestrial en-
vironment. The use of materials that
contain industrial by-products is pos-
sible when such materials posses ap-
propriate technical characteristics [3, 6]
and are environmentally acceptable.
[3–5, 9] Industrial by-products that can
be potentially re-used may contain
various inorganic and organic pollut-
ants. Among pollutants in wastes from
steel making industry, metals repre-
sent the potential environmental threat.
It is well known that the toxicity and
mobility of particular metal depends
not only on the total concentration,
but also on its chemical form. An ex-
ample is chromium that is extremely
toxic in its hexavalent form (carcino-
genic, mutagenic, provoker of contact

dermatitis), while trivalent chromium compounds (Cr(III)) are essential for glucose metabolism and are much less toxic than those of hexavalent chromium (Cr(VI)).[10] When waste materials and industrial by-products are re-used for road construction and in civil engineering, toxic substances may be successfully immobilised with asphalt [7] and cement.[8, 11, 12] However, before the use, the environmental risk due to the potential release of contaminants from alternative aggregates should be critically apprised.[4, 5, 7, 8, 13] Although it is important to predict the possible long-term effects of alternative aggregates to the environment, there are only few papers reported in the literature on such investigations. In order to estimate the long-term environmental impact, leaching tests based on diffusion were proposed in the Netherland's NEN 7345 standard [14] and applied in the leaching protocol developed for concrete.[15]

The aim of this work was to appraise the long-term environmental impacts of the re-use of EAF dust as additive to asphalt and cements. We report estimation of the results from the leachability tests based on diffusion that were performed in a time span of six months [7, 8] with particular emphasis to critically evaluate the concentrations of Cr(VI) in leachates. Finally, the conclusion was made on the environmental acceptability of the use of EAF dust in road construction and in other civil engineering applications.

MATERIALS AND METHODS

Filter dust generated at the steelwork Štore Steel steelworks, Slovenia was mixed with asphalt and/or cements into stable composites. It was found experimentally that the maximal amount of filter dust added to asphalt that ensured the optimal physico-mechanical characteristics was 2 % by mass of asphalt composite [7] and 1.5 % by mass of cement composite.[8]

In order to assess the long-term environmental impact of asphalt and cement composites with addition of filter dust, the leachability test was carried out in water and salt water (3.8 % NaCl). The salt water simulated the salting of roads during the winter time and the marine environment. Leachability was investigated in compact and ground composites. Ground composites simulated the long term environmental conditions when asphalt disintegrates with time.

To perform the leachability test, NEN standard (NEN 7345, 1995), based on diffusion [14] and the leaching protocol that was developed for concrete [15] were considered. Accordingly, the ratio between volume of a testing composite and the volume of added leaching solution was 1 : 5. In the leaching solutions

pH and Cr(VI) concentrations were followed for six months. Concentrations of Cr(VI) were determined either by the spectrophotometry or by anion-exchange fast protein liquid chromatography – electrothermal atomic absorption spectrophotometry.[16] In the leaching solutions from the last samplings some selected metals were also determined by atomic absorption spectroscopy.

RESULTS AND DISCUSSION

Chemical characteristics of EAF dust
EAF dust is a material with a rather constant composition. The major components of filter dust represent Zn (23–24 %) and Fe (18–22 %), the minor components Pb (1.3–1.5 %), Ca (3.1–3.6 %), Mg (1.6–2.0 %) and Mn (3.5–3.9 %) while in lower concentrations Cr (0.3 %), Cu (0.2 %), K (0.4 %), Ba (0.2 %) and Al (0.2 %) are present.[7] The leachability of these metals in water is low. However, it should be taken into consideration that total leached chromium (0.8 mg kg^{-1}) is present exclusively in its toxic hexavalent form. Despite neutral pH of filter dust water extracts, leaching of Cr(VI) was significant (0.8 mg kg^{-1}), due to very high specific area of filter dust (particle size < 5 μm).[7] Therefore, when filter dust is re-used as additive in road construction and in civil engineering, long-term environmental impacts of new materials should be investigated.

Investigation of the environmental impact of asphalt composites with addition of EAF dust
In order to estimate the environmental impact of EAF dust used as additive to asphalts, four different asphalts were mixed with EAF dust (2 % by mass) so that stable composites with optimal physico-mechanical properties were formed.[7] To simulate the worst case scenario of salting of roads during the winter time and disintegration of asphalts with time, the leachability of chromium and Cr(VI) was investigated in a time span of six months in compact and ground composites using water and salt water as leaching agents. pH was determined in leachates throughout the experiment and was found to be 7.0 ± 0.1. The analytical data indicated that during the course of the experiment Cr(VI) was not leached with water and salt water from compact asphalt composites with addition of filter dust. However, in ground asphalt composites with addition of filter dust Cr(VI) was leached with water and salt water. The results are presented in Figure 1.

The data from Figure 1 indicate that leaching of Cr(VI) from water and salt water is similar for all four samples of asphalt composites with addition of EAF dust. From Figure 1 (A) it is further evident that leaching of Cr(VI) in water from ground asphalt composites with addition of filter dust
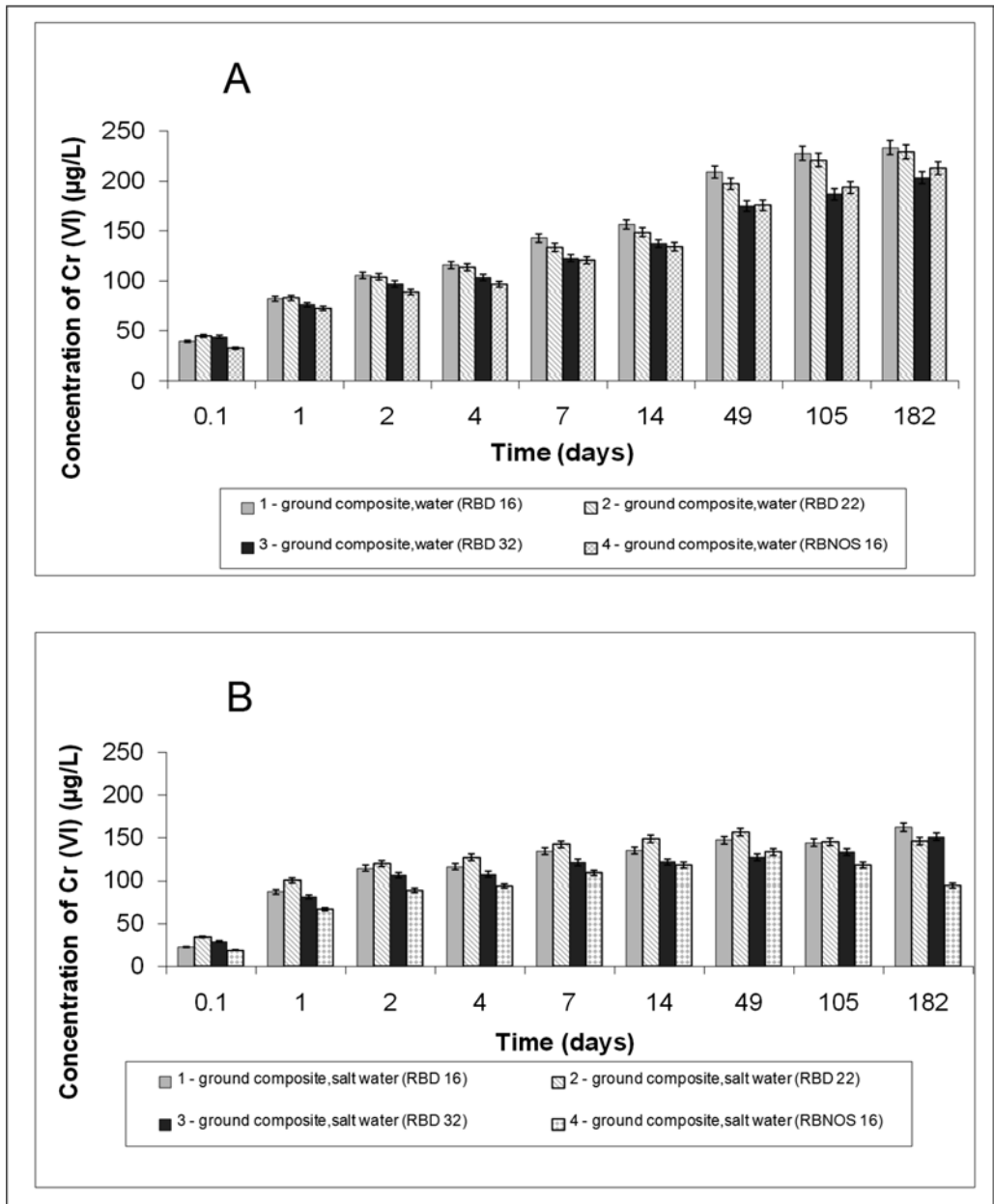
Figure 1. Leaching of Cr(VI) in water (A) and salt water (B) with time from ground asphalt composites with addition of 2 % of EAF dust by mass (resumed from reference 7).

gradually increases with time and reaches constant values (concentrations about 220 µg L⁻¹ Cr(VI)) after approximately 100 d. In salt water (Figure 1 (B)) lower concentrations from ground composites with addition of filter dust are leached in comparison to leaching in water. The constant values (concentrations about 150 µg L⁻¹ Cr(VI)) are reached faster, after 7 d. It was experimentally found the 90 % of total chromium was leached in its hexavalent form. The relatively low Cr(VI) concentrations that are leached from ground asphalt composites with addition of filter may possibly represent the environmental hazard only if the leachates reach the ground and/or drinking water reservoirs. However, due to the reducing characteristics of the bitumen and neutral pH of aggregate, it may be expected that concentration of Cr(VI) will be slowly decreased in the environment after decades. At more acidic environmental conditions, in the case of acid rain precipitations (pH about 4), Cr(VI) would be readily reduced in the presence of organic matter arising from bitumen. According to the Slovenian legislation [17] the maximal allowed Cr(VI) concentration in leachates from disposals of inert waste is 100 µg L⁻¹. Leaching of other metals: Pb, Ni, Cu, Cd and Zn in ground asphalt composites with addition of filter dust in water and salt water was negligible.

Investigation of the environmental impact of cement composites with addition of EAF dust

For estimation of environmental consequences of the use of EAF dust as an additive to cement, stable cement composites and cement composites with addition of 1.5 % of EAF dust by mass were investigated [8]. The leachability of total chromium and Cr(VI) was studied in compact and ground composites in water and salt water. The pH in leachates was not changed during the course of the experiment. high concentrations of water soluble calcium in the form of hydroxides regulated the pH of aqueous extracts and salt water leachates, which was highly alkaline. In aqueous and salt water leachates of cement composites and cement composites with addition of EAF dust the pH ranged between 11 and 13. In ground composites the pH was for one unit higher than in compact composites as a result of higher specific surface and consequently higher leachability of $CaCO_3$ and $Ca(OH)_2$. Due to higher ionic strength, the pH was for one unit higher in salt water composites. As a consequence of the high alkaline pH, the leachability of metals (with the exception of calcium) is generally very low. However, attention should be paid to soluble Cr(VI) concentrations.

Data of the leaching test indicated that during the course of the experiment

the total chromium and Cr(VI) were not leached with water in compact cement composites and compact cement composites with addition of EAF dust, while in ground cement composites and ground cement composites with addition of EAF dust total chromium and Cr(VI) were leached with water, but in very low concentrations (below 5.5 µg L^{-1} of total chromium). The leaching was more pronounced in salt water. In Figure 2 leaching from compact composites and in Figure 3 leaching from ground composites in salt water are presented. The data from Figures 2 and 3 indicate that more than 90 % of chromium in leachates was present in its haxavalent form. Namely, the traces of dissolved trivalent chromium are almost completely oxidized to its hexavalent state due to the high alkaline pH and the presence of oxygen. The extent of leaching of Cr(VI) in salt water was higher than in water due to the higher ionic strenght of salt water as leaching solution that causes more efficient leaching of Ca(OH)$_2$ and CaCO$_3$ and consequently higher pH of the leachate. It is known that higher pH values favour the existence of Cr(VI). Data from Figures 2 and 3 further indicate that leaching of Cr(VI) in salt water from compact and ground cement composites and cement composites with addition of EAF dust gradually increased with time and reached constant values after three months. During the course of the experiment the concentrations of Cr(VI) in leachates from compact cement composites in salt water (Figure 2(A)) did not exceed 20 µg L^{-1} and in leachates from compact cement composites with addition of EAF dust 40 µg L^{-1} (Figure 2 (B)).The difference (20 µg L^{-1} of Cr(VI)) corresponded to the leachability of Cr(VI) from EAF dust added to cement composite. More intensive leaching in salt water is observed from ground cement composites (up to 80 µg L^{-1} of Cr(VI)) (Figure 3 (A)) and ground cement composites with addition of EAF dust (up to 100 µg L^{-1} of Cr(VI)) (Figure 3 (B)). Again, the difference (20 µg L^{-1} of Cr(VI)) corresponded to the leachability of Cr(VI) from EAF dust added to cement composite. Therefore, Cr(VI) that originates from cement, mainly contributed to the leachability from cement composites with addition of EAF dust. The highest Cr(VI) concentrations that were observed in salt water leachates from ground cement composite with addition of EAF dust did not exceed 100 µg L^{-1}, that is according to the Slovenian legislation [17] the maximal allowed Cr(VI) concentration in leachates from disposals of inert waste. Leaching of other metals: Ni, Cu, Zn, Fe, Mg, Mn, Mo, Co, V, Cd and Pb from compact and ground cement composites and cement composites with addition of EAF dust is negligible in water and salt water.

Figure 2. Leaching of total chromium and Cr(VI) in salt water with time from compact cement composite (A) and compact cement composite with addition of 1.5 % of EAF dust by mass (B) (resumed from reference 8).
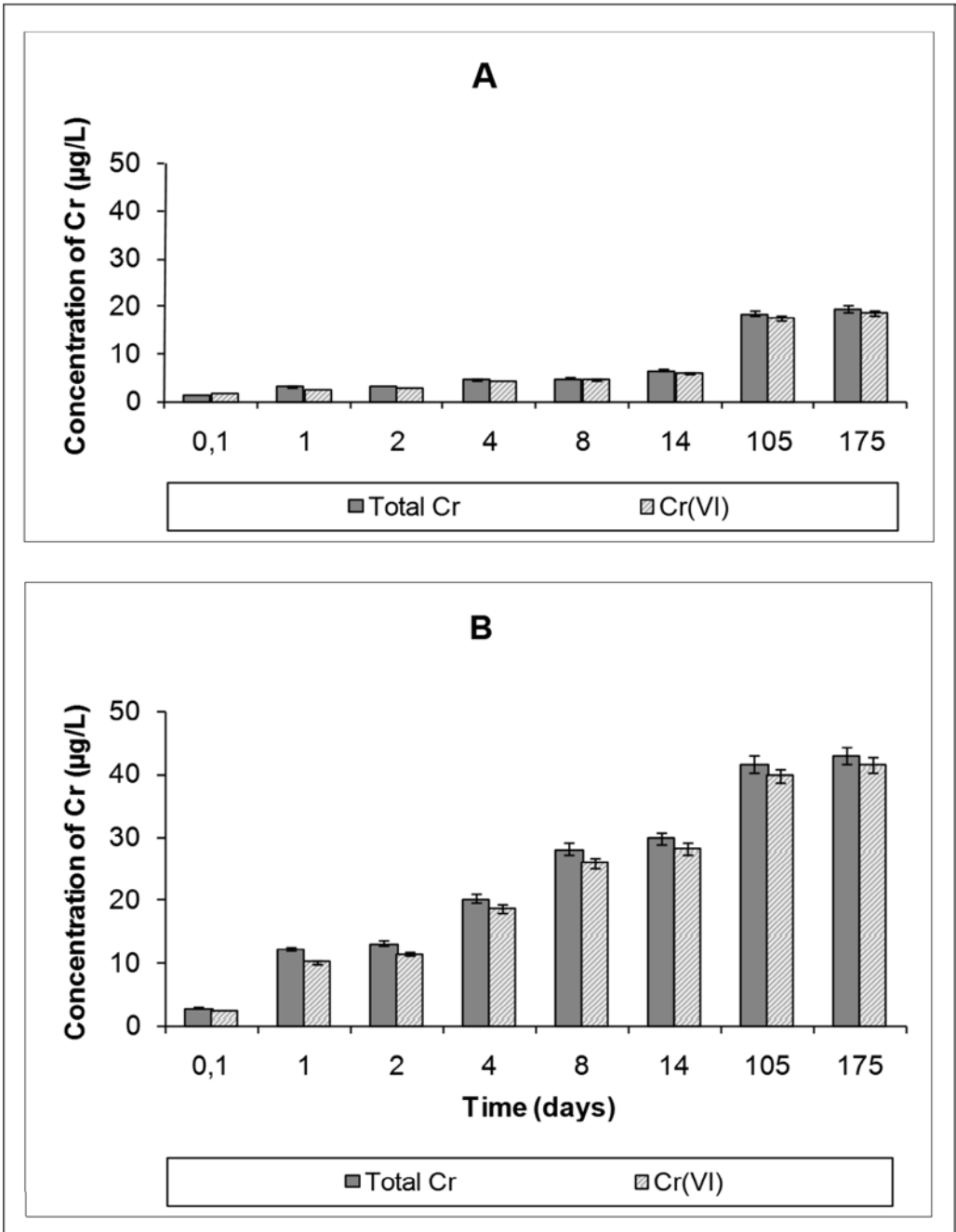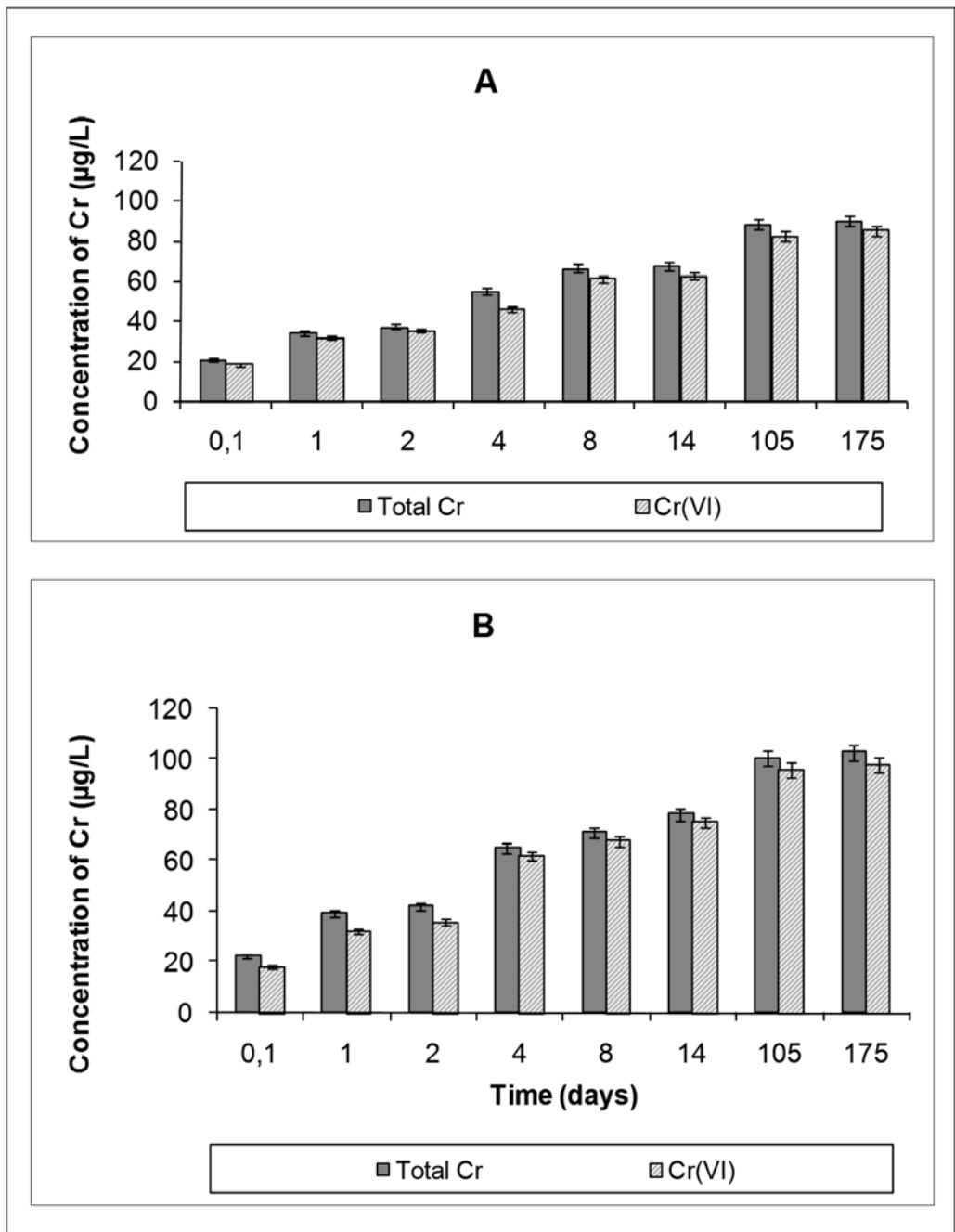
Figure 3. Leaching of total chromium and Cr(VI) in salt water with time from ground cement composite (A) and ground cement composite with addition of 1.5 % of EAF dust by mass (B) (resumed from reference 8).

Conclusions

In the present work long-term environmental impacts of asphalt and cement composites with addition of EAF dust were evaluated, on the basis of the literature data. Leachability tests based on diffusion were considered. The data demonstrated that leaching of metals from stable asphalt and cements with addition of EAF dust is negligible in water and in salt water. Salt water simulated the marine environment and salting of roads during the winter time. The only important metal species that was leached was Cr(VI). However, neither in ground asphalt and cement composites with addition of EAF dust, that simulated the worst case scenario when composites decomposes with time, nor when the salt water was used as leaching agent, concentrations of Cr(VI) that were leached did not represent an environmental hazard. Nevertheless, attention should be paid to ensure the conditions that prevent the leaching into the ground and/or drinking water reservoirs. From the environmental point of view, EAF dust in maximal addition of 2 % by mass can be used as an additive to asphalts for road construction and in civil engineering for all purposes, including applications in the external environment. Cement composites to which a maximum of 1.5 % by mass of EAF dust has been added can also be used in civil engineering for all purposes as well as for balances in washing machines. Such

balances can be, at the end of their service life, safely disposed in landfills. It is also important to stress that the re-use of EAF dust disburdens the landfills and prevents the latent environmental threat due to the dusty nature of EAF dust that contains also toxic Cr(VI). The re-use of EAF dust in road construction and in civil engineering represents positive environmental aspects. Since the recycling of EAF dust and its disposal on landfills are expensive, the re-use of EAF dust has also positive economic aspects.

References

[1] Geiseler, J. (1996): Use of steelwork slag in Europe. *Waste Management, 16*, pp. 59–63.

[2] Shi, C., Qian, J. (2000): High Performance cementing materials from industrial slags – a review. *Resources, Conservation and Recycling, 29*, pp. 195–207.

[3] Motz, H., Geiseler, J. (2001): Products of steel slags an opportunity to save natural resources. *Waste Management, 21*, pp. 285–293.

[4] Lind, B. B., Fallman, A. M., Larsson, L. B. (2001): Environmental impact of ferrochrome slag in road

construction. *Waste Management, 21*, pp. 255–264.

[5] CHAURAND, P., ROSE, J., BRIOIS, V., OLIVI, L., HAZEMANN, J. L., PROUX, O., DOMAS, J., BOTTERO, J. Y. (2007): Environmental impacts of steel slag reused in road construction: A chrystallographic and molecular (XANES) approach. *Journal of Hazardous Materials, B139*, pp. 537–542.

[6] PIORO, L. S., PIORO, I. L. (2004): Reprocessing of metallurgical slag into materials for the building industry. *Waste Management, 24*, pp. 371–379.

[7] VAHČIČ, M., MILAČIČ, R., MLADENOVIČ, A., MURKO, S., ZULIANI, T., ZUPANČIČ, M., ŠČANČAR, J. (2008): Leachability of Cr(VI) and other metals from asphalt composites with addition of filter dust. *Waste Management, 28*, pp. 2667–2674.

[8] ŠTURM, T., MILAČIČ, R., MURKO, S., VAHČIČ, M., MLADENOVIČ, A., STRUPI-ŠUPUT, J., ŠČANČAR, J. (2009): The use of EAF dust in cement composites: Assessment of environmental impact. *Journal of Hazardous Materials, 166*, pp. 277–283.

[9] U. S. Environmental Protection Agency, Guide for Industrial Waste Management [cited 3. 11. 2010]. Accessible on Internet: http://www.epa.gov/epaoswer/non-hw/industd/guide.htm 2, 1–20.

[10] KATZ, S. A., & SALEM, H. (1994): The Biological and Environmental Chemistry of Chromium. *220 East 23rd Street, New York: VCH Publishers, Inc*, pp. 1–10.

[11] LAFOREST, G., DUCHESNE, J. (2005): Immobilization of chromium(VI) eveluted by binding isotherms for ground granulated blast furnace slag and ordinary Portland cement. *Cement and Concrete Research, 35*, pp. 2322–2332.

[12] BATCHELOR, B. (2006): Overview of waste stabilisation with cement. *Waste Management, 26*, pp. 689–698.

[13] FLYHAMMAR, P., BENDZ, D. (2006): Leaching of different elements from subbase layers of alternative aggregates in pavement constructions. *Journal of Hazardous Materials, B137*, pp. 603–611.

[14] NEN 7345, (1995): Leaching characteristics of solid earthy and stony building and waste materials. Leaching tests. Determination of the leaching inorganic components from buildings and monolithic waste materials with diffusion test.

[15] HOHBERG, I., DE GROOT, G. J., VAN DER VEEN, A. M. H., WASSING, W. (2000): Development of a leaching protocol for concrete. *Waste Management, 20*, pp. 177–184.

[16] ŠČANČAR, J., MILAČIČ, R., SÉBY, F., DONARD, O. F. X. (2005): Determination of chromium in cement by the use of HPLC-ICP-MS, FPLC-ETAAS, spectrophotometry and selective extraction techniques. *Journal of Analytical Atomic Spectrometry, 20*, pp. 871–875.

[17] Regulation on waste disposal (2000). *Official Gazzete of Republic of Slovenia, 5*, pp. 511.

Adsorption capacity of the Velenje lignite: methodology and equipment

Adsorptivnost velenjskega lignita: metodologija in oprema

Janja Žula[1,*], Jože Pezdič[2], Simon Zavšek[1], Edi Burič[1]

[1]Velenje Coal Mine, Velenje, Slovenia
[2]GEORIS, Radovljica, Slovenia

*Corresponding author. E-mail: janja.zula@rlv.si

Abstract: Laboratory study of adsorption-desorption characteristics of various lignite lithotypes is very important for prevention of coal dust and gas outbursts that represent a dangerous and unpredictable phenomenon in underground mining of the Velenje lignite. The performed study consists of adsorption investigations carried out in the geotechnical laboratory of the Velenje Coal Mine (VCM). Lignite samples contained in the reaction cell were exposed for a limited time to a gas pressure of up to 100 bar. The measurements were performed on an updated instrument according to the improved volumetric gas sampling method. The gas was sampled from the reaction cell during the sorption simulation. Updating of the instrument affected positively the data quality. The performed three sets of measurements led to results that were crucial for further research. In the experiment, the amount of adsorbed and desorbed gas was calculated from the pressure difference in the known cell volume. The obtained results could permit the risk assessment of possible coal dust and gas outbursts. The performed tests shall enable a more exact determination and understanding of gas effects, possibly add some new knowledge to understanding of the dangerous phenomena, maybe also improve their prediction and lead to better safety in mining.

Izvleček: Laboratorijske raziskave adsorpcijsko-desorpcijskih lastnosti različnih litotipov lignita v Premogovniku Velenje so zelo pomembne pri raziskovanju in preprečevanju izbruhov plina in premogovega prahu, ki so nevarni in nepredvidljivi pojavi pri rudarjenju v omenjenem premogovniku.

Original scientific paper

Raziskovanje je zajemalo meritve sorpcijskih lastnosti lignita v geotehničnem laboratoriju Premogovnika Velenje, kjer so bili različni vzorci lignita zaprti v reakcijski celici in obremenjeni z do 100 bar plina za določen čas. Vzpostavili smo sistem meritev na posodobljeni napravi, izpopolnili volumetrično metodo in način vzorčevanja plina iz reakcijske celice med potekom simulacije sorpcije. Posodobitev naprave je vplivala na kvaliteto pridobljenih podatkov. Izvedli smo tri sklope meritev, ki so pokazali odločilne rezultate za nadaljnje raziskave. Po končanih meritvah sorpcije smo matematično določili količino adsorbiranega in desorbiranega plina iz razlike tlaka plina v znanem volumnu celice. S količino plina ocenimo stopnjo tveganja pri odkopavanju različnih plasti premoga, kjer lahko pride do vdora plina. S temi poskusi bo mogoče bolj natančno opredeliti in razumeti plinske efekte v Premogovniku Velenje in morda tudi prispevati k razumevanju nevarnih dogodkov, njihovemu morebitnemu napovedovanju in s tem k večji varnosti.

Key words: sorption, lignite, lithotype, laboratory experiments, Velenje Coal Mine – Slovenia

Ključne besede: sorpcija, lignit, litotip, laboratorijski poskusi, Premogovnik Velenje – Slovenija

Introduction

Various lignite lithotypes are of microporous structure in which the gas occurs compressed in the pores, cleats and capillaries. The gas in these tiny spaces can be in gaseous, liquid or even solid state. The basic lignite lithotypes are determined macroscopically, and they can be recognized with an unaided eye. The lithotypes are named according to the classification of the International Committee for Coal and Organic Petrology (ICCP, 1993) (e.g. in Taylor et al. (1998), p. 280).

A gas-mix accumulated in a coal, termed as the coalbed gas, can be of various origins and migration paths and this is also an outstanding fact in the case of the Velenje lignite. This thematic was thoroughly studied by Pezdič and his co-workers for almost 15 years - from 1998 onwards - and is in details well documented in yearly-made elaborations for the VCM company as "Monitoring of gas components" in the Velenje Coal Mine as well as published in papers by Kanduč et al. (2003), Kanduč (2004), and Kanduč & Pezdič (2005). The content presented in this paper is mainly a summary from the B.Sc. thesis work of the first author (Žula, 2006), which was also mentored by professor Pezdič.

Coalbed gases, together with rock-mechanical properties of the lignite in different areas of the Velenje lignite mining are highly responsible for dynamical processes during advancement of mine workings. Among them, the most dangerous events are sudden coal-falls, gas exhalations, gas and lignite outbursts, and pillar chocks. This thematic was studied and evidenced for decades. More recently, it was summarized and interpreted in representative works of LIKAR (1995), ZAVŠEK (2004) and in many working reports and studies cited by these two authors. In connection with rock-mechanics, LIKAR and his co-workers studied in the 1990 and 2000 also sorption of gases in lignite at different strain conditions (PEZDIČ et al. 1999 a, b). Results and long-term investigation are also archived at the VCM in the form of annual reports and elaborations.

The coalbed gas occurs in pores and cleats of coal under the lithostatic pressure of rocks above the coal seam and under the pore pressure. When pressure decreases, the gas is released from the coal, and can migrate freely. Migration of gas is especially enhanced in tectonized zones along fault systems. Gases can be accumulated in the void volumes (pores, cleats, crushed zones, chambers) of various sizes both adsorbed on the surfaces and dissolved in water. Studying gases in coals and their adsorption/desorption behavior is

of great interest in the last two decades especially in connection with efforts to assess potential of coals as a geological medium for eventual storage of CO_2, particularly in combination with enhanced methane recovery. In this context, at least studies of sorption on different coals worldwide should be mentioned here: LITWINISZYN (1990), GAMSON et al. (1996), PEZDIČ et al. (1999b), MASTALERZ et al. (2004), MAJEWSKA et al. (2009), GRUSZKIEWICZ et al. (2009), WENIGER et al. (2010). In 2009, a special issue of the International Journal of Coal Geology (Vol. 77/1–2) was devoted to CO_2 sequestration in coals and enhanced coalbed methane recovery.

The origin of gases can be inferred from the isotope composition of its gas components. Such a pioneering study for the Velenje lignite was carried out by KANDUČ & PEZDIČ (2005). On the basis of carbon isotope composition of carbon dioxide and methane they concluded that the following types of origin of CO_2 and methane can be recognized: microbial methane and CO_2, methane generated by microbial CO_2 reduction and/or methane affected by processes of oxidation, and endogenic CO_2.

The isotope composition of coal-bed gases is affected by a range of factors: the original organic matter composition, temperature, Eh-pH conditions, microbiological activity, so called secondary processes (diffusion, migration,

oxidation), and by mixing of gases of various origin (Kanduč & Pezdič (2005); and references there-in).

Gases in the Velenje basin are of a highly variable composition both within the lignite seam and the non-coaly basin sediments. According to data from Kanduč & Pezdič (2005), the CDMI (carbon dioxide to methane index expressed as $\varphi(CO_2) \times 100/\varphi(CO_2 + CH_4)$) varies between 80 % and 99 % in the lignite-seam gases (with very rare exceptions of the CDMI being considerably below 80 %), whereas this index is from 1 % to ca. 55 % in the gases as coming from the subsurface wells penetrating different basin sediments and the pre-Pliocene basement rocks. Considerably variable is also content of N_2, i.e. between 0 % and almost 55 % (as reported in Kanduč & Pezdič (2005)), but this range is highly dependent on the sampling approach (see samples of the A and B types in Table 1 in Kanduč & Pezdič (2005)). It is evident that the gases in the Velenje lignite (as well as in other lithologies) have various origins and are affected by possible mixing and changes owing to different physicochemical properties of methane and CO_2 during gas migration (Kanduč et al. (2003), Kanduč & Pezdič (2005)). Amount of the gas sorbed in the coal depends also on pressure, temperature, mineral matter, moisture and the coal lithotype. Rate of achieving the adsorption equilibrium depends on the sorption rate in pores and on gas diffusion into the porous coal matrix (Pezdič (1999), Kanduč (2004)).

In closed systems, as e.g. in areas of still un-excavated and relatively undisturbed parts of coal/lignite seams, accumulations of gases at high pressures may occur. In a final stage, they may attain or exceed the value of the lithostatic pressure. Such circumstances are characteristic for zones ahead of mining longwalls and mine-road faces (Kanduč et al. (2003), Kanduč & Pezdič (2005)). Opening of such a zone is often a highly dynamic process that can lead to a coal-dust and gas outburst. As the total and partial pressure of the adsorbed gases decreases, this can affect a wider area of the coal seam. In dependence of conditions and properties of the coal matter, the gas desorption can be a sudden, momentary event (e.g. Likar (1995), Zavšek (2004)).

Sorption method, equipment and measurements

The quantity of adsorbed gas was determined according to the sorption method, as described in Pezdič et al. (1999b). For measuring the adsorption-desorption properties of various lignite lithotypes at high pressures (up to almost 100 bar), the volumetric method was applied.

For calculating the quantities of adsorbed gas the theoretical bases were used as cited in PEZDIČ et al. (1999b) and in ŽULA (2006), taken mostly after MOORE (1974). We proceeded from the general gas law (1) and the real gas law (2) (see e.g. in LAZARINI & BRENČIČ, 1992):

$$PV = nRT \qquad (1)$$

For gases deviating from ideal conditions the gas equation for real gases is used, the so-called van der Waals equation.

$$(P + an^2/V^2)\,(V - nb) = nRT \qquad (2)$$

We calculate the volume of the adsorbed gas V_a after equation (3):

$$(P_0 - P_t)\,V_{free} = V_a\,P_a \qquad (3)$$

P_0 is the initial pressure, P_t is the pressure determined after a certain time period t, P_a is 1.013 bar and V_{free} the volume in autoclave.

Amount of the adsorbed gas is given in three different ways (4, 5, 6):

$$V_{adsorb} = V_a/m_{material} \quad (L/\,kg) \qquad (4)$$
$$n = V_{adsorb}/V_0 \qquad (mmol/kg) \qquad (5)$$
$$m_{gas} = nM/1000 \quad (g/kg) \qquad (6)$$

Equipment
The apparatus for gas sorption measurements has been set in the Geotechnical laboratory of the VCM. Measurements of sorption were performed on the third modification of the high-pressure system as initially used by PEZDIČ in 1998 (Figure 1).

The apparatus has been meanwhile improved by adding a new measurement registering system. Readings of pressure and temperature are now directly transformed to graphic signals that are continuously monitored on a display (Figure 2). In this way, by updating the computer program (SUPOVEC & FILIPIČ, 2004), detection of temperature and pressure signals became more accurate, since being performed in one second time intervals. This permitted registration of the most important data during the first minute after dosing, when adsorption is at the highest. Added were also two additional temperature sensors for registration of temperature in the system and in the room. The system temperature (T_{system}) is measured on the housing of autoclave with a temperature sensor (PT1000) fixed to the housing. An additional construction improvement was done on net volume of autoclave. The robe for pressure measurements was placed closer to autoclave, and the volume reduced by valve (V). The additional valve on the autoclave permits the extraction of gas during adsorption (Figure 3).

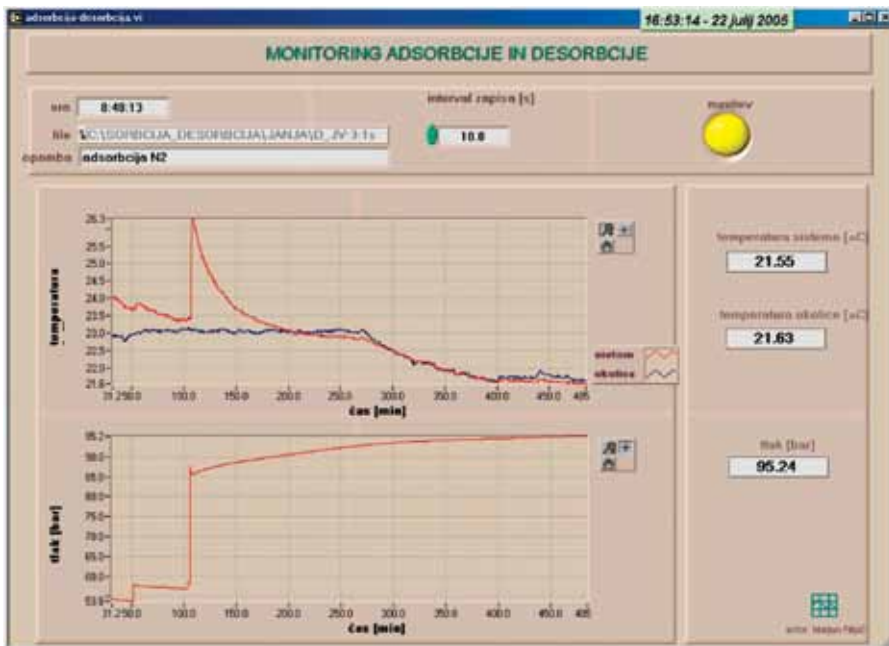**Figure 1.** Modernized apparatus for sorption measurements - autoclave, probe, valves, software application

Figure 2. Computer output of pressure and temperature measurements (Supovec & Filipič, 2004).
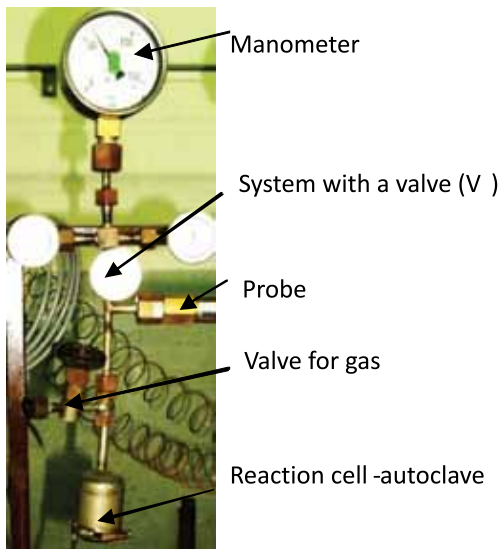
Figure 3. System with the reaction cell

Sampling of lignite
Lignite was sampled in borehole cores, and from mine road and longwall faces (Table 1).

Six distinct samples differing in their lithotype composition were prepared and classified according to the ICCP classification (1993) (in: Taylor et al. (1998), p. 280). Sample 1 was pure xylite (X), and samples 3 and 4 were xylite-rich and xylite very rich lignite lithotypes. Samples 2, 5 and 6 were lithotypes of fine detrital lignite. Among them, sample 2, which was taken from a fault zone, and sample 5, both exhibited a pronounced degree of gelification. Generally speaking, fine detrital and gelified lignite is more characteristic for the upper and the inner part of the Velenje lignite seam, whereas more or less xylite-rich lignite predominates in the lower and the outer part of the seam (Markič & Sachsenhofer, 1997, 2010). In Table 1, petrographic composition is also expressed in terms of lithotype components (in percents and by code values) as introduced by Markič et al. (2001) and Markič & Sachsenhofer (2010).

For a sorption measurement around 100 g of crushed lignite material of 2−4 mm grain size was used.

Measurement process
The whole sorption measurement process consisted of five steps. In the first step, after dosing to ca. 60 bar CO_2, adsorption was measured for 45 min. In the following step, dosing to ca. 60 bar CO_2 was repeated and adsorption was measured again for 45 min. After that, the type A gas sampling was performed. As during the gas sampling some pressure in the flask was lost, the missing CO_2 was replaced.

Into the equilibrated sample, we added nitrogen N_2 overpressure up to a total pressure around 85 bar. Adsorption of the gas mixture (CO_2+N_2) lasted for additional six hours. After completed adsorption of the (CO_2+N_2) gas mixture, we performed the B type gas sampling and then exposed the sample to atmospheric pressure (1 bar). Desorption followed, and was measured for 15 h.

Table 1. Samples chosen for sorption tests

Sample 1: Xylite; X 100 %

Petrographic code: 3

Sample 2: Fine detrital gelified lignite
(from a fault zone !)

fD 90 % G 10 %

Petrographic code: 9.5

Visible are milimeter thick white
CaCO3coatings over vegetal remains

Samp. 3: Xylite-rich lignite

dXxD 20 % fD 80 %

Petrographic code: 8.4

Samp. 4: Xylite very rich lignite

X 80 % dXxD 10 % fD 10 %

Petrographic code: 3.75

Samp. 5: Fine detrital gelified lignite

X 15% fD 65% G 20%

Petrographic code: 9.5

Visible are milimeter thick white
CaCO3coatings over vegetal remains

Sample 6: Fine detrital lignite

dXxD 7% fD 93 %

Petrographic code: 8.95

Sampling of gas components from an autoclave

For gas sampling during sorption a special equipment shown in Figures 4, 5 was used. Gas capture from an autoclave was a two-step procedure. First, the gas was captured into a piston ampoule (1 bar), and then transferred to a laboratory ampoule. Two types of sampling were differentiated, the type A and type B sampling.

The type A sampling was carried out at the end of the second CO_2 adsorption phase i.e. after 90 min from the beginning of the adsorption measurements.

The type B sampling was capture of gas mixture ($CO_2 + N_2$) in autoclave. It was carried out 6 h after N_2 dosing, just before desorption.

Gas analysis was performed on a homemade NIER mass spectrometer at the J. Stefan Institute in Ljubljana.

RESULTS

Because gas sorption in a coal is dependent on coal´s solid matter composition, moisture content, pressure, time and kind of gas dosed, and because gas composition is alternating due to dosing of different gases and due to adsorption/desorption effects, three sets of measurements were performed. The 1st set represents measurements at varying moistures, the 2nd set comprises measurements on various lignite lithotypes, and the 3rd set represents comparison of composition of gases as sampled at varying pressures (ŽULA, 2006).

First set of measurements

The 1st set of measurements was done on sample Nº 3 (see Table 1) of the following lithotype composition: fD 80 % dXxD 20 %. In order to study influence of moisture on sorption, the whole sample was split into three

Figures 4. (left) and **5.** (right): Gas sampling into a piston ampoule (1 bar) from autoclave (at 60 bar to 100 bar), and then transferring of gas to a laboratory ampoule.

parts to measure moisture contents at three stages/conditions:

- at the initial stage (sample-part S-1),
- after moistening with 20 mL of distilled water, before sorption (sample-part M-1),
- after moistening with 10 mL distilled water, after sorption (sample part M-2).

Measurements were performed by a simple experiment. As gas, only CO_2 was used. The autoclave with lignite sample was dosed by CO_2 and left for 45 min for the adsorption to take place. The same time duration was applied for desorption.

The results are given in Tables 2–4:

Moisture content at the as received (a. r.) basis of the "initial" sample-part S-1 was 50.00 % (Table 2). This moisture content is very close to a real bed-moisture content (at the ash-free basis) as typical for the Velenje lignite regarding its coalification rank (Markič & Sachsenhofer (2010), p. 141-153).

Additional moistening of the sample-part M-1 with 20 mL distilled water (Table 3) resulted in an increase of moisture from 50.00 % (S-1) to 83.60 % (M-1). Additional moistening of the sample-part M-2 with "only" 10 mL distilled water

Table 2. Measurement results for S-1

Sample	Test	m(p1) (g)	m(p2) (g)	P_0 (bar)	$\Delta p_{ads.}$ (bar)	Ads. (g/kg)	$\Delta p_{des.}$ (bar)	Des. (g/kg)	Moisture1 (%)	Moisture2 (%)
S-1 a. r. moisture	CO_2	57.52	57.62	52.69	−1.30	**2.47**	1.39	**1.65**	**50.00**	**42.25**

Table 3. Measurement results for M-1

Sample	Test	m(p1) (g)	m(p2) (g)	P_0 (bar)	$\Delta p_{ads.}$ (bar)	Ads. (g/kg)	$\Delta p_{des.}$ (bar)	Des. (g/kg)	Moisture1 (%)	Moisture 2 (%)
M-1 a.r. moisture + 20 mL distilled water	CO_2	58.71	58.80	55.05	−4.05	**7.48**	2.71	**5.16**	**83.60**	**81.02**

Table 4. Measurement results for M-2

Sample	Test	m(p1) (g)	m(p2) (g)	P_0 (bar)	$\Delta p_{ads.}$ (bar)	Ads. (g/kg)	$\Delta p_{des.}$ (bar)	Des. (g/kg)	Moisture1 (%)	Moisture 2 (%)
M-2 a.r. moisture + 10 mL distilled water	CO_2	59.98	60.12	52.98	−2.78	**5.10**	2.51	**4.61**	**59.74**	**59.49**

(Table 4) resulted in an increase of moisture from 50.00 % (S-1) to "only" 59.74 % (M-2). Both additionally moistened sample-parts showed significantly larger adsorption and desorption than the initial sample (S-1) (Tables 2−4). CO_2 adsorption in additionally moistened sample-parts M-1 and M-2 was 2 to 3 times greater (more effective) than in S-1, and similarly was desorption. After sorption, moisture content of the sample-parts was measured again ("moisture 2" data in Tables 2−4). After sorption, the moistures decreased as follows: in sample S-1 for 7.75 %, in sample (M-1) for 2.58 %, and in sample M-2 for 0.25 %.

Second set of measurements

Sorption measurements were performed on six samples (1, 2, 3, 4, 5, 6), differing in lithotype composition (Table 1). Detailed measurements for all samples are given in Žula (2006), whereas in this paper, measurements for all samples are given only graphically (Graphs 3, 4, 5), and only exampling tabular data will be presented and discussed (Table 5).

On each sample, two identical measurements were done. Between the two measurements on the same sample, slight deviations appeared - most probably due to heterogeneity of samples, different initial sample weights, dosage velocities, amounts of dosed gas, slight temperature differences and slight differences in moisture.

As an example, results for sample N° 2 are presented in Table 5.

Explanation of results in Table 5 and pressure conditions shown in Figures 6, 7, 8.

- After first dose (56.50 bar CO_2), lignite adsorbs in 45 min 3.65 bar or 6.65 g/kg (grams of gas per kilogram of coal).
- After second dose (58.15 bar CO_2), in the next 45 min, lignite adsorbs 1.28 bar or 2.33 g/kg.
- In total it adsorbs 4.93 bar or 8.98 g/kg.
- Third dose (58.60 bar CO_2) represents a maximal filling of reaction cell with CO_2.
- The fourth stage is dosing 87.26 bar N_2 onto equilibrated sample. At the first moment, in less than 1 minute, the total pressure decreases for 2.15 bar, but then, after ca. six hours, it increases up to 95.12 bar. In total, 10.02 bar of gas or 18.25 g/kg (grams of gas per kg of coal) became released. A momentary pressure decrease after N_2 dosing is also characteristic for other samples (as measured by Žula (2006)). Subsequent slowly permanent increase in pressure for about 10 bar to 11 bar in six hours or so, indicates release of gas from coal. This is maybe the most important phenomenon in sorption investigations of the Velenje lignite. It was already clearly

Table 5. Adsorption and desorption key data for sample № 2 from Table 1 based on two repeated measurements (2-1 and 2-2). Sample composition: fD 90 %, G 10 %, autoclave volume: 105 mL, coal mass: 60 g, environmental temperature: 22 °C, V_0: 24.12 mL/mmol, specific mass: 1.33 g/cm³, free volume: 59.9 mL. Dots indicate gas sampling. Abbreviations W1 and W2 mean two measurements of mass of coal samples analyzed. T_{sist}/K is temperature of system in autoclave in Kelvin scale. P_1 to P_4 are starting pressure (e.g. 56.50 bar) and pressure after a certain time (e.g. 52.85 bar). P_x is increased pressure at adsorption. Δp_{ads} is difference in pressures due to adsorption, and Δp_{des} is difference in pressures due to desorption. Ads. and Des. are amounts of adsorbed and desorbed gas(es), respectively, expressed in grams of gas per kilogram of lignite.

Sample	Test	W1 (g)	W2 (g)	Time (h)	Tsist. (K)	P (bar)	Δp ads. (bar)	Ads. (g/kg)	Δp des. (bar)	Des. (g/kg)
2-1		60.0	60.11	0						
	(CO₂)			0.001	297.18	(P1) 56.50	-3.65	6.65		
				0.75		52.85				
	(CO₂)			0.76	296.43	(P2) 58.15	-1.28	2.33		
•				1.50		56.87				
	(CO₂)			1.63	295.90	(P3) 58.60				
	(N₂)			1.75	296.02	(P4) 87.26	-2.15			
				1.76		85.11				
				1.76			+10.02	18.25		
•				8		(Px) 95.13				
	Drop of pressure to 1 bar and desorption of gas (mainly CO₂+N₂) lasting for 15 hours								6.67	**12.09**
2-2		60.0	60.22	0						
	(CO₂)			0.001	296.72	(P1) 57.48	-2.92	**5.31**		
				0.75		54.56				
	(CO₂)			0.76	296.89	(P2) 59.05	-1.01	**1.84**		
•				1.51		58.04				
	(CO₂)			1.63	296.48	(P3) 59.55				
	(N₂)			1.76	296.56	(P4) 87.05				
						85.01	-2.04			
							+10.70	19.48		
•				8		(Px) 95.71				
	Drop of pressure to 1 bar and desorption of gas (mainly CO₂+N₂) lasting for 15 hours								6.89	**12.55**

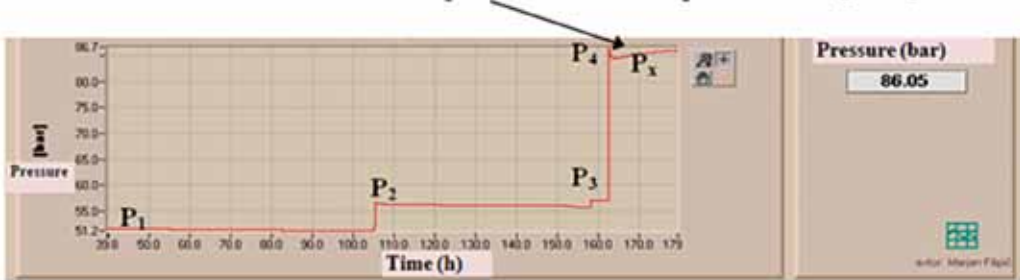**Decrease and then increase of pressure at adsorption of CO₂ + N₂**

Figure 6. Graphic presentation of the used starting pressures (P_1, P_2, P_3, P_4) with adsorption in particulate phase and especial event (P_x) with decrease and then increase of pressure during the adsorption process of CO₂ + N₂ mixture.
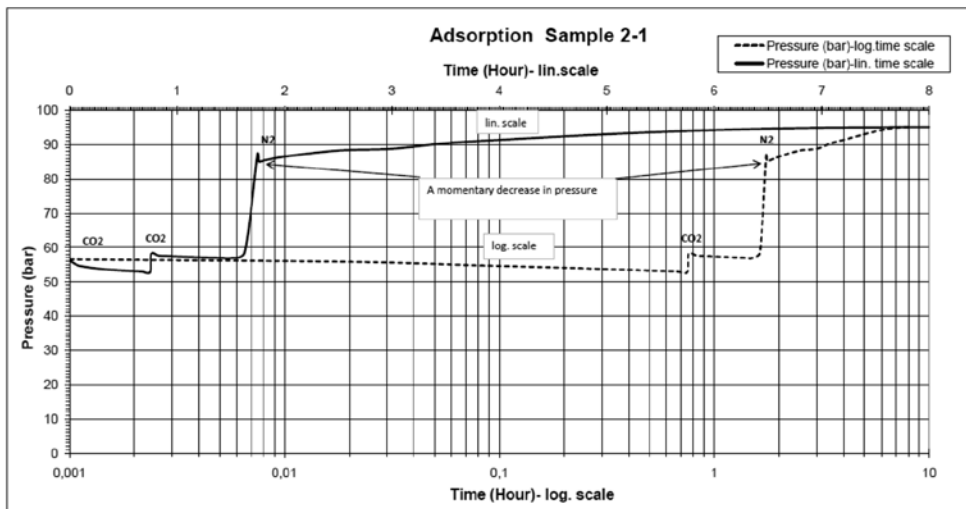
Figure 7. Pressure behaviour as measured in autoclave after 1st and 2nd dosing by CO_2, and after dosing by N_2 (in a linear and the logarithmic scale). Note that dosing by CO_2 causes adsorption of gas into coal substance (detected as two slight decreases of pressure in the first two 45 min lasting steps), and that N_2 dosing causes - after an instant time of adsorption - a release of gas from coal (detected as slight increase and then stabilizing of pressure in the time interval between 1.75 h and 8 h). Note also considerably higher pressure of N_2 dosing in comparison to CO_2.
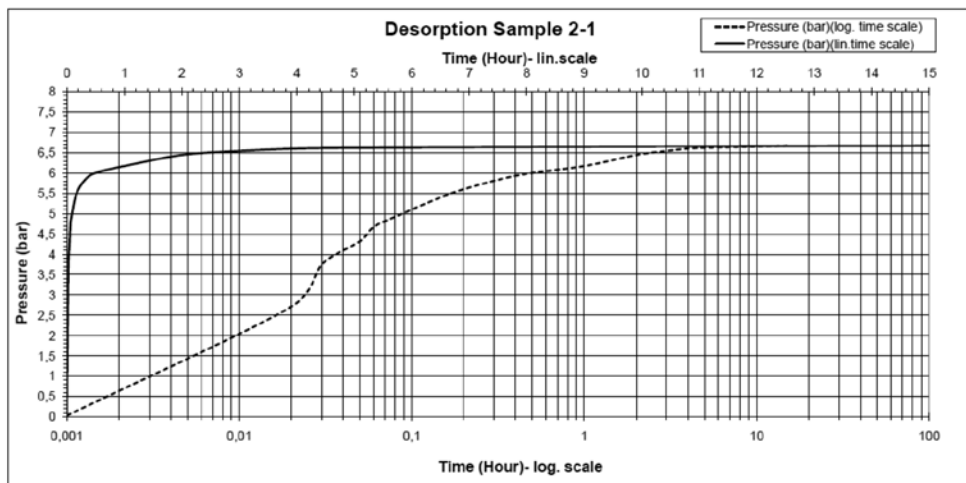

Figure 8. Desorption of gas from sample 2-1. Measurements expressed by Δ pressure values are shown in a normal linear scale and the logarithmic scale, respectively.

detected by Pezdič at el. (1999b) and was explained by different possible processes, which would need additional investigations. One explanation is enhanced release of gases from coal, and some other explanations are thoroughly given in Pezdič et al. (1999b), Pezdič et al. (2007) .

- Comparing results for sample 2-1 and 2-2, adsorption due to CO_2 dosing is slightly more effective for the first sample, whereas gas release due to N_2 dosing is somewhat higher in the second sample.
- Desorption is 6.67 bar or 12.09 g/kg in the first measurement case (2-1), and 6.89 bar or 12.55 g/kg in the second case (2-2), respectively.

Sample 1-1 and Sample 4-1:
Samples 1-1 (X 100 %) and 4-1 (X 80 %, dXxD 10 %, fD 10 %) are very similar in lithotype composition, but demonstrate quite diverse sorption characteristics (Figure 10). In the first and the second CO_2 loading stage together, sample 4-1 adsorbed 3.26 g/kg or 43.10 % less of CO_2 than sample 1-1 with 5.73 g/kg.

Additional N_2 pressure caused initially a slight decrease of the total pressure in both samples, but then the pressure started to rise (as principally visible from Figure 7), and reached after six hours the value of 90.25 bar for sample 1-1 and the value of 92.57 bar for sam-

ple 4-1. Sample 1-1 released 5.87 bar of gas or 10.44 g/kg, whereas sample 4-1 released 11.09 bar of gas or 19.01 g/kg i.e. for almost 80 % more than sample 1-1.

Proportion of released gas depends on the proportion of adsorption in the first two steps, on CO_2 compression at the time of addition of N_2 overpressure, and on velocity of gas mixture release, as we decreased the pressure to 1 bar. For the same reason desorption varies too. The desorption for sample 1-1 equals to 5.30 g/kg or to 32.78 % of the wholly adsorbed gas (5.73 + 10.44 g/kg), and for 4-1 to 3.74 g/kg or 16.80 %. Already our findings so far categorized the samples of such entirely xylite, and xylite-very-rich lignite lithotypes as the most resistant for sorption. In this sense, our present measurements published in this paper confirm this finding once again.

Sample 3-1 and Sample 6-1:
Samples 3-1 (dXxD 20 %, fD 80 %) and sample 6-1 (dXxD 7 %, fD 93 %) differ significantly in content of xylite-detrite (dXxD) component. Even though this difference (20–7 %) is numerically not very big it seems to be decisive to give the two samples quite distinctive gas adsorption characteristics.

As visible from Figure 10, total CO_2 adsorption in the sample 3-1 amounts

to 6.06 g/kg, and in sample 6-1 to 7.62 g/kg. In the second stage, less than a half of gas than in the first stage was adsorbed.

Additional N_2 pressure caused initially a slight decrease of the total pressure for both samples, but afterwards the pressure started to rise and reached the value of 95.25 bar for sample 3-1, and 93.93 bar for sample 6-1. Sample 3-1 released 16.06 g/kg of gas and sample 6-1 16.69 g/kg of gas. Desorption of the sample 3-1 equals 8.09 g/kg or 36.57 %, and of the sample 6-1 7.09 g/kg or 29.90 %.

Sample 2-1 and Sample 5-1:
Samples 2-1 (fD90%, G10%) and sample 5-1 (X 15 %, fD 65 %, G 20 %) have the same lithotype code (9.5), although their composition is different. The sample 2-1 comes from a fault zone and the sample 5-1 from a borehole. What is common to both samples is remarkable degree of gelification which was most probably enhanced due to alkalinity evidenced by e.g. carbonate coatings of vegetal remnants (see Table 1). Their gas adsorption and desorption values are much higher than for all previous samples, and this feature is connected to our opinion to gelification. Total adsorption of sample 2-1 is 8.98 g/kg, and of sample 5-1 9.80 g/kg (Figure 10). Compared to the sample 4-1 with the lowest adsorption, this is around 60 % more.
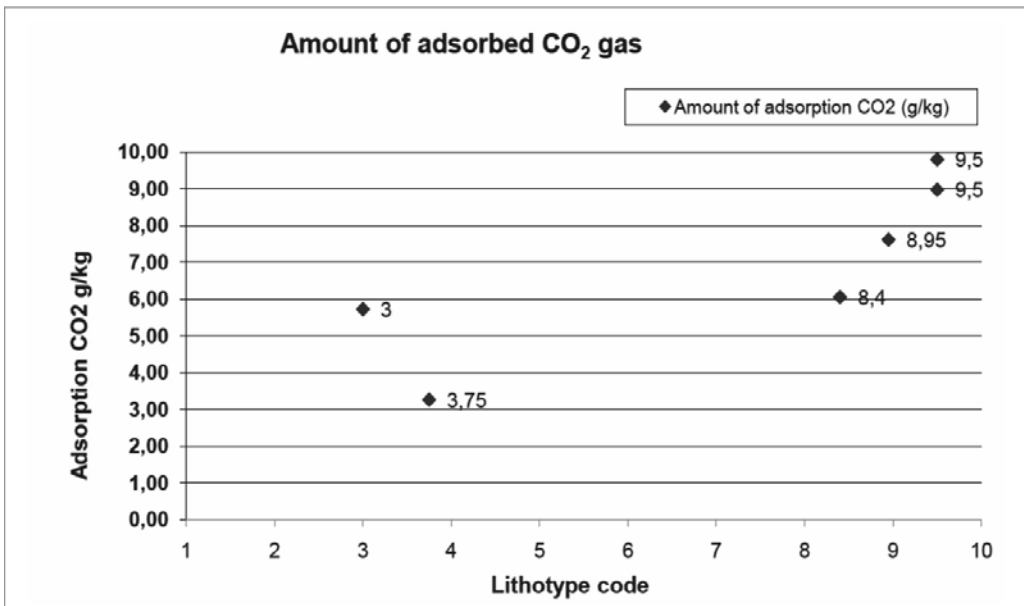

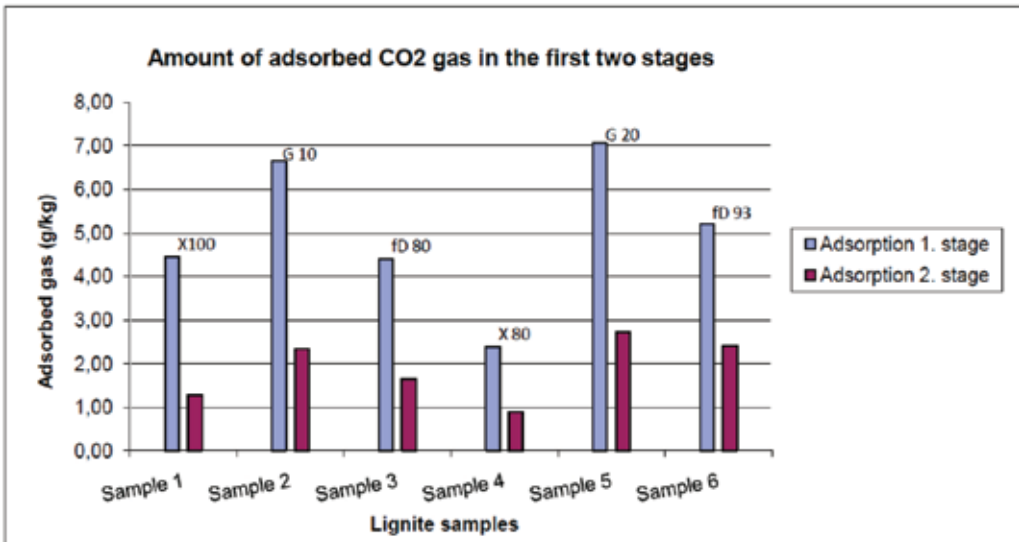**Figure 9.** Amount of adsorbed CO_2 gas depends on lithotype code

Figure 10. Amounts of adsorbed CO_2 as achieved by 1st and 2nd step of dosing by CO_2 at pressures of between 55 bar and 59 bar. Time of adsorption was 45 min for each step.
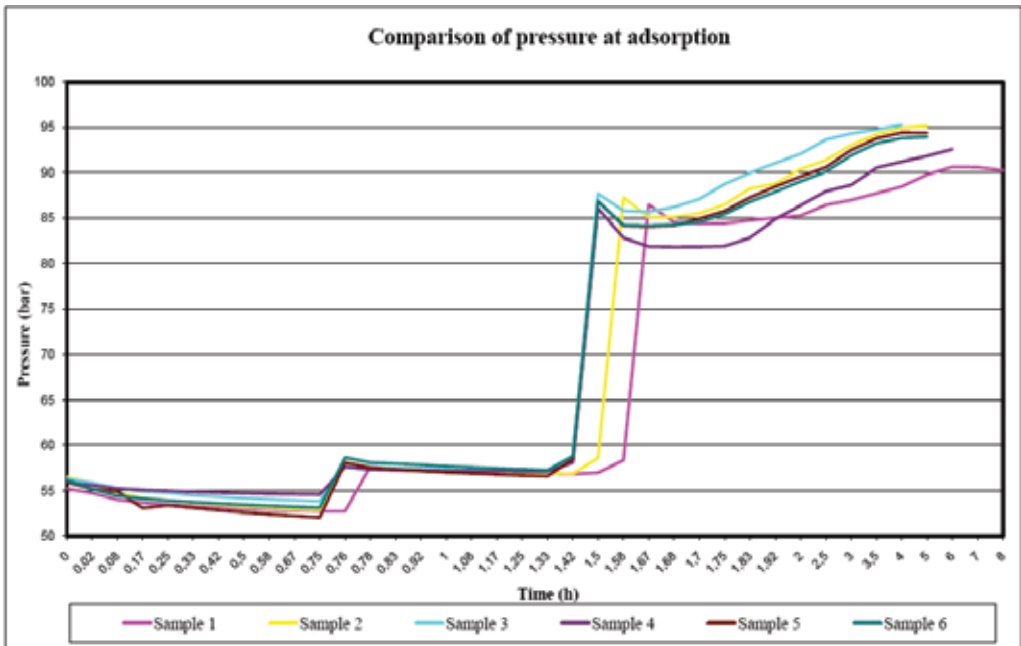

Figure 11. Pressure-to-time behaviour for all samples during adsorption.
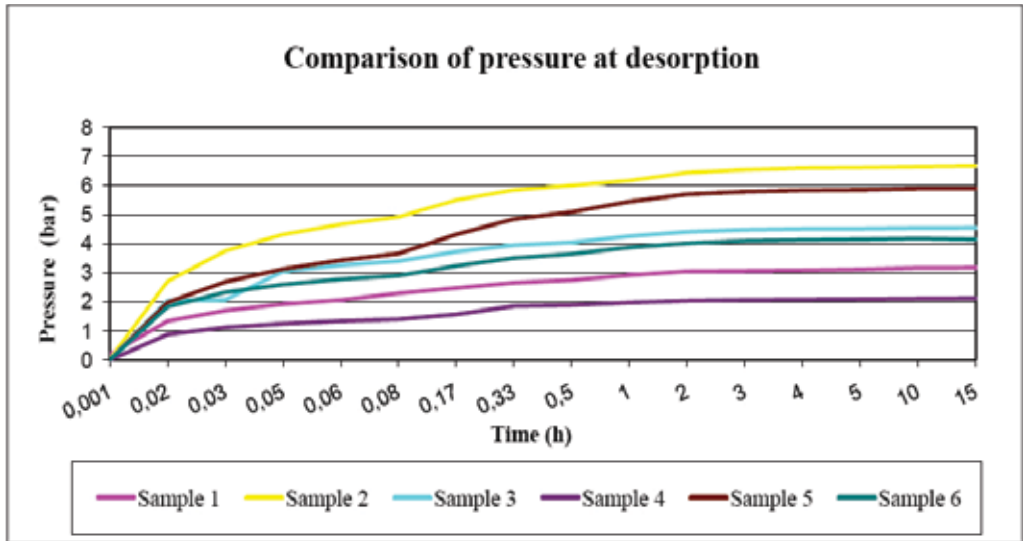
Figure 12. Pressure increase in autoclave during desorption of gas from the 1 to 6 samples.

Also in these two cases the additional N_2 pressure caused initially a slight decrease of the total pressure at both samples, but then the pressure started to rise and it reached the value of 95.13 bar for sample 2-1 and 94.38 bar for sample 5-1, respectively. Sample 2-1 released 10.02 bar of gas or 18.25 g/kg, and sample 5-1 released 10.03 bar of gas or 18.78 g/kg. As the proportion of adsorption is considerably higher than for other samples, also the proportion of desorption will be higher. Desorption of the sample 2-1 equals 12.09 g/kg or 44.40 %, and of the sample 5-1 10.74 g/kg or 37.58 %.

Third set of measurements
With the intention to explain the appearance of the newly arisen P_x of gas, we

have sampled the gas for analysis from autoclave during the adsorption process. During each sorption process, the gas components were sampled twice - by **sampling A** (at the end of the second step of adsorption of CO_2 - i.e. after 90 min), and **sampling B** (after dosing by N_2, just before desorption) (see also chapter about sampling of gas components). Into a piston ampoule, one bar of gas sample was taken. Results of gas composition of the A and B samplings in the case of samples 2-1 and sample 2-2 (in fact two parts of the same lignite lithotype) are presented in Table 6.

In all cases of the type A sampling, the gas analysis resulted to more than 90 % of CO_2 (in the case of 2-1 in Ta-

Table 6. Gas composition of sampling A and B during sorption of a gelified fine detrital lignite (fD90 G10) sample duplicates 2-1 and 2-2. Time of sampling, temperature and pressure in autoclave are given for complete information.

Sample	Composition	Sampling	t/h	T/K	P/bar/	Gas sample composition, φ/%				
						CH4	N2	O2	CO2	Ar
2-1	fD 90 % G 10 %	A	1.5	295.9	(P_3) 58.6	0.1	1.1	0.7	98.2	0
		B	6	294.4	(P_x) 90.7	1.5	67.2	0.9	30.1	0.4
2-2	fD 90 % G 10 %	A	1.5	296.4	(P_3) 58.0	0.3	2.5	0.6	96.6	0
		B	6	295.9	(P_x) 95.6	0.2	69.0	0.3	30.2	0.4

ble 6 even more than 95 %), and the remaining 10 % of CH_4, N_2 and O_2. In the case of the type B sampling the gas analysis resulted (Table 6) to more than 60 % of N_2, around 30 % of CO_2, and the rest represented by CH_4, N_2, O_2 and Ar. Minimal amounts of the last two gases appear owing to presence of air in the dosing pipes. The CH_4 is the residue from the coal matrix.

In the procedure, the proportion of the added N_2 pressure reached only around 30 % of the total pressure. Gas analysis resulted into around 60 % of N_2.

Regarding these results it can be inferred that the additional N_2 overpressure caused CO_2 compression and consequently condensation. Instead of 30 % N_2 as much as 60 % (i.e. ca. two times more) of N_2 could be dosed on account of CO_2 compression.

Results of gas analysis permit to explain the reasons for appearance of the newly arisen P_x pressure after the third dosing step in the confined system. It can be affirmed that 10 bar were released from the sample's structure, as two times more N_2 gas than supposed entered the system.

Discussion

Experience with coal mining and coal dust and gas outbursts so far (e.g. overview in Likar (1995); and references there-in) indicates that these events are connected to a considerable degree to occurrences of masses of fine detrital lignite varieties, especially if the lignite is gelified (Markič et al. (2001)). On the laboratory level, an outstanding gas proneness of the fine detrital gelified lignite variety was already ascertained by several studies, such as those of Zapušek & Hočevar (1998), Likar (1999), Pezdič et al. (1999a,b), Zavšek (2004), Likar et al. (2008).

1. We established a measurement system on the modernized apparatus

and improved the volumetric method (PEZDIČ et al. (1999b), DOBNIKAR (2003), MIHELČIČ (2004)). We also improved the gas sampling from reaction cell during sorption simulation progression.

When updating the device, we acquired a new factor in the sorption process through   monitoring the temperature of temperature sensors (T_{system}, $T_{environment}$). This is very important as it affects all other parameters involved in sorption process. The net volume of the reaction container has been changed, the sound for pressure change measurements has been moved closer to autoclave and the volume reduced with the valve (V).

2. Comparable   adsorption/desorption investigations were performed on various lignite lithotypes. High pressure measurements of adsorption and desorption were done on six samples varying in their lithotype composition. Owing to the size of autoclave opening the lignite samples had to be correspondingly prepared. We simplified the sample preparation using grinding in the grinder and sowing on sieves with aperture 2−4 mm.

Sorption measurements progressed in a reaction cell (autoclave) where we kept a lignite sample. The sample has been loaded in two steps with CO_2 (up to 60 bar) and in the

third step with N_2 (up to 85 bar). Measurement for determination of moisture's impact on sorption were done. Measurements results show sorption's dependence on moisture content as sorption increases regarding increased moisture content in the sample. All measurements show that in the second adsorption step much less gas is adsorbed as in the first step (Figure 10).

The most CO_2 gas was adsorbed, in the first two steps, in the samples 2, 5 and 6. (Figure 10). Second adsorption step adsorbed only around half or 50 % amount of adsorbed gas in the first step. The comparative amounts of measured adsorption (first plus second step) indicate the dependence of the amount of adsorption upon the sample lithotype. Samples higher in contents of fine detric matrix tend to adsorb more gas (Figure 9).

Comparative   adsorption   values (Figure 11) of the first and the second CO_2 dosage and of the N_2 overpressure value show differences owing to different lithotype composition of samples. Major deviations between curves are seen at the third N_2 loading step when after the initial pressure decrease the curve starts to rise (pressure rises), and reaches around (+10 bar) after six hours.

The newly arosen (P_x) pressure, appearing after the third dosing stage

in the confined system, is explicit and means a considerable loading of the firm coal's skeleton.

The comparative desorption readings (Figure 12) show pressure changes during desorption. Desorption depends on the proportion of adsorption in the first two stages and on released gas in the third stage. The lowest measured desorption value after 15 hours is shown for the 4-1 sample. This sample is the most heterogeneous (X 80 %, cD 10 %, fD 10 %), and the desorption value is 2.12 bar. The highest measured desorption value after 15 hours shows the 2-1 sample. This sample comes from a fault zone (fD 90 %, G 10 %), and it desorption value is 6.67 bar.

3. Of the key importance was also the sampling of gas in autoclave. Gas analysis showed that at N_2 dosing in autoclave a high compression of CO_2 was achieved. When in the third step 30 bar of N_2 was dosed, the gas ration in autoclave should have been 2 : 1 in favour of CO_2. Chemical analysis proved the achievement of compression, but the achieved ratio of gases was reversed, 1 : 2 in favour of N_2.

4. After addition of the N_2 pressure, the adsorption tests for all samples showed first a slight initial decrease of total pressure (from 1.70 to 4.19

bar) - that means an instant gas adsorption into the lignite matter - and then the pressure increase - this means release of gas out from the lignite matter (for an example see Figures 2, 7; whereas data for all samples are in Žula, (2006)). After six hours, the pressure reached the maximal value, while temperature decreased markedly, for almost 5 °C (Figure 2 - upper graph). This phenomenon indicates that the coal samples were additionally affected owing to P_x of the gas. The P_x pressure can be related to the conditions in mine. During advanced exploitation of lignite by the longwall working face method (longwalls being ca 100 m wide and 4 m high, with additional vertical concentration of excavation), substantial deformations and (differentially) increased pressures occur ahead of the longwall faces. These factors have an impact on strength of the lignite's skeleton (Zavšek, 2004), and may lead in some extreme situations to coal and gas outbursts.

5. In the further research, more accent should be put on influence of temperature and moisture on sorption. Owing to influence of environment temperature on temperature changes in autoclave, the autoclave will have to be insulated. Planned is also a new concept of reaction vessel with a wider input opening

to allow passing of larger coal fragments. With this also dosing tubes will have to be enlarged to permit faster gas input. Measurements will be supplemented with additional gas mixtures of varying ratios of CO_2, CH_4 and N_2 Sorption properties of lignites will be shown with isotherms. Micropetrographic description of samples will be supplemented with the scanning electron microscopy (SEM).

CONCLUSION

From these reasons, to clarify gas sorption characteristics of the Velenje lignite and to supplement previous investigations with some new aspects, gas sorption tests on different lithotypes at different laboratory (autoclave) conditions of dosing gases, pressures and moistures have been studied in the experimental work which is presented in this paper. The main conclusions of our work, starting with some technical improvements, are cited below:

1. The methodology of adsorption/desorption was tested on various lignite lithotypes by introducing additional parameters (temperature, moisture, speed of dosing). Upgraded was the hardware and software of the sorption research system as originally described by ŽULA (2006), PEZDIČ et al. (2008–

2009). As during dosing the adsorption (amount of adsorbed gas) cannot be measured, it was important that we accelerated the speed of dosing. The dosing time of 3−5 s was achieved, although the entire adsorption process has not yet been properly registered.
Modernization of software makes detection of the signal more accurate as it is read each second assuring to capture the most important data in the first minute after dosage when the adsorption is maximal.

2. Desorption depends on the adsorption share in the first two steps, on the compressed CO_2 gas in the third steps, and on the gas mixture release velocity when the pressure was decreased to one bar.
The lowest measured desorption value after 15 hours was shown by the 4-1 sample (by composition the most heterogeneous sample), namely 2.12 bar or 3.74 g/kg, and the highest value the 2-1 sample (from fault zone), namely 6.67 bar or 12.09 g/kg.
Samples with fine detrite (Samples 2, 5, and 6) adsorbed the highest amounts of gas. The best result of sorption was achieved with sample 2 (fine detrite from foult zone) which adsorbed 27.23 g/kg of gas and desorbed 12.09 g/kg respectively 44.4 % adsorption.

3. The sorption methodology is still in the development phase. The principal future research trends will be aimed at collecting new data on coal petrology, calculation of bulk coal sorptive capacities and perfecting the mechanical gaseous mathematical model of the lignite - gas system. Results from sorption tests will be used to verify and fit the mentioned mathematical model which is being developed in the last few years in order to study the influence of structural and petrographical changes of the Velenje lignite depending on various stress states and presence of gases.

Acknowledgements

References

Dobnikar, P. (2003): Metode določanja sorpcijskih lastnosti lignita pri visokih tlakih: diplomsko delo. Naravoslovnotehniška fakulteta, Oddelek za geologijo, Ljubljana, p. 104.

Gamson, P., Beamish, B. & Johnson, D. (1996): Coal microstructure and secondary mineralization: their effect on methane recovery. In: Gayer R. & Harris, I. (Eds.), Coalbed Methane and Coal Geology. The Geological Society London, pp. 165–179.

Gruszkiewicz, M. S., Naney, M. T., Blencoe, J. G., Cole, D. R., Pashin, J. C. & Carroll, R. E. (2009): Adsorption kinetics of CO_2, CH_4, and their equimolar mixture on coal from the Black Warrior Basin, West-Central Alabama. *International Journal of Coal Geology*, Vol. 77, pp. 23–33.

Kanduč, T. (2004): Izotopske značilnosti premogovega plina v Velenjskem bazenu: magistrsko delo. Naravoslovnotehniška fakulteta, Oddelek za geologijo, Ljubljana, 17–30, 67–72.

Kanduč, T., & Pezdič. J. (2005): Origin and distribution of coalbed gases from the Velenje basin, Slovenia. *Geochemical Journal*, Vol. 39, 397–409.

Kanduč, T., Pezdič, J., Lojen, S. & Zavšek, S. (2003): Study of the gas composition ahead of the working face in a lignite seam from the Velenje basin. *RMZ - Materials and geoenvironment*, Vol. 50/2, 503–511.

Kanduč, T., Pezdič, J., Lojen, S., Zavšek, S. (2003): Izvor premogovnega

plina v Velenjskem bazenu: 16. Posvetovanje geologov: Geološki zbornik 17 - razprave in poročila. Naravoslovnotehniška fakulteta, Oddelek za geologijo, Ljubljana, 76–78.

LAZARINI, F., BRENČIČ, J. (1992): Splošna in anorganska kemija. Državna založba Slovenije, Ljubljana, p. 557.

LIKAR, J. (1995): Analiza mehanizmov nenadnih izbruhov premoga in plina v premogovnikih. - Univerza v Ljubljani (doktorska disertacija), p. 216.

LIKAR, J. (1999): Sorpcijski pojavi v lignitu pri različnih napetostnih stanjih v povezavi z migracijskimi procesi plinov : zaključno poročilo o rezultatih raziskovalnega projekta v letu 1998. Ljubljana: IRGO.

LIKAR, J., RUNOVEC, F., DAEBELAK, B., MALAVAŠIČ, H. (2008): Behaviour of CO_2 saturated lignite in the different states of stresses. - In (Eds. Pezdič, J., Zavšek, S., Jamnikar S.): International workshop Velenje 08 - Mine (green-house) gases CO_2, CH_4, mine safety, prevention, managing and utilization), p. 51–64.

LITWINISZYN, J. (1990): Rare fraction shock waves, outbursts and consequential coal damage. International Journal of Rock Mechanics and Mining Science & Geomechanics Abstracts, Vol. 27, p. 535–540.

MAJEWSKA, Z., CEGLARSKA-STEFANSKA, G., MAJEWSKI, S. & ZIETEK, J. (2009): Binary gas sorption/desorption experiments on a bituminous coal: Simultaneous measurements on sorption kinetics, volumetric strain and acoustik emission. International

Journal of Coal Geology, Vol. 77, p. 90–102.

MARKIČ M. & SACHSENHOFER R. F. (1997): Petrographic composition and depositional environments of the Pliocene Velenje lignite seam (Slovenia). International Journal of Coal Geology, Vol. 33, p. 229–254.

MARKIČ, M., SACHSENHOFER, R. F. (2010): The Velenje lignite - its petrology and genesis. Ljubljana: Geološki zavod Slovenije, VIII, p. 218.

MARKIČ, M., ZAVŠEK, S., PEZDIČ, J., SKABERNE, D., KOČEVAR, M. (2001): Macropetrographic characterization of the Velenje lignite (Slovenia). Acta Univ. Carol., Geol., Vol. 45, 2/4, p. 81–97.

MASTALERZ, M., GLUSKOTER, H. & RUPP, J. (2004): Carbon dioxide and methane sorption in high volatile bituminous coals from Indiana, USA. International Journal of Coal Geology, Vol. 60/1, p. 43–55.

MOORE, W. J. (1974): Physical Chemistry. Longman, 997 str.

MIHELČIČ, D. (2004): Visokotlačne sorpcijske lastnosti nepremoških komponent v Premogovniku Velenje: diplomsko delo. Naravoslovnotehniška fakulteta, Oddelek za geologijo, Ljubljana, 45 str.

PEZDIČ, J. (1998): Adsorpcijsko - desorpcijske lastnosti različnih litotipov lignita pri visokih tlakih (Premogovnik Velenje), Projekt: Sorpcijski pojavi v lignitu pri različnih stanjih v povezavi z migracijskimi procesi plinov. Delovno poročilo za leto 1997. Ljubljana: Naravoslovnotehniška fakulteta, Oddelek za geologijo,

Ljubljana.

Pezdič, J., 1999: Izotopi in geokemijski procesi: univerzitetni učbenik. Naravoslovnotehniška fakulteta, Oddelek za geologijo, Ljubljana, 114 – 117.

Pezdič, J., Popovič, A., Ogrinc, N., Lojen, S., Zavšek, S., 1999a: Sledenje plinskih komponent v Premogovniku Velenje, 1. Fazno poročilo: Naravoslovnotehniška fakulteta, Oddelek za geologijo, Ljubljana, 23 Str.

Pezdič, J., Markič, M., Lojen, S., Čermelj, B., Ulrich, M., Zavšek, S., 1998: Carbon isotope composition in the Velenje lignite mine - its role in soft brown coal genesis (Izotopska sestava ogljika v velenjskem lignitu - vloga pri določanju njegovega nastanka), *RMZ* - Materials and Geoenvironment, Vol. 45, No. 1-2, 149–153.

Pezdič, J., Markič, M., Letič, M., Popovič, A, Zavšek, S., 1999b: Laboratory simulation of adsorption - desorption processes on different lignite lithotypes from Velenje lignite mine, *RMZ* - Materials and Geoenvironment, Vol. 46, No. 3, 555–568.

Pezdič, J., Žula, J., Zavšek, S., 2008/2009: Sledenje plinskih komponent v Premogovniku Velenje - SORPCIJA, poročilo: HGEM in GEORIS, Ljubljana.

Pezdič, J., Zavšek S., Žula, J., 2007: High pressure sorption of CO_2 on lignite coal, 20th NZGG Conference, Dunedin, New Zealand.

Supovec, I., Filipič, M., 2004: Izdelava računalniškega programa za moni-toring adsorpcije in desorpcije - avtorsko delo, (neobjavljen vir), Ljubljana.

Taylor, G.H., Teichmüller, M., Davis, A., Diessel, C.F.K., Littke, R. & Robert, P., 1998: Organic Petrology. Gebrüder Borntraeger, Berlin, 704 str.

Weniger, P., Kalkreuth, W, Busch, A. & Krooss, B.M., 2010: High-pressure methane and carbon dioxide sorption on coal and shale samples from the Parana Basin, Brazil. International Journal of Coal Geology, 84/3–4, 190–205.

Zavšek, S., 2004: Model za raziskavo sprememb strukturnih in petrografskih lastnosti velenjskega lignita pri različnih napetostnih stanjih in ob prisotnosti plinov: doktorska disertacija (Model for research of structural and petrographical changes of the Velenje lignite depending on various stress states and presence of gasses): Ph. D. Thesis. Ljubljana, 114 str.

Zapušek, A. & Hočevar, S., 1998: Adsorption and desorption properties of lignite. In: Meunier, F. (ed.), 1998, Fundamentals of adsorption 6. Proceedings of the 6th International Conference of fundamentals of adsorption, Presqu'île de Giens, 24–28 May. Elsevier, 653–658.

Žula, J., 2006: Sorpcijske lastnosti različnih litotipov velenjskega premoga pri visokih tlakih. Diplomsko delo, Ljubljana: Naravoslovnotehniška fakulteta, Oddelek za geologijo, 26–76.

Strokovni posvet Podnebni ekstremi in varna oskrba s pitno vodo

Kolikšne so podnebne spremembe na območju jugovzhodne Evrope in kako podnebni ekstremi vplivajo na vodne vire, so vse pogostejša družbena vprašanja, ki vplivajo na različne vidike človekovega življenja. Evropska okoljska agencija (The European Environmental Agency – EEA) je dala pobudo za regionalne in lokalne projekte in študije z namenom oceniti obseg podnebnih sprememb in določiti vpliv le-teh na vodne vire. Glavni problemi oskrbe s pitno vodo na območju jugovzhodne Evrope v zadnjih desetletjih sta zmanjševanje razpoložljivih količin in slabšanje kakovosti podzemne vode, kar je posledica neprimerne rabe prostora in podnebnih sprememb.

V okviru programa Jugovzhodna Evropa poteka projekt Podnebne spremembe in njihov vpliv na oskrbo s pitno vodo (Climate Change and Impacts on Water Supply – CC-WaterS), v katerega so kot projektni partnerji vključene tri slovenske ustanove: Univerza v Ljubljani, Naravoslovnotehniška fakulteta, Javno podjetje Vodovod-Kanalizacija, d. o. o., in Agencija RS za okolje. Gre za mednarodni projekt, ki združuje 18 ustanov iz devetih držav območja jugovzhodne Evrope z namenom zagotoviti trajnostno in varno oskrbo s pitno vodo v prihodnosti ob upoštevanju vplivov rabe prostora in podnebnih sprememb.

Spremembe vremenskih dogodkov so zaznane tudi na območju Slovenije, ravno tako časovna prerazporeditev vremenskih dogodkov in njihova jakost, kar neposredno vpliva na razpoložljivost in kakovost vodnih virov. Za prilagoditev podnebnim spremembam in načrtovanje varne oskrbe s pitno vodo je treba prepoznati probleme in vzpostaviti ustrezne prilagoditvene ukrepe. Slovenski partnerji smo se odločili, da v sklopu projekta analiziramo sedanje stanje in na osnovi scenarijev modelov podnebnih sprememb pripravimo ukrepe za zmanjšanje kvarnih vplivov in za ohranitev vodnih virov na dveh prodnih vodonosnikih: na Ljubljanskem polju in Murskem/Prekmurskem polju, ki pa se med seboj razlikujeta tako po razpoložljivosti vodnih virov kakor tudi po prevladujoči rabi prostora. Zaradi raznolikosti problematike smo v projekt vključili tudi zunanje institucije in strokovnjake s področja meteorologije, kmetijstva, matematičnega modeliranja podzemnih voda ter prostorske in okoljske sociologije.

Dne 9. junija 2011 je v hotelu Mons potekal strokovni posvet z naslovom Podnebni ekstremi in varna oskrba s pitno vodo, kjer so bile predstavljene ugotovi-

---

Short paper

tve, dileme in rezultati projekta s poudarkom na Ljubljanskem polju. Posvet je odprl župan Mestne občine Ljubljana g. Zoran Janković. Dr. Jernej Stritih, direktor Službe vlade RS za podnebne spremembe, je na kratko predstavil Strategijo prehoda Slovenije v maloogljično družbo. Udeležence posveta so nagovorili tudi direktor družbe JP Vodovod-Kanalizacija, d. o. o., g. Krištof Mlakar, generalni direktor Agencije RS za okolje dr. Silvo Žlebir in dekan Naravoslovotehniške fakultete izr. prof. dr. Jakob Likar. V nadaljevanju je doc. dr. Barbara Čenčur Curk predstavila projekt Podnebne spremembe in njihov vpliv na oskrbo s pitno vodo (CC-WaterS). Doc. dr. Klemen Bergant (Agencija RS za okolje) je udeležence seznanil s podnebno spremenljivostjo in z ekstremi ter s scenariji podnebja v prihodnosti. Branka Bračič Železnik (Javno podjetje Vodovod-Kanalizacija, d. o. o.) je preučila javno oskrbo s pitno vodo v Ljubljani in vpliv podnebnih sprememb ter rabe prostora na vodni vir. Matej Knapič s Kmetijskega inštituta je prikazal oceno sedanjega izpiranja nitratov in pesticidov v podzemno vodo ter projekcij izpiranja zaradi podnebnih sprememb. Marko Fatur (LUZ, d. d.) je obravnaval problematiko prostorskega načrtovanja in varovanje virov pitne vode. Zaznavanje prebivalstva, sprejemanje in odnos do prilagoditev podnebnim spremembam ter odnosov do okolja ter pitne vode je podal prof. dr. Drago Kos s Fakultete za družbene vede.

Slika 1. Strokovni posvet »Podnebni ekstremi in varna oskrba s pitno vodo«, Hotel Mons, 9. 6. 2011. (z leve: dekan NTF izr. prof. dr. Jakob Likar; Branka Bračič Železnik, JP VO-KA, d. o. o.; Tina Zajc, NTF; dr. Petra Souvent, ARSO; župan Mestne občine Ljubljana g. Zoran Janković; doc. dr. Barbara Čenčur Curk, NTF; direktor družbe JP VO-KA, d. o. o., g. Krištof Mlakar; generalni direktor ARSO dr. Silvo Žlebir)

Doc. dr. Barbara Čenčur Curk

In Memoriam

Prof. dr. inž. Ciril Pelhan
(4. 11. 1921–20. 5. 2011)

Dne 20. maja 2011 je nenadoma, v 90. letu starosti umrl prof. dr. C. Pelhan, pionir naše livarske stroke, utemeljitelj in prvi predavatelj samostojnega predmeta Livarstvo, mednarodno priznan raziskovalec in pisec več knjig, prvi in dolgoletni urednik časopisa Livarski vestnik ter soustanovitelj in predsednik Društva livarjev Slovenije. Že kot študent je napovedal svojo vsestransko dejavnost, bil je odličen plavalec, l. 1945 je v tedanji skupni državi postal državni prvak na 100 m hrbtno in na olimpijskih igrah v Londonu l. 1948 kot član štafete 4 × 200 m prosto z njo dosegel odmevno 5. mesto.

Na tedanji Tehniški fakulteti v Ljubljani je l. 1949 diplomiral iz metalurgije, kjer je l. 1960 nato tudi doktoriral. Zaposlil se je na Fakulteti za rudarstvo in metalurgijo, kjer je bil l. 1969 imenovan za rednega profesorja. Pogosto se pozablja njegov trud in zasluga za ustanovitev, razvoj in delovanje Livarskega laboratorija na fakulteti, ki je bil dolgo edini v tedanji državi in v katerem se uspešno raziskuje še danes. S tem je omogočil izdelavo kakovostnih diplom s področja livarstva. Do konca službovanja l. 1990 je bil mentor 107 diplomantom, ki so kot inženirji postali nosilci razvoja livarske industrije ne samo v Sloveniji, temveč tudi v celotni Jugoslaviji.

Raziskoval je strjevanje in kristalizacijo sive litine, rast grafita, oksidacijo nelegiranih in legiranih sivih litin, livne bakrove zlitine in livarska pomožna sredstva. O svojem raziskovalnem delu je poročal na številnih svetovnih, mednarodnih in nacionalnih livarskih kongresih in si pridobil mednarodni sloves. Objavljal je v vodilnih evropskih znanstvenih časopisih s področja livarstva, največkrat v Nemčiji, pa tudi v Avstriji, Poljski, Italiji, redno pa tudi v domačih revijah.

Pripravil je celoten slovenski dodatek k 4-jezičnemu Mednarodnemu livarskemu slovarju, vendar do izdaje ni prišlo. Napisal je več učbenikov za predmet Livarstvo in za Uvod v metalurgijo. Za livarsko industrijo je napisal še 7 monografij,

ki obravnavajo posamezna, tedanja najbolj pereča tehnološka vprašanja. Tako je l. 1957 napisal knjižico Livarski peski, v kateri je zajel vse podatke o kvaliteti in zalogah peskokopov v Sloveniji.

Izpopolnjeval se je v tujini: v Franciji, Nemčiji, Poljski in Avstriji, in si poleg strokovnega znanja pridobil tudi pomembne mednarodne stike. Znanje je prenašal ne samo na študente in diplomante, temveč tudi v industrijo. V tem času je že sodeloval z današnjim podjetjem Termit pri razvoju pomožnih livarskih sredstev in peskov v obratih v Ihanu in Moravčah in jih redno obiskoval. Danes to ne zveni nič posebno, tedaj pa je vsak obisk pomenil večurno vožnjo po razdrapanem cestišču s kolesom kot edinim prevoznim sredstvom.

L. 1953 je bilo ustanovljeno Društvo livarjev, kjer je postal najprej tajnik in urednik Livarskega vestnika, nato pa v obdobju od l. 1966 do l. 1979 predsednik, vodenje pa je nadaljeval tudi kot podpredsednik. Pri uspešnem delu so prišli do izraza njegovi obširni mednarodni stiki in bogate izkušnje, k nam so začeli prihajati priznani strokovnjaki in znanstveniki iz tujine. Skupaj s tedanjim predsednikom prof. Fettichom sta razvijala sodelovanje z nemškim, avstrijskim, poljskim in čehoslovaškim društvom livarjev, ki poteka dejavno še danes. Neizogibno je treba pri tem navesti nekaj vodilnih evropskih znanstvenikov, ki so se že v prvih letih delovanja odzvali povabilu in predavali pri nas: tedaj vodilni profesor livarstva v Evropi prof. W. Patterson iz Aachna, naš rojak prof. B. Marinček iz ETH v Zürichu, direktor novega Livarskega inštituta v Leobnu dr. R. Ziegler, prof. M. Skarbinski iz Varšave, kasneje pa številni drugi, med temi je tudi očitno tesno sodelovanje s prof. E. Schürmannom, vodilnim nemškim znanstvenikom na področju celotne metalurgije, iz TU Clausthal.

V 60. letih je uvedel redna vsakoletna livarska posvetovanja v Portorožu, ki so pritegnila predavatelje in udeležence iz cele tedanje skupne države, vedno pa je sodelovalo tudi več priznanih strokovnjakov in znanstvenikov iz tujine. Portorož pomeni še vedno kraj, kjer se srečujejo livarji in izmenjujejo strokovna mnenja na mednarodnem nivoju, posvetovanja pa so eden od središčnih vsakoletnih dogodkov na področju livarstva v celotni srednje- in južnoevropski regiji.

Uvedel je študijska potovanja livarjev iz Slovenije v tujino. Med začetnimi naj omenimo dve. Kljub tedanji zaprtosti meje je l. 1956 vodil skupino 17 livarskih strokovnjakov iz Slovenije na tedaj prvo povojno svetovno livarsko razstavo v Düsseldorfu, kjer so se odpirala v livarstvu povsem nova obzorja. V okvi-

ru Združenja rudnikov in industrije nemetalov pa je l. 1958 vodil direktorje na 10-dnevni ogled peskokopov v Belgiji, Franciji in Nemčiji, ki je po mnenju udeležencev spodbudil nadaljnji uspešni razvoj tudi v Sloveniji.

Prof. C. Pelhan je bil prvi urednik Livarskega vestnika, ki je začel izhajati l. 1954 in še vedno redno izhaja. Priznati moramo, da so bila tedanja začetna snovanja časopisa zelo temeljita, saj se je izkazalo, da nobena sprememba ne bi bila smotrna, zato izhaja časopis še vedno v enaki obliki, obsegu in formatu, slovenski livarji in avtorji iz tujine pa še vedno zagotavljajo v začetku začrtano število kakovostnih člankov. Prof. C. Pelhan ga je urejeval vse do leta 1982, torej 28 let.

Za njegovo ustanoviteljsko večdesetletno delo ga je Društvo livarjev Slovenije l. 1993 imenovalo za častnega predsednika.

S prof. dr. Cirilom Pelhanom smo izgubili pionirja razvoja slovenske livarske stroke ne samo v pedagoškem, raziskovalnem, izdajateljskem in društvenem smislu, temveč tudi pri vzpostavljanju izjemno obširnega mednarodnega sodelovanja na področju livarstva in uveljavljanja v tujini.

Iz bogatega spomina nanj se nam vedno znova izrisujejo značilnosti njegove močne osebnosti, to so korektnost in spoštovanje ter pozitiven in svetovljanski odnos do sogovornika; s svojim samoniklim in pronicljivim načinom razmišljanja, s katerim se je dokopal do povsem novih ocen in sklepov, je presenečal tako doma kot v tujini. Zato je bilo druženje z njim vedno zanimivo, polno posebne privlačnosti in šarma. Svojih stališč ni skrival in tudi ne vsiljeval drugim. Ponudil je le svoj lasten vzor, vedno z vedrino, ki jo je izžareval in s katero je obdaril sogovornika. Zato je tudi na začetku delovanja Društva livarjev, ki je s časom dobil mednarodni značaj, gradil na povsem prijateljskem navezovanju stikov, saj nismo imeli ničesar drugega, kar bi lahko enakovredno ponudili. Za zanj značilno sredozemsko lahkotnostjo se je skrival trden, do popolnosti izoblikovan in urejen značaj, ki smo ga spoznali tisti, ki smo z njim tesneje sodelovali.

Z njim odhaja velik del naših svetlih skupnih časov, ko smo v zrelih letih skupaj reševali vsakodnevna vprašanja v zelo prijetnem ozračju, ne da bi pri tem pomislili na grenkobo slovesa, ki je nepričakovano in neizprosno prihajal. S hvaležnostjo se bomo spominjali njegovih strokovnih nasvetov, še bolj pa kot življenjskega vzornika.

<div align="right">Prof. dr. M. Trbižan</div>

In Memoriam

Prof. dr. Bogdan Sicherl
(16. 8. 1927–26. 4. 2011)

Bogdan Sicherl je luč sveta ugledal v Beogradu 16. 8. 1927. Maturiral je l. 1947 na drž. Realni gimnaziji v Ljubljani, l. 1954 pa diplomiral na Oddelku za rudarstvo in metalurgijo Tehniške fakultete Univerze v Ljubljani (UL).

Po diplomi se je zaposlil kot asistent za toplotno tehniko na Oddelku za rudarstvo in metalurgijo Tehniške fakultete UL. L. 1971 je zagovarjal doktorsko disertacijo z naslovom Untersuchungen über den Verlauf der Ausbrandkurve von Difussionsflammen unter Besonderer Berüscksichtigung der Flammentemperatur und der Flammenlänge na Montanistični visoki šoli v Leobnu, Avstrija. L. 1974 je bil izvoljen v naziv docenta za predmete Toplotna tehnika v metalurgiji, Metalurške peči ter Toplotnotehnične meritve in regulacija. Od l. 1972 dalje je bil stalni in zaprisežeini sodni izvedenec za področje industrijskih peči, plinskih armatur in regulacijo. Od l. 1975 je bil predsednik komisije za energetiko projektnega sveta za črno metalurgijo Slovenskih železarn. L. 1979 je bil izvoljen v naziv izrednega, l. 1985 pa rednega profesorja za predmete Toplotna tehnika v metalurgiji, Metalurške peči ter Toplotnotehnične meritve in regulacija.

Takoj po diplomi se je strokovno izpopolnjeval v tujini, kjer si je nabiral izkušnje na področju ognjevzdržnih gradiv in pri toplotnotehničnih in plinskoanalitičnih meritvah tehničnih naprav. Strokovne izkušnje pa je pridobival tudi pri slovenskih podjetjih, predvsem v Železarni Jesenice, in v drugih metalurških podjetjih v takratni državi Jugoslaviji. Kmalu je tudi pokazal željo po pedagoškem delu, saj je že l. 1954 predaval na Tehniški srednji šoli v Ljubljani, aktivno pa je sodeloval tudi pri izvajanju tečajev, ki sta jih organizirala Društvo livarjev Slovenije in Združenje železarn Jugoslavije.

Znanstvenoraziskovalno in strokovno delo prof. dr. Bogdana Sicherla je bilo osredinjeno na preučevanje zgorevanja plinastih in tekočih goriv, toplotnotehnične

bilance metalurških peči, na študij in obravnavo plinskih sistemov s posebnim poudarkom na zamenljivosti kurilnih plinov. Tako je raziskoval in podal osnovne usmeritve pri uporabi tekočega naftnega plina v mešanici z zrakom, kar je omogočilo industrijskim uporabnikom v Sloveniji hitrejši in racionalnejši prehod na uporabo zemeljskega plina. Poleg tega je intenzivno delal pri raziskavah metalurških peči, jih projektiral in pripravljal računalniške programe za njihovo vodenje. Posebno področje, ki ga je prof. Sicherl obdelal, so bili sevalni, konvekcijski in kombinirani sevalno-konvekcijski rekuperatorji, za katere je pripravil projektno izvedbeno dokumentacijo in jih glede na toplotno bilanco tudi klasificiral. Uspešnost razvojnega in raziskovalnega dela prof. Sicherla na omenjenih področjih se kaže v 18 prijavljenih in priznanih tehničnih izboljšavah. Tako je npr. l. 1975 prejel nagrado SBK za patente in inovacije kot zaslugo za razvoj patentiranega industrijskega gorilnika. Prav tako je l. 1984 prejel s sodelavci zlato plaketo za najboljše delo, tj. za izboljšave kombiniranega sevalno-konvekcijskega rekuperatorja pri kupolki na vroči zrak z dodatnim izkoriščanjem odpadne toplote.

Kot strokovnjak s področja toplotne tehnike in toplotnotehničnih meritev je z referati sodeloval na mednarodnih in domačih konferencah ter posvetovanjih.

Pri raziskovalnem delu je bil natančen zlasti na področju meritev in zbiranja podatkov, potrebnih za izdelavo toplotnih in materialnih bilanc ogrevnih peči. Zato so imeli rezultati njegovih ekspertiz veliko uporabno vrednost in verodostojnost. Loteval se je praktičnih tem v metalurški industriji, kjer si je ustvaril velik krog zvestih sodelavcev, s katerimi je reševal naloge, ki so izhajale iz aktualnih problemov, s ciljem izboljšave energijskih izkoristkov naprav ter večje storilnosti. Bil je med prvimi strokovnjaki, ki so v slovensko metalurško energetiko uvajali tekoči naftni plin in kasneje tudi zemeljski plin ter se z veliko vnemo ukvarjal z razvojem gorilnikov za zgorevanje tekočih in plinastih goriv. Njegovo raziskovalno delo je potekalo v času, ko ni bili samoumevno, da se lahko kupijo na trgu posamezne komponente, ki so potrebne pri raziskovalnem delu. Ker je pri zgorevanju goriv pomembno, da prideta v stik in se mešata gorivo in zrak (kisik), si je posamezne potrebne dele naredil sam na stružnici. S tem je pokazal veliko tehnično/inženirsko iznajdljivost.

Pedagoške obveznosti je izpolnjeval prizadevno in poglobljeno, tako da so si študentje lahko ustvarili bogate zapiske o strokovnih in znanstvenih temah, ki jih je predaval. Čeprav ni vodil evidence prisotnosti študentov, je bila predavalnica

vedno zasedena. Prav tako je od študentov zahteval natančnost pri poznanju področja iz toplotne tehnike, peči in meritev. Kdor se tega ni držal, je moral večkrat priti k njemu na izpit.

Prav tako je treba omeniti, da je po nenadni smrti predstojnika katedre za toplotno tehniko prof. Pavka kot najstarejši uspešno prevzel težo vodenja katedre. Ob tem je moral poskrbeti tudi za izpolnjevanje habilitacijskih pogojev. V tem pogledu je naredil za oddelek zelo veliko. Namreč, z delom na katedri za toplotno tehniko in energetiko smo bili, tudi po njegovi zaslugi, tesno povezani z industrijo.

Napisal je obsežna skripta o toplotni tehniki v metalurgiji z dodanimi diagrami in nazornimi shemami merilnih aparatov in posebnih izvedb pripomočkov za merjenje tlakov, pretokov in temperatur. Delo je bilo takrat med prvimi takšne vrste in je bilo napisano v slovenskem jeziku.

Ob praznovanjih je bil gostoljuben in zabaven gostitelj, ki je rad, kadar je bil v domačem okolju, delil veselje do resne glasbe s svojimi sodelavci s fakultete in Metalurškega inštituta. Rad se je pohvalil s svojo vrhunsko avdioopremo. Imel je še enega zvestega sodelavca, ki ga je spremljal v pisarno ob popoldanskih in večernih urah. To je bil čudovit koker španjel Raudi.

V začetku l. 1991 se je prof. Sicherl odpravil v zaslužen pokoj.

Prof. dr. Bogdana Sicherla bomo sodelavci Oddelka za materiale in metalurgijo Naravoslovnotehniške fakultete ohranili v lepem spominu.

Izr. prof. dr. Boštjan Markoli

Author`s Index, Vol. 58, No. 2

INSTRUCTIONS TO AUTHORS

RMZ-MATERIALS & GEOENVIRONMENT (RMZ- Materiali in geookolje) is a periodical publication with four issues per year (established 1952 and renamed to RMZ-M&G in 1998). The main topics of contents are Mining and Geotechnology, Metallurgy and Materials, Geology and Geoenvironment.

RMZ-M&G publishes original Scientific articles, Review papers, Preliminary notes, Professional papers **in English**. In addition, evaluations of other publications (books, monographs,...), In memoriam, Professional remarks and reviews are welcome. The Title, Abstract and Key words in Slovene will be included by the author(s) or will be provided by the referee or the Editorial Office.

* Additional information and remarks for Slovenian authors:
Only Professional papers, Publications notes, Events notes, Discussion of papers and In memoriam, will be exceptionally published in the Slovenian language.

Authorship and originality of the contributions. Authors are responsible for originality of presented data, ideas and conclusions as well as for correct citation of data adopted from other sources. The publication in RMZ-M&G obligate authors that the article will not be published anywhere else in the same form.

Specification of Contributions

RMZ-M&G will publish papers of the following categories:

<u>*Full papers*</u> *(optimal number of pages is 7 to 15, longer articles should be discussed with Editor prior to submission). An abstract is required.*
- **Original scientific papers** represent unpublished results of original research.
- **Review papers** summarize previously published scientific, research and/ or expertise articles on the new scientific level and can contain also other cited sources, which are not mainly result of author(s).

- **Preliminary notes** represent preliminary research findings, which should be published rapidly.
- **Professional paper**s are the result of technological research achievements, application research results and information about achievements in practice and industry.

Short papers (the number of pages is limited to 1 for Discussion of papers and 2 pages for Publication note, Event note and In Memoriam). No abstract is required for short papers.

- **Publication notes** contain author's opinion on new published books, monographs, textbooks, or other published material. A figure of cover page is expected.
- **Event notes** in which descriptions of a scientific or professional event are given.
- **Discussion of papers (Comments)** where only professional disagreements can be discussed. Normally the source author(s) reply the remarks in the same issue.
- **In memoriam** (a photo is expected).

Supervision and review of manuscripts. All manuscripts will be supervised. The referees evaluate manuscripts and can ask authors to change particular segments, and propose to the Editor the acceptability of submitted articles. Authors can suggest the referee but Editor has a right to choose another. **The name of the referee remains anonymous.** The technical corrections will be done too and authors can be asked to correct missing items. The final decision whether the manuscript will be published is made by the Editor in Chief.

The Form of the Manuscript

The manuscript should be submitted as a complete hard copy including figures and tables. The figures should also be enclosed separately, both charts and photos in the original version. In addition, all material should also be provided in electronic form on a diskette or a CD. The necessary information can conveniently also be delivered by E-mail.

Composition of manuscript is defined in the attached Template

The original file of Template is available on RMZ-Materials and Geoenvironment Home page address:

http://www.rmz-mg.com

References - can be arranged in two ways:
- first possibility: alphabetic arrangement of first authors - in text: (Borgne, 1955), or
- second possibility: [1] numerated in the same order as cited in the text: example[1]

Format of papers in journals:
   LE BORGNE, E. (1955): Susceptibilite magnetic anomale du sol superficiel. *Annales de Geophysique*, 11, pp. 399–419.

Format of books:
   ROBERTS, J. L. (1989): Geological structures, *MacMillan*, *London*, 250 p.

Text on the hard print copy can be prepared with any text-processor. The electronic version on the diskette, CD or E-mail transfer should be in MS Word or ASCII format.
Captions of figures and tables should be enclosed separately.
Figures (graphs and photos) and tables should be original and sent separately in addition to text. They can be prepared on paper or computer designed (MSExcel, Corel, Acad).
Format. Electronic figures are recommended to be in CDR, Al, EPS, TIF or JPG formats. Resolution of bitmap graphics (TIF, JPG) should be at least 300 dpi. Text in vector graphics (CDR, Al, EPS) must be in MSWord Times typography or converted in curves.
Color prints. Authors will be charged for color prints of figures and photos.
Labeling of the additionally provided material for the manuscript should be very clear and must contain at least the lead author's name, address, the beginning of the title and the date of delivery of the manuscript. In case of an E-mail transfer the exact message with above asked data must accompany the attachment with the file containing the manuscript.

Information about RMZ-M&G:

Editor in Chief prof. dr. Peter Fajfar (phone: ++386 1 4250-316) or
Secretary Barbara Bohar Bobnar, univ. dipl. ing. geol. (phone: ++386 1 4704-630),
Aškerčeva 12, 1000 Ljubljana, Slovenia
or at E-mail addresses:
peter.fajfar@ntf.uni-lj.si,
barbara.bohar@ntf.uni-lj.si

Sending of manuscripts. Manuscripts can be sent by mail to the **Editorial Office** address:

*   RMZ-Materials & Geoenvironment
    Aškerčeva 12,
    1000 Ljubljana, Slovenia

or delivered to:

*   **Reception** of the Faculty of Natural Science and Engineering (for RMZ-M&G)
    Aškerčeva 12,
    1000 Ljubljana, Slovenia
*   E-mail - addresses of Editor and Secretary
*   You can also contact them on their phone numbers.

These instructions are valid from August 2009

NAVODILA AVTORJEM

RMZ-MATERIALS AND GEOENVIRONMENT (RMZ- Materiali in geookolje) – kratica RMZ-M&G - je revija (ustanovljena kot zbornik 1952 in preimenovana v revijo RMZ-M&G 1998), ki izhaja vsako leto v štirih zvezkih. V reviji objavljamo prispevke s področja rudarstva, geotehnologije, materialov, metalurgije, geologije in geookolja.

RMZ- M&G objavlja izvirne znanstvene, pregledne in strokovne članke ter predhodne objave samo v angleškem jeziku. Strokovni članki so lahko izjemoma napisani v slovenskem jeziku. Kot dodatek so zaželene recenzije drugih publikacij (knjig, monografij …), nekrologi In Memoriam, predstavitve znanstvenih in strokovnih dogodkov, kratke objave in strokovne replike na članke objavljene v RMZ-M&G v slovenskem ali angleškem jeziku. Prispevki naj bodo kratki in jasni.

Avtorstvo in izvirnost prispevkov. Avtorji so odgovorni za izvirnost podatkov, idej in sklepov v predloženem prispevku oziroma za pravilno citiranje privzetih podatkov. Z objavo v RMZ-M&G se tudi obvežejo, da ne bodo nikjer drugje objavili enakega prispevka.

Vrste prispevkov

Optimalno število strani je 7 do 15, za daljše članke je potrebno soglasje glavnega urednika.
Izvirni znanstveni članki opisujejo še neobjavljene rezultate lastnih raziskav.
Pregledni članki povzemajo že objavljene znanstvene, raziskovalne ali strokovne dosežke na novem znanstvenem nivoju in lahko vsebujejo tudi druge (citirane) vire, ki niso večinsko rezultat dela avtorjev.
Predhodna objava povzema izsledke raziskave, ki je v teku in zahteva hitro objavo.
Strokovni članki vsebujejo rezultate tehnoloških dosežkov, razvojnih projektov in druge informacije iz prakse.
Recenzije publikacij zajemajo ocene novih knjig, monografij, učbenikov, razstav …(do dve strani; zaželena slika naslovnice in kratka navedba osnovnih podatkov - izkaznica).

In memoriam (do dve strani, zaželena slika).

Strokovne pripombe na objavljene članke ne smejo presegati ene strani in opozarjajo izključno na strokovne nedoslednosti objavljenih člankov v prejšnjih številkah RMZ-M&G. Praviloma že v isti številki avtorji prvotnega članka napišejo odgovor na pripombe.

Poljudni članki, ki povzemajo znanstvene in strokovne dogodke (do dve strani).

Recenzije. Vsi prispevki bodo predloženi v recenzijo. Recenzent oceni primernost prispevka za objavo in lahko predlaga kot pogoj za objavo dopolnilo k prispevku. Recenzenta izbere Uredništvo med strokovnjaki, ki so dejavni na sorodnih področjih, kot jih obravnava prispevek. Avtorji lahko sami predlagajo recenzenta, vendar si uredništvo pridržuje pravico, da izbere drugega recenzenta. **Recenzent ostane anonimen**. Prispevki bodo tudi tehnično ocenjeni in avtorji so dolžni popraviti pomanjkljivosti. Končno odločitev za objavo da glavni in odgovorni urednik.

Oblika prispevka

Prispevek predložite v tiskanem oštevilčenem izvodu (po možnosti z vključenimi slikami in tabelami) ter na disketi ali CD, lahko pa ga pošljete tudi prek E-maila. Slike in grafe je možno poslati tudi risane na papirju, fotografije naj bodo originalne.

Razčlenitev prispevka:

Predloga za pisanje članka se nahaja na spletni strani:

http://www.rmz-mg.com/predloga.htm

Seznam literature je lahko urejen na dva načina:
-po abecednem zaporedju prvih avtorjev ali
-po [1]vrstnem zaporedju citiranosti v prispevku.

Oblika je za oba načina enaka:
Članki:

> LE BORGNE, E. (1955): Susceptibilite magnetic anomale du sol superficiel. *Annales de Geophysique*; Vol. 11, pp. 399–419.

Knjige:

Roberts, J. L. (1989): Geological structures, *MacMillan*, *London*, 250 p.

Tekst izpisanega izvoda je lahko pripravljen v kateremkoli urejevalniku. Na disketi, CD ali v elektronskem prenosu pa mora biti v MS Word ali v ASCII obliki.

Naslovi slik in tabel naj bodo priloženi posebej. Naslove slik, tabel in celotno besedilo, ki se pojavlja na slikah in tabelah, je potrebno navesti v angleškem in slovenskem jeziku.

Slike (ilustracije in fotografije) in tabele morajo biti izvirne in priložene posebej. Njihov položaj v besedilu mora biti jasen iz priloženega kompletnega izvoda. Narejene so lahko na papirju ali pa v računalniški obliki (MS Excel, Corel, Acad).

Format elektronskih slik naj bo v EPS, TIF ali JPG obliki z ločljivostjo okrog 300 dpi. Tekst v grafiki naj bo v Times tipografiji.

Barvne slike. Objavo barvnih slik sofinancirajo avtorji

Označenost poslanega materiala. Izpisan izvod, disketa ali CD morajo biti jasno označeni – vsaj z imenom prvega avtorja, začetkom naslova in datumom izročitve uredništvu RMZ-M&G. Elektronski prenos mora biti pospremljen z jasnim sporočilom in z enakimi podatki kot velja za ostale načine posredovanja.

Informacije o RMZ-M&G: urednik prof. dr. Peter Fajfar, univ. dipl. ing. metal. (tel. ++386 1 4250316) ali tajnica Barbara Bohar Bobnar, univ. dipl. ing. geol. (tel. ++386 1 4704630), Aškerčeva 12, 1000 Ljubljana
ali na E-mail naslovih:
peter.fajfar@ntf.uni-lj.si
barbara.bohar@ntf.uni-lj.si

Pošiljanje prispevkov. Prispevke pošljite priporočeno na naslov **Uredništva:**
- RMZ-Materials and Geoenvironment
  Aškerčeva 12,
  1000 Ljubljana, Slovenija
oziroma jih oddajte v
- **Recepciji** Naravoslovnotehniške fakultete (pritličje) (za RMZ-M&G)
  Aškerčeva 12,
  1000 Ljubljana, Slovenija
- Možna je tudi oddaja pri uredniku oziroma pri tajnici.

Navodila veljajo od avgusta 2009.

TEMPLATE

The title of the manuscript should be written in bold letters (Times New Roman, 14, Center)

Naslov članka (Times New Roman, 14, Center)

Name Surname[1], …. , & Name Surname[x] (Times New Roman, 12, Center)

[x] University of ..., Faculty of ..., Address…, Country ... (Times New Roman, 11, Center)

*Corresponding author. E-mail: ... (Times New Roman, 11, Center)

Abstract (Times New Roman, Normal, 11): The abstract should be concise and should present the aim of the work, essential results and conclusion. It should be typed in font size 11, single-spaced. Except for the first line, the text should be indented from the left margin by 10 mm. The length should not exceed fifteen (15) lines (10 are recommended).

Izvleček (Times New Roman, navadno, 11): Kratek izvleček namena članka ter ključnih rezultatov in ugotovitev. Razen prve vrstice naj bo tekst zamaknjen z levega roba za 10 mm. Dolžina naj ne presega petnajst (15) vrstic (10 je priporočeno).

Key words: a list of up to 5 key words (3 to 5) that will be useful for indexing or searching. Use the same styling as for abstract.

Ključne besede: seznam največ 5 ključnih besed (3–5) za pomoč pri indeksiranju ali iskanju. Uporabite enako obliko kot za izvleček.

Introduction (Times New Roman, Bold, 12)

Two lines below the keywords begin the introduction. Use Times New Roman, font size 12, Justify alignment.

There are two (2) admissible methods of citing references in text:

1. by stating the first author and the year of publication of the reference in the parenthesis at the appropriate place in the text and arranging the reference list in the alphabetic order of first authors; e.g.:
    "Detailed information about geohistorical development of this zone can be found in: ANTONIJEVIĆ (1957), GRUBIĆ (1962), ..."
    "… the method was described previously (HOEFS, 1996)"
2. by consecutive Arabic numerals in square brackets, superscripted at the appropriate place in the text and arranging the reference list at the end of the text in the like manner; e.g.:
    "... while the portal was made in Zope environment. [3]"

MATERIALS AND METHODS (TIMES NEW ROMAN, BOLD, 12)

This section describes the available data and procedure of work and therefore provides enough information to allow the interpretation of the results, obtained by the used methods.

RESULTS AND DISCUSSION (TIMES NEW ROMAN, BOLD, 12)

Tables, figures, pictures, and schemes should be incorporated in the text at the appropriate place and should fit on one page. Break larger schemes and tables into smaller parts to prevent extending over more than one page.

CONCLUSIONS (TIMES NEW ROMAN, BOLD, 12)

This paragraph summarizes the results and draws conclusions.

Acknowledgements (Times New Roman, Bold, 12, Center - optional)

This work was supported by the ****.

References (Times New Roman, Bold, 12)

In regard to the method used in the text, the styling, punctuation and capitalization should conform to the following:

FIRST OPTION - in alphabetical order

Casati, P., Jadoul, F., Nicora, A., Marinelli, M., Fantini-Sestini, N. & Fois, E. (1981): Geologia della Valle del'Anisici e dei gruppi M. Popera - Tre Cime di Lavaredo (Dolomiti Orientali). *Riv. Ital. Paleont.*; Vol. 87, No. 3, pp. 391–400, Milano.

Folk, R. L. (1959): Practical petrographic classification of limestones. *Amer. Ass. Petrol. Geol. Bull.;* Vol. 43, No. 1, pp. 1–38, Tulsa.

SECOND OPTION - in numerical order

[1] Trček, B. (2001): *Solute transport monitoring in the unsaturated zone of the karst aquifer by natural tracers.* Ph. D. Thesis. Ljubljana: University of Ljubljana 2001; 125 p.

[2] Higashitani, K., Iseri, H., Okuhara, K., Hatade, S. (1995): Magnetic Effects on Zeta Potential and Diffusivity of Nonmagnetic Particles. *Journal of Colloid and Interface Science, 172*, pp. 383–388.

Citing the Internet site:

CASREACT-Chemical reactions database [online]. Chemical Abstracts Service, 2000, updated 2. 2. 2000 [cited 3. 2. 2000]. Accessible on Internet: http://www.cas.org/CASFILES/casreact.html.

Texts in Slovene (title, abstract and key words) can be written by the author(s) or will be provided by the referee or by the Editorial Board.

PREDLOGA ZA SLOVENSKE ČLANKE

Naslov članka (Times New Roman, 14, Na sredino)

The title of the manuscript should be written in bold letters (Times New Roman, 14, Center)

IME PRIIMEK[1], …, IME PRIIMEK[X] (TIMES NEW ROMAN, 12, NA SREDINO)

[X]Univerza…, Fakulteta…, Naslov…, Država… (Times New Roman, 11, Center)

*Korespondenčni avtor. E-mail: ... (Times New Roman, 11, Center)

Izvleček (Times New Roman, Navadno, 11): Kratek izvleček namena članka ter ključnih rezultatov in ugotovitev. Razen prve j bo tekst zamaknjen z levega roba za 10 mm. Dolžina naj ne presega petnajst (15) vrstic (10 je priporočeno).

Abstract (Times New Roman, Normal, 11): The abstract should be concise and should present the aim of the work, essential results and conclusion. It should be typed in font size 11, single-spaced. Except for the first line, the text should be indented from the left margin by 10 mm. The length should not exceed fifteen (15) lines (10 are recommended).

Ključne besede: seznam največ 5 ključnih besed (3–5) za pomoč pri indeksiranju ali iskanju. Uporabite enako obliko kot za izvleček.
Key words: a list of up to 5 key words (3 to 5) that will be useful for indexing or searching. Use the same styling as for abstract.

UVOD (TIMES NEW ROMAN, KREPKO, 12)

Dve vrstici pod ključnimi besedami se začne Uvod. Uporabite pisavo Times New Roman, velikost črk 12, z obojestransko poravnavo. Naslovi slik in tabel (vključno z besedilom v slikah) morajo biti v slovenskem jeziku.

Slika (Tabela) X. Pripadajoče besedilo k sliki (tabeli)

Obstajata dve sprejemljivi metodi navajanja referenc:

1. z navedbo prvega avtorja in letnice objave reference v oklepaju na ustreznem mestu v tekstu in z ureditvijo seznama referenc po abecednem zaporedju prvih avtorjev; npr.:

    "Detailed information about geohistorical development of this zone can be found in: Antonijević (1957), Grubić (1962), ..."

    "… the method was described previously (Hoefs, 1996)"

ali

2. z zaporednimi arabskimi številkami v oglatih oklepajih na ustreznem mestu v tekstu in z ureditvijo seznama referenc v številčnem zaporedju navajanja; npr.;

    "... while the portal was made in Zope[3] environment."

Materiali in metode (Times New Roman, Krepko, 12)

Ta del opisuje razpoložljive podatke, metode in način dela ter omogoča zadostno količino informacij, da lahko z opisanimi metodami delo ponovimo.

Rezultati in razprava (Times New Roman, Krepko, 12)

Tabele, sheme in slike je treba vnesti (z ukazom Insert, ne Paste) v tekst na ustreznem mestu. Večje sheme in tabele je po treba ločiti na manjše dele, da ne presegajo ene strani.

Sklepi (Times New Roman, Krepko, 12)

Povzetek rezultatov in sklepi.

Zahvale (Times New Roman, Krepko, 12, Na sredino - opcija)

Izvedbo tega dela je omogočilo ………

Viri (Times New Roman, Krepko, 12)

Glede na uporabljeno metodo citiranja referenc v tekstu upoštevajte eno od naslednjih oblik:

PRVA MOŽNOST (priporočena) - v abecednem zaporedju
Casati, P., Jadoul, F., Nicora, A., Marinelli, M., Fantini-Sestini, N. & Fois, E. (1981): Geologia della Valle del'Anisici e dei gruppi M. Popera – Tre Cime di Lavaredo (Dolomiti Orientali). *Riv. Ital. Paleont.*; Vol. 87, No. 3, pp. 391–400, Milano.
Folk, R. L. (1959): Practical petrographic classification of limestones. *Amer. Ass. Petrol. Geol. Bull.;* Vol. 43, No. 1, pp. 1–38, Tulsa.

DRUGA MOŽNOST - v numeričnem zaporedju
[1] Trček, B. (2001): *Solute transport monitoring in the unsaturated zone of the karst aquifer by natural tracers.* Ph. D. Thesis. Ljubljana: University of Ljubljana 2001; 125 p.
[2] Higashitani, K., Iseri, H., Okuhara, K., Hatade, S. (1995): Magnetic Effects on Zeta Potential and Diffusivity of Nonmagnetic Particles. *Journal of Colloid and Interface Science, 172*, pp. 383–388.

Citiranje spletne strani:
CASREACT-Chemical reactions database [online]. Chemical Abstracts Service, 2000, obnovljeno 2. 2. 2000 [citirano 3. 2. 2000]. Dostopno na svetovnem spletu: http://www.cas.org/CASFILES/casreact.html.

Znanstveni, pregledni in strokovni članki ter predhodne objave se objavijo v angleškem jeziku. Izjemoma se strokovni članek objavi v slovenskem jeziku.